The *Skyscraper Revolution*: Global Economic Development and Land Savings*

Gabriel M. Ahlfeldt † Nathaniel Baum-Snow ‡ Remi Jedwab §

July 22, 2023

Abstract

The construction of tall buildings has been central in facilitating sustainable urbanization and growth in cities around the world. Using supply side variation for identification, we demonstrate that the average elasticity of city population to aggregate city building heights is 0.12, and that of city built area to heights is -0.17. Land saved from development by post-1975 tall building construction is over 80% covered in vegetation. To isolate the effects of technology-induced reductions in the cost of height from correlated demand shocks, we use interactions of static demand differences and the geography of bedrock as instruments for observed changes in height, a triple difference identification strategy. Central to the analysis is newly organized data on the population, land area, and a measure of total height for 1975-2015 in 12,877 cities worldwide. Quantification using a canonical urban model suggests that about two-thirds of the potential benefits from reductions in the cost of heights has been realized. Worker welfare would increase by 1% if constraints to vertical development were relaxed, though aggregate land rents would decline by 2%.

Key words: Density; International Buildings Heights; Skyscrapers; Sustainable Urbanization; Commercial Real Estate; Housing Supply; Sprawl; Land Savings; Affordability; Geographical Constraints

JEL: R11, R12, R14, R31, R33, O18, O13

*We thank Jason Barr, Adrian Bilal, Jan Brueckner, Federico Curci, Klaus Desmet, Rebecca Diamond, Gilles Duranton, Edward Glaeser, Gabriel Kreindler, Jessie Handbury, Christian Hilber, Matthew Kahn, Jeffrey Lin, Megha Mukim, Guy Michaels, John Morrow, David Nagy, Victor Ortego Marti, Lindsay Relihan, Tanner Regan, Frederic Robert-Nicoud, Esteban Rossi-Hansberg, Mark Roberts, Michael Storper, Nick Tsivanidis, Matthew Turner, Tony Venables, C. Luke Watson, Michael Wong, and numerous seminar audiences for helpful comments.

†London School of Economics. Email: g.ahlfeldt@lse.ac.uk

‡University of Toronto. Email: nate.baum.snow@rotman.utoronto.ca

§George Washington University and NYU Marron Institute of Urban Management. Email: jedwab@gwu.edu and rj2513@nyu.edu

1 Introduction

Chicago's ten-storey 42-meter tall Home Insurance Building, built in 1884-85 and often regarded as the world's first *skyscraper* (Schleier, 1986), was among the first uses of technologies that would prove to transform cities around the world. Since then, technological improvements that have lowered the marginal cost of building high have facilitated the construction of the more than 16,000 km of buildings over 55 meters tall in cities worldwide. Most of this construction has occurred since 1975 for residential use in developing economies. With the equivalent of almost 43,000 Empire State Buildings, which cost 572 million in 2020 dollars to construct, the stock of tall buildings worldwide holds an aggregate asset value of more than 15 trillion dollars, after accounting for depreciation since construction. Indeed, a look at many global cities today leaves no doubt that the skyscraper revolution has been transformative (Glaeser, 2012). Each of the world's largest cities now hosts over 100 km of heights in tall buildings. In cities of over 1 million people, tall buildings account for about 10% of the stock and 18% of aggregate construction costs for existing structures. Like currently developed countries during the 19^{th} and 20^{th} centuries, many developing economies are now in a process of rapid urbanization, growth, and structural transformation. With these great pressures, the technology of building high has allowed cities to accommodate greatly increased populations while saving land for non-urban uses.

In this paper, we empirically and theoretically investigate the extent to which the skyscraper revolution has facilitated sustainable urbanization and urban growth, with a particular focus on cities in developing economies. Our empirical analysis recovers causal effects of the component of 1975-2015 tall building construction driven by technical progress and declines in the marginal cost of height on urban population growth, urban form, and land use. Using data from 12,877 urban agglomerations worldwide, we estimate an average elasticity of city population to height of 0.12 and an average elasticity of built-up land area to height of -0.17. These estimates are driven by cities in the developing world but also apply to cities in North America. While built land area elasticities are quite stable across cities of different sizes, estimated population elasticities are above average at about 0.15 for the largest cities and are largest at about 0.30 for the smallest cities. Tall buildings have facilitated substantial growth in the developing world's largest 100 cities since 1975. Had the technological advances driving declines in the cost of height not occurred, these cities would be up to 50 percent smaller in population and be up to one-third larger in land area. The skyscraper revolution has been critical to the growth and success of the world's largest cities and the preservation of surrounding rural land, over 80% of which is covered in tree canopy or short vegetation.

For identification, we use an instrumental variables strategy that leverages both cross-sectional and time series variation in the marginal cost of building high. In the cross-section, we use variation in city mean bedrock depth as a key source of identifying variation. Descriptive analysis and building cost function estimates indicate marginal cost of height per building floor area that is U-shaped in bedrock depth, consistent with engineering standards for foundation depth and the narrative in Barr et al. (2011). Bedrock that is too close to the surface must be blasted away at high cost to make room for building foundations. Foundations built above

bedrock that is beyond the optimal depth must either be reached with the costly installation of deep wide piles, placed on a more costly raft, or engineered to be underpinned by many very long deeply bored piles. Favorable bedrock depth thus acts as a cost shifter, promoting more construction of tall buildings for a given level of demand. As a result, the elasticity of tall building construction with respect to historical city population, a proxy for the level of demand, is greater at more favorable bedrock depths. Finally, differencing over time 1975-2015 leverages secular reductions in the marginal cost of height for identification. Particularly in the developing world, costs were sufficiently prohibitive in 1975 to preclude the existence of many tall buildings. Put together, our identification strategy leverages triple difference comparisons of historically large versus small cities on more versus less favorable bedrock depths over time.

To implement the empirical strategy, we compile a unique data set of all 12,877 cities with populations over 50,000 worldwide (in 182 countries), covering about 90% of the world's total urban population. For these cities, we collect census-based population and satellite-based area estimates going back to 1975, allowing us to measure population and land use in and around these cities over time. To capture the vertical size of cities, we use a data set of 750 thousand tall buildings from *Emporis*. This data set has comprehensive information on the location, use, and construction year of all buildings over 55 meters tall worldwide.

To conceptually ground the empirical work and evaluate the welfare consequences of policies that influence building heights, we incorporate building height into a neoclassical urban general equilibrium "representative city" model with frictional rural-urban migration. Potential floorspace rents for the commercial and residential sectors capitalize differences in production and residential amenities, respectively, across space within the city. Developers respond to higher floorspace rents by building taller, facing construction costs that are convex in height (Ahlfeldt and McMillen, 2018), consistent with our empirical evidence. In a competitive market, the land rent is the residual in the profit function that determines whether land is developed for commercial or residential use (Duranton and Puga, 2015). This setup draws from Ahlfeldt and Barr (2022), though it adds migration frictions through heterogeneity in tastes for urban life (McFadden, 1974), incorporating ideas from Harris and Todaro (1970), Bryan and Morten (2018) and Desmet et al. (2018) to accommodate domestic migration. Imperfect mobility of workers means that population *and* the utility of residents are endogenous objects.[1]

In the model, as in the data, reductions in the cost of height cause cities to grow vertically and become more productive and compact. Under our model parameterization, a reduction in the cost of height leads to an increase in the sum of heights across all buildings in the city, a measure of vertical size that we adopt from Jedwab et al. (2020). The vertical expansion is partially offset by a horizontal contraction. Due to the positive net effect on housing supply, the average floorspace rent falls. Lower rents, in conjunction with higher wages that arise from agglomeration economies, result in greater urban utility. Rural-urban migration (Harris and Todaro, 1970) is a central element in the model, as it is the way that cities grow in population in response to reductions in the cost of height. Matching estimated population and land area elasticities

[1]Our setup nests the closed-city and open-city models as special cases under extreme and negligible taste heterogeneity. See Brueckner (1987) for a discussion of these cases in the standard urban model.

with respect to height for a sub-sample of cities inferred to have the least burdensome land-use regulations to their model simulated counterparts yields an associated estimated elasticity of migration with respect to the urban real wage of 1.8, which is similar to other evidence in the literature (Caliendo et al., 2019).

Using the model, we undertake two counterfactual exercises which together indicate that about one-third of the potential welfare gains from heights have been realized. First, we compare the welfare consequences of the full relaxation of a 15 floor height limit to market allocations for all cities worldwide. Results indicate that relative to this height limit, the market allocation increases worker welfare by 3.2% and reduces aggregate land rents by 3.1%. Population gains and regulatory cost declines associated with going to the market allocation increase steeply in city size. Aggregate land rents decline most in the largest cities due to the horizontal contraction facilitated by the greater allowed heights. Hence, reducing height regulation redistributes welfare from land to labor. Landlords lose with the lower rents associated with the supply expansion that comes with new heights but workers gain more due to slightly higher wages, enhanced access to preferred locations, and lower rents. The second exercise is to compute the aggregate effects of going from a 15 floor height limit to the current existing heights observed in the data. This increases worker welfare by 2.2% and reduces aggregate land rents by 1.3%. Once again, landlords lose through the relaxation of the supply constraint but workers benefit from higher wages and improved access to their preferred location. Put together, the implication is that about two-thirds of the welfare potential of tall buildings has been realized globally. Relaxations of restrictions on building tall buildings thus has the potential to increase potential residents' welfare by 1.0%. This number is as large as 1.9% for cities in South Asia and as low as 0.3% in East Asia and the Pacific. These gaps are driven by both the differing costs of heights in these regions and the amount of existing tall building construction.

Our analysis builds on the more focused existing evidence on the consequences of building heights, which mostly uses data from the US. Rosenthal and Strange (2008) and Curci (2020) provide evidence that skyscrapers catalyze nearby densification and productivity gains, with complementary evidence of within structure productivity advantages for tall buildings in Liu et al. (2020). Danton and Himbert (2018), Koster et al. (2013), and Liu et al. (2018) provide empirical evidence on the returns to height in residential and commercial buildings. Our model also has many features in common with that in Curci (2017), which examines the consequences of vertical versus horizontal city expansion.

While this is the first paper to comprehensively study how declines in the costs of building tall have contributed to urban growth and change in cities around the world, our analysis has many parallels with the large empirical literature exploring the impacts of transport infrastructure on cities. Like highways, railroads, and subways, tall buildings are a central component of city capital stocks. Similar to the research on transport, we face the identification challenge of isolating variation in infrastructure supply across cities and over time that is unrelated to local demand conditions. Indeed, our identification challenge is perhaps more demanding than that for transport, as there are few systematic institutional reasons for building heights to vary across cities. Somewhat analogous to Faber (2014)'s use of least cost paths driven by topography as

instruments for highway routes in China, we use natural bedrock depth as a source of exogenous variation in changes in the cost of building taller. Duranton and Turner (2012) estimate an elasticity of urban population growth with respect to urban highway infrastructure of 0.15 for the US, which is quite similar to our estimate of 0.12 for the world. Our estimated population density elasticity for tall buildings of 0.29 is about 3 times as large as those found for urban radial highways in the US and China (Baum-Snow, 2007; Baum-Snow et al., 2017).[2]

Conceptually, our study perhaps most closely relates to the large literature studying land use, housing supply, and regulation. Our modeling framework incorporates insights from the land use and housing production literatures to accommodate height restrictions and general equilibrium linkages across labor and housing markets within and between residential and commercial sectors. Following in the tradition of Muth (1969), we incorporate residential and commercial real estate production into the neoclassical monocentric land use theory of Alonso (1964) and Mills (1967), with some elements of the more recent quantitative spatial models summarized in Redding and Rossi-Hansberg (2017). Qualitative conclusions thus mirror those from the more targeted modeling frameworks in Bertaud and Brueckner (2005) and Henderson et al. (2021), though we put more emphasis on accommodating variation across cities in the marginal cost of height. The use of the simple monocentric city structure allows our model to reasonably characterize cities of many different sizes and shapes, in part as captured by differences in fundamental productivities and amenities. Our model parameterization uses as important inputs results from the more focused empirical studies of the cost of height (Ahlfeldt and McMillen, 2018) and returns to height (Liu et al., 2018, 2020). These central parameters shape the verticality of cities in our model (Barr, 2010, 2012), with the dominant idea that tall buildings are a reflection of economic activity at the time they were built (Ahlfeldt and Barr, 2020).

Much research on the existence and implications of housing market regulation has been carried out for developed economies, including Gyourko and Molloy (2015); Hilber and Vermeulen (2016); Hsieh and Moretti (2019); Baum-Snow and Han (2019); Brueckner and Singh (2020), and Duranton and Puga (2020). The more limited work for cities in the developing world has mostly come to the same conclusion, that height regulations are broadly binding and have negative welfare consequences. There is evidence in Brueckner and Sridhar (2012) for Indian cities, Brueckner et al. (2017) and Tan et al. (2020) for Chinese cities, Henderson et al. (2021) for Nairobi, along with Jedwab et al. (2020)'s meta-analysis for cities around the world. We provide a comprehensive quantitative evaluation of the extent to which reductions in the cost of building high have influenced affordability, rural-urban migration, productivity, and welfare for all cities worldwide. Moreover, we quantify the prospects for further gains through relaxation of height regulations.

The use of geological conditions as instruments has been particularly common in the literature concerned with the economic (productivity and amenity) effects of urban density, as summarized

[2]Other papers studying impacts of different types of transport infrastructure on cities include Storeygard (2016); Gonzalez-Navarro and Turner (2018); Gibbons et al. (2019); Heblich et al. (2020); Baum-Snow (2020); Baum-Snow et al. (2020), and Jedwab and Storeygard (2021). Redding and Turner (2015) provides a comprehensive overview of much of this extensive literature.

by Ahlfeldt and Pietrostefani (2019). Similar to our empirical approach, a few studies in this literature use soil and subsoil geological conditions to instrument for density in the identification of agglomeration spillovers (Rosenthal and Strange, 2008; Combes et al., 2011). These papers argue that solid bedrock, or favorable geological conditions more generally, reduce the cost of building tall structures, leading to greater employment and population densities for reasons unrelated to features that may have a direct impact on productivity or amenities such as access to coastlines and navigable rivers. This paper builds on these ideas and the more direct evidence in Barr et al. (2011) and Barr (2016) to directly document the causal connections from bedrock depths to building heights, a required intermediate step to density that has heretofore not been comprehensively explored. The large applied agglomeration and urban growth literature, as summarized in Combes and Gobillon (2015), does not closely consider the requirements of the built environment for generating density. This lack of inquiry is likely due to the challenges associated with putting together data appropriate for the analysis. Our estimates indicate that the lower costs of tall building construction have facilitated cities' vertical expansions as a central vehicle to densification and associated enhanced productivities and amenities.

Understanding how the skyscraper revolution fits into the process of urban development is all the more important as cities that do not develop vertically tend to sprawl (Burchfield et al., 2006) and/or become inefficiently spatially configured. Odd urban spatial structures impede growth (Harari, 2020), and associated sprawl typically occupies land that is particularly valuable in non-urban uses. According to World Bank (2022), urban areas occupied 3.6 million sq km in 2011, whereas 48.0 million sq km of land was in agriculture. As cities are more likely to be sited on agriculturally productive land (Henderson et al., 2018), land savings through increased urban compactness frees up more space for agriculture and tree canopy. Taller cities make us "greener" (Glaeser, 2012) by accommodating more people on less land. In that, the skyscraper revolution has parallels with the Green Revolution, whose goal was to use rural land more intensively in order to use less land globally (Gollin et al., 2021).

2 Data and Descriptive Evidence

2.1 The Growth in Tall Buildings

Until the 1960s, the vast majority of the world's tall buildings (over 55 meters tall) were office buildings found in the largest cities of the highest income countries. Starting in the 1970s, the construction of tall buildings spread through many middle income countries and into medium sized and smaller cities worldwide. Moreover, most such construction was for residential rather than commercial use. Figure 1 depicts these patterns. As seen in the left panel, the world's total stock of tall building heights increased slowly from 1884, when the first skyscraper was built, until the 1970s. During our primary study period of 1975-2015, the total stock of heights in buildings for which we observe construction year increased from 868 km to 12,387 km. This growth corresponds to more than 70% of the total stock today and is about three times the distance between New York and Los Angeles.

Figure 1: Evolution of Aggregate Tall Building Heights

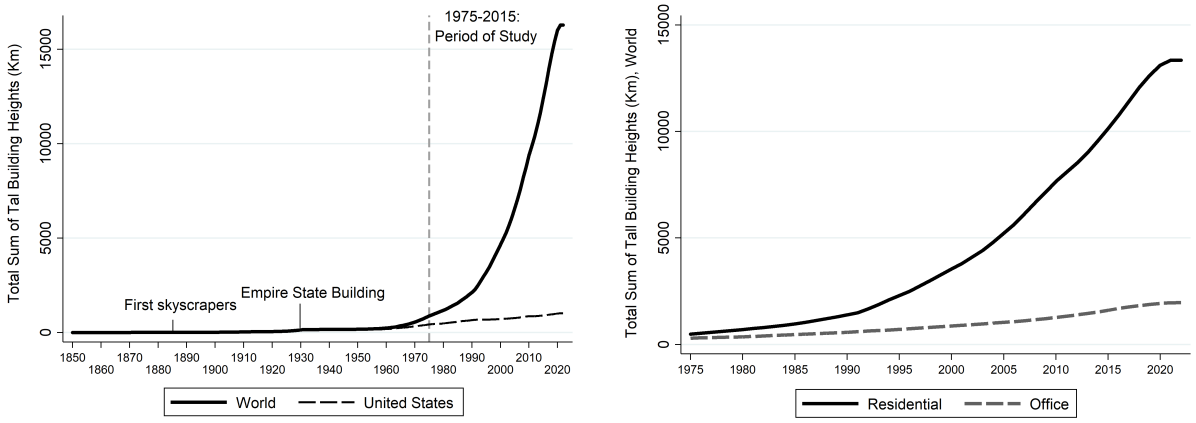

(a) All Buildings

(b) Residential vs. Office Towers

Notes: The left panel shows the evolution of the total stock of tall building heights (km) for the world and the United States. The right panel shows the evolution of the stock of tall building heights (km) separately for residential and office buildings. Only buildings above 55 meters are included.

During our primary study period of 1975-2015, total heights increased seven times more for residential buildings than for office buildings (right panel of Figure 1). While most buildings over 100 meters host offices, most buildings between 55 and 100 meters are residential, and these make up the lion's share of tall building construction since 1975.

The rapid increase in construction starting in the 1970s came with advances in technology. Until the 1960s, most tall buildings were steel construction. In the 1970s, there was a shift toward concrete construction. Concrete buildings use lower cost materials but cannot be easily built as tall as steel construction buildings. In the 1975-2015 period, concrete accounts for 80 percent of height in new construction buildings over 55 meters, with the remainder about evenly split between steel and composite. As concrete is heavier than steel, more recently built tall buildings have required more robust foundations to accommodate the extra weight.

Figure 2 shows how widespread tall buildings have become around the world. For an exhaustive data set of 12,877 cities worldwide, it shows the absolute change (km) in aggregate tall building heights between 1975 and 2015. While the highest-stock cities included New York, Chicago, Hong Kong, Moscow, London, Sao Paulo and Philadelphia in 1975, in 2015 the list is dominated by Seoul, Hong Kong, Moscow, Sao Paolo, Singapore, New York, Guangzhou and Tokyo. In terms of absolute changes per capita 1975-2015, some of the most dynamic cities include Seoul, Hong Kong, Panama City, Singapore, Moscow, Kuala Lumpur, Dubai, and Tel Aviv, reflecting the spread of tall building construction to lower income economies.

The remarkable 1975-2015 tall building construction boom can be explained by both supply and demand factors. On the demand side, the 1975-2015 period saw both rapid urbanization and income growth in many countries. This has manifested as particularly strong demand growth in larger cities. On the supply side, there was technical progress in tall building construction, bringing costs down.

Figure 2: Sum of Tall Building Heights, World Cities, 1975-2015

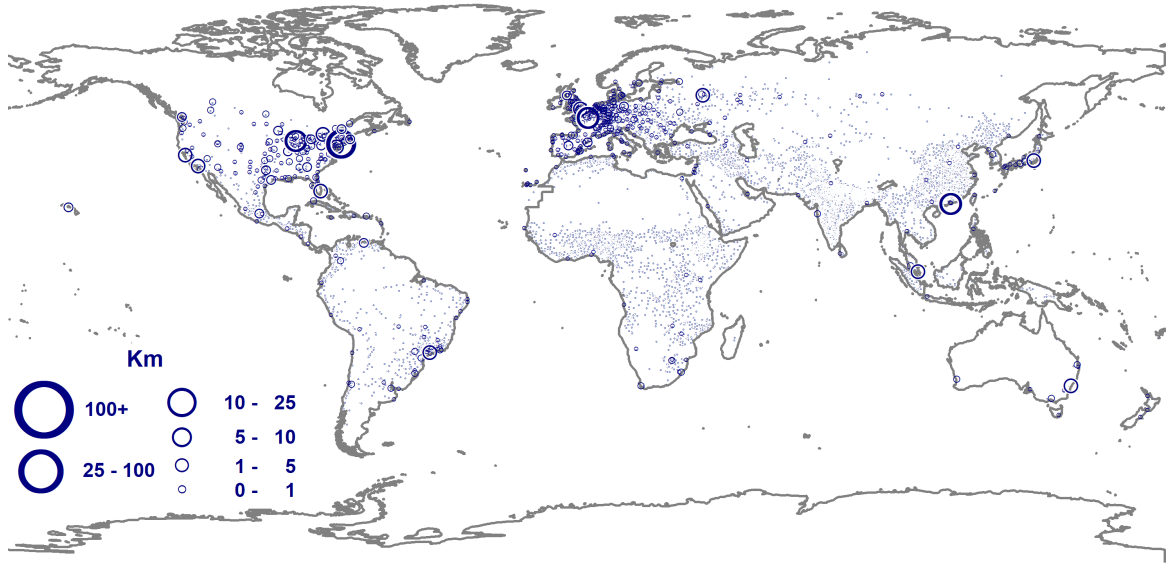

(a) 1975

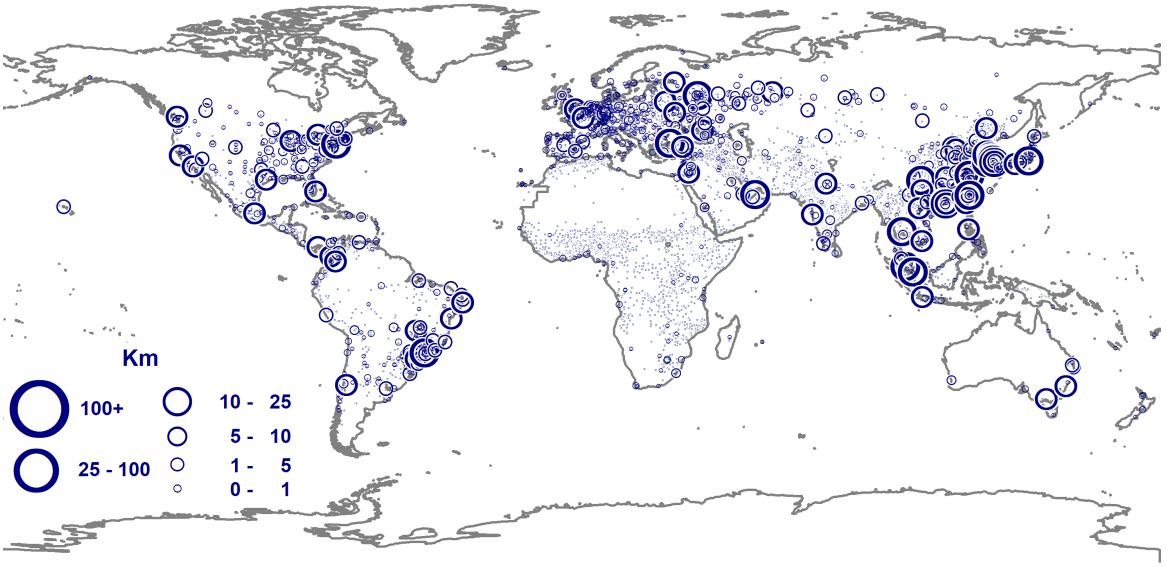

(b) 2015

Notes: This figure shows the total stock of tall building heights (km) for 12,877 world cities of at least 50,000 residents in 2015. Only buildings above 55 meters are included.

Figure 3 provides evidence on reductions in the cost of height over time. For this figure, we use building level data from Emporis on construction cost and floor area for the United States, described in more detail in the following sub-section.[3] This figure is created in two steps. First, a construction cost index is created by residualizing city and country-decade of construction fixed effects from log cost per building floor area. This residualization partials out local input cost differences across cities and over time. Second, this index is smoothed over construction year and building height using a bivariate Gaussian kernel. Because time effects are removed, construction cost per floor area is (approximately) mean 0 by construction in each year. Therefore, this figure speaks only to the relative change in construction costs in taller versus shorter buildings.

Figure 3: Construction cost as function of height and construction year

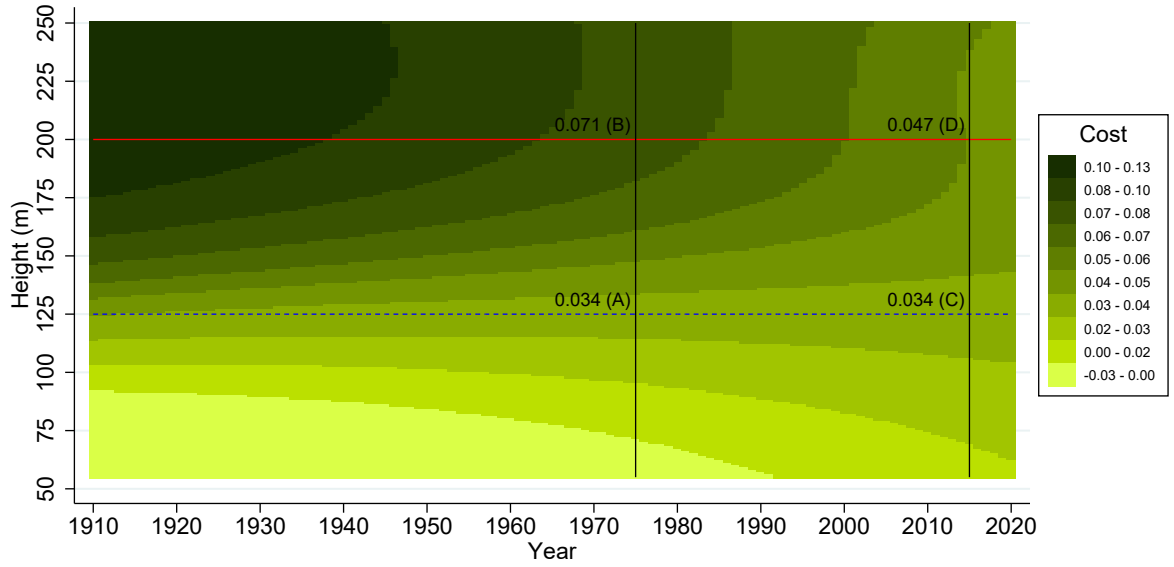

Notes: Cost is the log cost per floor area, residualized for city and country-by-decade of construction fixed effects. The sample consists of 591 buildings in US cities (see Panel A in Table A2 in the Appendix). We use locally weighted regressions with a bivariate Gaussian kernel to estimate local means of the residualized cost measure within the height-bedrock plane with a bandwidth parameter for both covariates of $\kappa = 50$. Appendix Section H.3 has details and provides results from locally weighted regressions with univariate kernels that deliver confidence bands for height categories that roughly correspond to the dotted blue and solid red lines.

Evident in Figure 3 are steep declines in the cost of height over the past century that continued throughout our study period of 1975-2015. In 1975, buildings of 200 meters were on average 3.5% higher cost to build per square meter than 125 m tall buildings. By 2015, that gap had fallen to just 1.3% greater. Appendix Section H.5 documents further evidence of secular declines in construction costs that were more rapid for tall buildings than shorter buildings. Our supply model in Section 2.4 below specifies how a combination of such secular cost declines and variation in levels of demand for real estate across cities of different sizes can have precipitated the post-1975 boom in tall building construction documented in Figure 1 that has been particularly oriented toward the world's largest cities.

[3]The United States is the only country for which we have enough construction cost data to build a reliable cost index prior to about 1990.

2.2 Data Sources

The empirical analysis uses historical information about urban agglomerations and building heights for 12,877 cities worldwide, 11,273 of which are in developing economies. Also incorporated into the data set are information on city bedrock depth and lights at night. Below we briefly describe each data source. Additional information is in Appendix H.

City Boundaries and Population: Using the *Global Human Settlements-Urban Centre Database* (GHS-UCDB) (Florczyk et al., 2019, version 1.2 from 18/04/2020), we obtain the GIS boundaries of all 12,877 current agglomerations of at least 50,000 inhabitants worldwide, which they call "urban centres" (UCs). These UCs correspond to commuting zones, as in US metropolitan statistical areas.[4] The GHS-UCDB reports the (satellite-based) total *land area* and *built-up area* of each city c. 1975, 1990, 2000 and 2015. Using the built-up area and population census data, the GHS-UCDB also reports population estimates for each city in these same years. As built-up area is more consistently measured over time, this is our main measure of urbanized land. The 12,877 cities account for about 90% of the world's total urban population in 2015 (United Nations, 2018).

Land Use: For additional measures of changes in land use in and near cities, we use the 1982-2015 *Global Land Change Data* (Song et al., 2018). For each ≈5X5 km pixel worldwide, this data set records agricultural suitability of the soil. Moreover, we observe whether there was tree canopy, short vegetation or urbanized/desertification land cover in 1982 and 2015. In 2000 and 2015, we observe whether the land was used for growing crops.

Building Heights and Construction Costs: Emporis (2022) (last accessed 02-07-2022) was a global provider of international skyscraper and high-rise building data.[5] Emporis collected information about the full life-cycle of each building, from conception to demolition, covering thousands of cities worldwide. The database contains data for 693,855 "existing [completed]" buildings.[6] For almost all buildings, we know the exact geographic coordinates, or at least the city in which it is located. This allows us to assign each building to a city in the GHS-UCDB data set. Since we know the year of construction (and demolition if demolished), we obtain the total *sum of heights* for each city-year from 1884 (when the first skyscraper – the Home Insurance Building in Chicago – was built) to date. For a select set of 1,053 buildings, the Emporis data set also reports the building's construction cost, though 20 of these do not have floorspace information.

Inspection of the kernel density of 2015 building heights in the Emporis data set (Figure A1) reveals a mode and large spike at 55 meters. Since cities are likely to have more buildings below than above 55 meters, and since the distribution of buildings is relatively smooth after 55 meters, we infer that the data set likely only captures the universe of buildings above 55 meters. As such, our *sum of heights* measure for each city and year only includes buildings of at least

[4] We refer to "UCs", "agglomerations" and "cities" interchangeably. For example, the New York UC includes "New York; Islip; Newark; Jersey City; Yonkers; Huntington; Paterson; Stamford; Elizabeth; New Brunswick."

[5] Since September, 2022, information in the Emporis data has been integrated into CoStar Group data products.

[6] We only consider buildings of the following types: "building with towers", "high-rise building", "low-rise building", "multi-story building", and "skyscraper".

55 meters.

In 1975, 5% of cities in our full sample had any tall buildings, including only 1% of cities in the developing world. The cities that did have tall buildings were mostly large and in the developed world. Of the 515 cities over 500,000 people in 1975 in our full sample, 41% had at least one tall building. But among the 347 large cities in the developing world, only 23% had any tall buildings. Between 1975 and 2015, cities of all sizes built some tall buildings, but this growth was disproportionately oriented toward larger cities. The fraction of cities under 100,000 that built their first tall buildings in the 1975-2015 period was only 0.02. This number rises to 0.13 for cities of 100,000-500,000 and 0.32 for cities over 500,000, despite both groups having larger 1975 bases.

To account for the fact that many cities have no buildings above 55 meters in some years, we primarily use $\ln(\text{Heights} + 1)$ to measure the sum of heights in each city. However, all results are robust to using scaling factors other than 1, the inverse hyperbolic sine transformation, or an indicator for whether the city had any tall buildings as alternative measures of city heights. One way to view our empirical approach is thus as treating heights in the base year as 0, especially for the sub-sample analysis that uses cities in developing economies only.

Bedrock Depth: Shangguan et al. (2017) reports bedrock depth in meters at a 30 second ($\approx$ 1 km) resolution for the entire world. (For example, there are 8,118 such pixels in the New York UC). We use our GIS city boundaries to obtain *mean bedrock depth* in meters (MBD) for each city. Shangguan et al. (2017) indicates "this data set is based on observations extracted from a global compilation of soil profile data (about 1,300,000 locations) and borehole data (about 1.6 million locations)." Looking across all pixels within our city boundaries, 90% of the variance in bedrock depth is between rather than within cities in our data. For pixels within cities of at least 300,000 people in 2015, a Theil decomposition indicates that about three-quarters is from between city variation, depending on whether it is calculated as unweighted or weighted by city population. Our results are not sensitive to the use of mean bedrock depth across all pixels in each city or the bedrock depth at each city's central business district inferred from the brightest cluster of lights at night pixels.

Lights at Night: While our main analysis considers city population and built area 1975-2015, we also study the effects of tall building construction on lights at night, for which only more recent data are available. Night lights data corresponding to the DMSP satellites are provided by NGDC (2015). We use the radiance calibrated version of this data, which is available for select years 1996-2011, to avoid issues related to top-coding.[7] The data are available at a fine spatial resolution and we use GIS to obtain *mean night light intensity per area* for each city.

2.3 Patterns of Vertical Growth in the Data

Conditional on bedrock depth, larger cities had both greater 1975 levels and 1975-2015 growth in heights. This holds true whether heights are measured in meters, growth rates, or at the extensive margin. For example, among cities of fewer than 100 thousand people in 1975, the

[7]This data set records levels of luminosity beyond the normal digital number upper bound of 63.

average city with medium depth bedrock built 63 meters of heights in buildings over 55 meters, whereas in the largest cities (over 500 thousand people in 1975) the average city built 26.5 km of heights between 1975 and 2015. In the following sub-section, we formally interpret this pattern, which is monotonic in 1975 city population, as reflecting the fact that technical progress which reduced the marginal cost of height allowed the greater levels of real estate demand in larger cities to be accommodated by building taller.

Conditional on 1975 city population, we see more tall building construction in cities on intermediate bedrock depths. Between 1975 and 2015, the average large city on mean bedrock depths below 10 meters built 5.2 km of tall buildings, relative to the 26.5 km built in cities on intermediate bedrock depths cited above. Among small cities on shallow bedrock depths, only 9 meters of heights were built, relative to the 63 meters on intermediate bedrock depths cited above. We note that secondary Chinese cities are heavily over-represented in the deep bedrock category. In many of these locations, the post-1990 construction boom did not respond to standard market forces. Moreover, the costs of installing foundations to support tall buildings depend more on soil conditions in areas where bedrock is very deep. As a result, there is more dispersion in height growth among cities on deep bedrock, meaning that they provide less identifying power than do cities on bedrock depths below 30 meters. Nonetheless, mean 1975-2015 height growth is lower in these deep bedrock cities than those on intermediate bedrock conditional on 1975 population.

Rapid 1975-2015 urbanization rates around the world manifested as population growth of 46% and built area growth of 55% in the average city. Our empirical results will indicate that this decline in average population density would have been even greater absent the contemporaneous boom in tall building construction, especially in the largest cities. On average across our sample, the typical city added 895 meters of heights on a base of 67 meters in 1975, with almost all of this growth among cities in the top tercile of the city size distribution. Table A1 presents means of our key outcome variables and three measures of city aggregate height of buildings over 55 meters tall by categories of 1975 city population and city mean bedrock depth (MBD).

2.4 The Data Generating Process for Heights

Here we demonstrate conceptually how greater levels of real estate demand, more favorable bedrock depths, and secular declines in the marginal cost of height have interacted to generate more tall building construction in certain cities. In 1975, only a few very high demand cities had tall buildings. With technical progress and declines in the marginal costs of height, it became viable for more cities to host tall buildings. This increased viability was particularly true for high population cities, where demand was high, with favorable intermediate bedrock depths, where costs of height were lower. As a result, we see more robust height growth in large relative to small cities with intermediate relative to low or high bedrock depths. This triple difference idea, which compares cities of different 1975 populations and bedrock depths over time, leads into our instrumental variables strategy of using 1975 log city population interacted with a flexible function of bedrock depth as a source of exogenous variation in the 1975-2015 growth in building

heights across cities.

Having established above that the marginal cost of height secularly declined after 1975, the next step is to provide evidence on how the cost of height is related to bedrock depth in cross-sectional comparisons. Structural engineers have a simple rule of thumb known as Rankine's Theory which indicates the depth of a building's foundation required for stability. Rankine's Theory lays out a proportional relationship between building weight (which is roughly proportional to height) and foundation depth, with the constant of proportionality differing as a function of soil conditions around the foundation. According to Rankine's Theory, the optimal foundation depth is around 10% of the building's height. In order for a building to be stable, the bottom of the foundation must either be anchored to bedrock, have a sufficiently wide base ("raft"), or incorporate many very deeply bored piles. As rafts and numerous deeply bored piles are more costly to construct and install, builders prefer to anchor to bedrock if it is not too deep. However, if bedrock is within only a few meters of the surface, expensive blasting is required to install the foundation.

Central to our empirical approach is the observation that construction cost per square foot varies with both building height and bedrock depth. Figure 4 provides descriptive evidence on how construction cost varies with bedrock depth. It is constructed using the the same methods as Figure 3, with the bivariate smoothing of residualized log construction cost per building floor area performed over bedrock depth and building height.

Figure 4 depicts both the non-monotonicity of construction costs in bedrock depth conditional on height and the rate at which construction costs increase in height. The descriptive evidence is that the cost-minimizing bedrock depth for 125 meter tall buildings is 18 meters (blue lines), while that for 200 meter tall buildings is 25 meters (red lines). Constructing a 125 meter tall building at the optimal bedrock depth saves more than 5% in cost per square meter relative to building on surface level or very deep bedrock. The associated cost savings are much larger for 200 meter tall buildings. Moreover, Figure 4 shows that unit costs increase in building height much more rapidly where bedrock is deep.[8] (Appendix H.4 has further discussion).

The engineering evidence thus suggests that a reasonable approximation of the cost function for developing a building of height S on bedrock depth B_{ac} in city a of country c at time t is

$$C_{act}(S) = c_{act} S^{1+\theta(B_{ac},\mu_t)}. \tag{1}$$

To be consistent with patterns seen in Figure 3, we allow the elasticity of unit cost with respect to height, $\theta(B_{ac}, \mu_t)$, to change over time, as governed by the μ_t parameters. To be consistent with patterns seen in Figure 4, we allow both the elasticity of unit cost with respect to height and the cost shifter c_{act} to depend on bedrock depth. It is evident from Figure 4 that, commensurate with the engineering discussion, the marginal cost of height per square meter is greater at low and high bedrock depths, meaning that θ is U-shaped in B_{ac} and $\theta_{BB} > 0$. As c is non-parameterically

[8] Below we demonstrate that the relatively low predicted unit costs on the bottom right of Figure 4, where bedrock is deep, are not significant. This region of the graph is mostly extrapolated, as 90% of the buildings with construction cost data are built on bedrock less than 30 meters deep.

Figure 4: Construction cost as function of height and bedrock depths

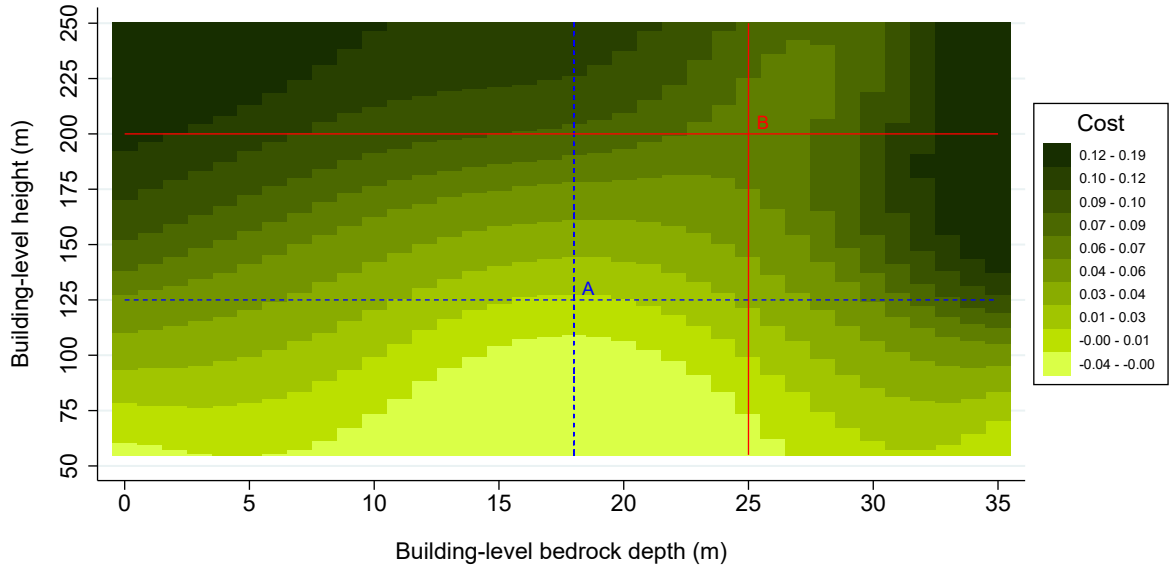

Notes: Cost is the log cost per floor area residualized for city and country-by-decade of construction fixed effects. The sample includes 1,033 buildings in 206 cities and 55 countries (see Panel A in Appendix Table A2). Locally weighted regressions with a bivariate Gaussian kernel are used to estimate local means of the residualized cost measure within the height-bedrock plane. We set the bandwidth parameter for bedrock, b, to $\kappa^b = 6$ and for building height, h, to $\kappa^h = 40$, which correspond to about one third of the standard deviation of each respective covariate. We bin height at the upper limit, so 250 m includes all buildings of at least 250 m height. Appendix Section H.3 has details and also provides results from locally weighted regressions with univariate kernels, delivering confidence bands for height categories that roughly correspond to the blue dotted and red solid lines.

indexed by city and time, it incorporates differences in bedrock depth in addition to labor and materials costs that may change over time. To maintain tractability and simplicity, we maintain separability of time effects from bedrock depth effects in the elasticity of unit cost with respect to height.[9]

To corroborate the descriptive evidence in Figure 4 that θ is U-shaped in B, we recover rough non-parametric estimates of the $\theta(B, \mu)$ function with our limited construction cost data. We regress log construction cost per floor area on building height for each bedrock depth using an instrumental variables locally weighted regression (IV-LWR) approach. CBD distance instruments for building height with controls for city and country-year fixed effects. As inAhlfeldt and McMillen (2018) and Ahlfeldt and Barr (2022), identifying variation comes from comparing construction costs of different buildings in the same city exposed to approximately the same bedrock depth but at different CBD distances. The result, depicted in Figure A4, supports the engineering-based hypothesis that bedrock at intermediate depths is associated with lower marginal costs of height. Estimates of θ range from 0.1 at intermediate bedrock depths to 1.1 at very low and moderate to high depths. While imperfect, these results support the idea that cities with bedrock in an intermediate range will have a greater ease of accommodating high real

[9]To allow this setup to fit fully into the general equilibrium model in Section 4, we will impose that all lots are of the same size and developers' only choice is building height. To be consistent with the empirical work and exclude the possibility of selection on bedrock depth within cities for siting tall buildings, we assume that bedrock depth is the same at all locations in each city.

estate demand, resulting in lower barriers to growth. Details of this estimation procedure and results are in Appendix Section H.4.

As construction cost differs by bedrock depth, the profit maximizing level of height also differs by bedrock depth conditional on demand conditions. Competitive building developers have the following profit function associated with building to height $S(x)$ at location x in city ac at time t.

$$\pi_{act}(S, x) = \int_0^S p_{act}(x, s)ds - C_{act}(S) - r_{act}(x). \tag{2}$$

As developers are price takers, they treat the sales price per unit of real estate at location x and height s $p_{act}(x, s)$ as exogenous. $r_{act}(x)$ denotes the fixed cost component of development, which includes both the land price and any regulatory development costs at location x. In Section 4, we lay out a demand structure that justifies the separable form $p_{act}(x, s) = p_{act}(x)s^{\omega}$, where ω is positive and close to 0. (In particular, for the model to be well-behaved we need that $\theta > \omega$.) A positive ω reflects the amenity value associated with improved views and reduced noise.[10] Profit maximization yields the log of the optimal height S^* that depends on the price per unit of real estate services and cost factors.

$$\ln S^*(p_{act}(x), c_{act}, B_{ac}, \mu_t) = \frac{1}{\theta(B_{ac}, \mu_t) - \omega}\left(\ln \frac{p_{act}(x)}{c_{act}} - \ln\left[1 + \theta(B_{ac}, \mu_t)\right]\right) \tag{3}$$

This expression highlights the fact that the developer's choice of log height depends on the interaction between bedrock depth, as included in $\theta(B_{ac}, \mu_t)$, and the level of demand, as included in $p_{act}(x)$.

To understand how optimal heights differ across space within cities, it is convenient to impose some restrictions on the $p_{act}(x)$ function. Following the model developed further in Section 4, we impose that the price per floor area of real estate decays with CBD distance.

$$p_{act}(x) = p^0_{act} f(x; \rho_{ac}) \tag{4}$$

Each city a in country c at time t faces its own real estate demand conditions, leading us to index CBD rents by this triplet. Each city also has its own transport network driving accessibility to the center, leading us to index the advantages of being near the center by city, where $f'(x; \rho_{ac}) < 0$ and ρ_{ac} governs the city-specific accessibility advantages to the center.

Equation (3) lays out the logic behind our triple difference empirical strategy as implemented with IV. First, compare two cities in 2015 at a given CBD distance x that are identical in all ways, including the same favorable bedrock depth of 15 meters, except for their CBD rents p^0_{act}. The difference in $\ln p^0_{act}$ between these two cities captures their difference in real estate or height demand. That is the first difference. Second, consider an analogous pair of cities with the same gap in $\ln p^0_{act}$ but with a less favorable bedrock depth of 0 meters. The form of the θ function documented above indicates that these second two cities have a smaller gap in heights, as the

[10] Evidence for both commercial and residential buildings indicate that real estate prices and rents are typically higher on higher floors of tall buildings, reflecting the amenity value of height (Liu et al., 2018; Ben-Shahar and Hongjia, 2022; Nase and Barr, 2023).

elasticity of height with respect to price has an inverse-U shape in bedrock depth. This is the second difference, which can be derived by calculating $\frac{\partial^2 \ln S^*}{(\partial \ln p^0)(\partial B)}$. Finally, the secular decline in the cost of height over time manifests as a reduction in μ_t. This reduction has facilitated taller construction in high demand locations, *and particularly so in cities with favorable bedrock.* This is the third difference. Differentiating (3) with respect to $\ln p^0_{act}$ then B_{ac} then μ_t derives this result, given that $d\mu_t < 0$. In 1975, building tall was very costly everywhere. As the marginal cost of height declined for all cities, it is the locations with strong demand conditions *and* favorable bedrock depths that are predicted to increase their heights the most.[11]

We are now in a position to characterize aggregate city building heights as observed in the Emporis data. As real estate prices decline in CBD distance, each city has a unique endogenous distance cutoff within which buildings of over 55 meters exist in each year. (In some cities, this cutoff is 0.) Call this distance cutoff x^{55}_{act}. Then the total stock of heights in city a at time t is

$$H^{55}_{act} = \left(\frac{p^0_{act}}{c_{act}(1+\theta(B_{ac},\mu_t))} \right)^{\frac{1}{\theta(B_{ac},\mu_t)-\omega}} \int_0^{x^{55}_{act}} f(x;\rho_{ac})^{\frac{1}{\theta(B_{ac},\mu_t)-\omega}} \mathcal{L}_{ac}(x)dx \tag{5}$$

In this expression, $\mathcal{L}_{ac}(x)$ is a city-specific function that captures the amount of land that can be developed at each distance. For example, it is $2\pi x$ for a circular city. This equation shows that the aggregate height in a city depends on the same factors as the profit-maximizing level of height at each specific location. The integral covers the land in use for tall buildings.

The aggregate stock of heights follow the same triple difference pattern as location-specific building height in Equation (3). Following the comparative statics on $\ln S^*$ in Equation (3) for each location within x^{55}_{act} delivers an aggregate of the location-specific gaps, which must follow the same pattern. Cities with greater heights at all locations x must also have a greater aggregate stock of heights when adding up over the same range of x. In addition, any city with a greater height at any location x must also have a greater CBD distance cutoff x^{55}_{act} beyond which heights are below 55 meters, representing an additional force increasing the gap in aggregate heights.

2.5 Predicting City Level Height Growth

Evidence in the prior sub-section indicates that more height should be constructed in larger cities, and even more so in those with favorable bedrock depth. Moreover, this phenomenon should have strengthened over time. We demonstrate these patterns empirically by graphing estimated coefficients γ_b in the following descriptive regression.

$$Const_{ac} = \gamma_{b(ac)} \ln Pop_{ac75} + \delta \ln Pop_{ac75} + \kappa_c + \phi_{b(ac)} + \epsilon_{ac}$$

The dependent variable is 1975-2015 construction in city a of country c with binned mean bedrock depth $b(ac)$. Construction is measured either as whether the city had any tall buildings in 2015 but not 1975 or as the change in the log sum of heights in the city. Each city is placed in a 5 meter wide bedrock bin (0-4 m, 5-9 m, etc.) and there are separate country and bin fixed

[11] The isomorphism between gaps in unit costs, through negative differences in $\ln c_{act}$, and demand, through positive differences in $\ln p^0_{act}$, is also evident in Equation (3).

effects. As the regression controls for ln city population, all γ_b coefficients are of the bin-specific impact of 1975 ln population on 1975-2015 construction relative to the population impact in the 0-4 meter bedrock depth bin.

γ_b coefficient estimates are graphed in Figure 5. Bubble sizes are proportional to the number of observations. Statistical significance (relative to 0) is indicated with stars. Quadratic and more flexible fractional polynomial lines of fit are also indicated.

Figure 5: Relationships Between Tall Buildings and ln 1975 Population by Bedrock Depth

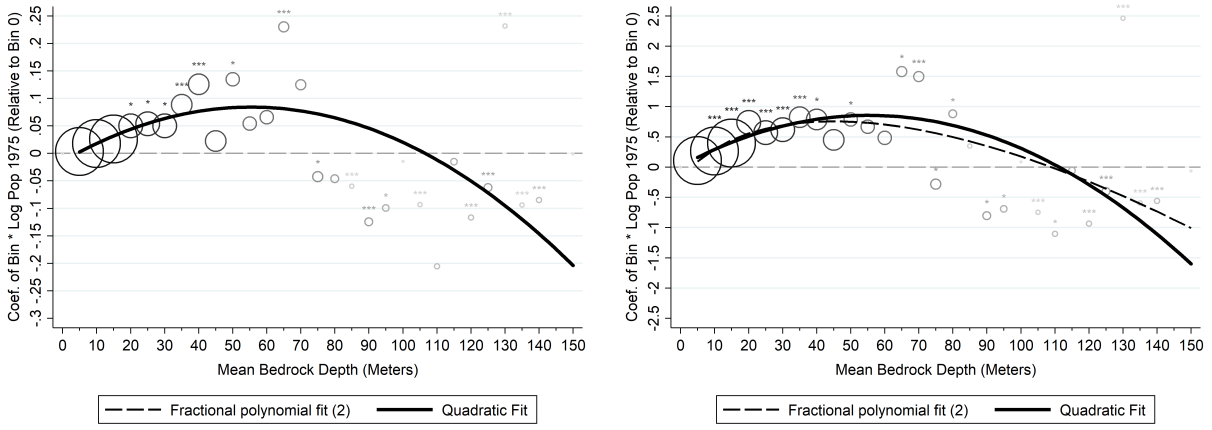

(a) Any Tall Building Construction

(b) Δln(Heights+1)

Notes: The left panel graphs coefficients on ln 1975 city population for each 5 meter bin of bedrock depth in which the dependent variable is an indicator for whether the city had any height growth. The right panel graphs analogous coefficients in which the dependent variable is the ln sum of heights constructed 1975-2015 plus one. Similar graphs with dependent variables measured as levels in 1975 are much flatter in bedrock depth than counterparts using 2015 levels.

Figure 5 shows the inverse U shaped impact of city mean bedrock depth on construction in strong relative to weak demand cities. In particular, the probability of having new tall building construction in response to a doubling of population is about 0.1 higher at a bedrock depth of 30-34 than at 0-4. Similarly, the elasticity of height growth with respect to 1975 population is about 0.65 greater for cities in the intermediate range of bedrock than the low or high ranges. As the quadratic fit (solid line) is similar to the more flexible fractional polynomial fit (dashed line), most of the empirical work uses a quadratic parameterization. We note that as 90% of cities are in the range of bedrock between 0 and 30, the upward-sloping portion of the population elasticities in bedrock depth seen in Figure 5 provides most of the identifying variation. The supply model predicts that the pattern seen in Figure 5 should be strongest in 2015 and muted in 1975. This is exactly what we see, as shown in Figure A6.

Put together, the first stage estimation equation takes the following form.

$$\begin{aligned} Const_{ac} = k_1 MBD_{ac} + k_2 MBD_{ac}^2 + \delta \ln Pop_{ac75} \\ +\gamma_1 MBD_{ac} \times \ln Pop_{ac75} + \gamma_2 MBD_{ac}^2 \times \ln Pop_{ac75} + \\ +X_{ac75}\xi + \kappa_c + \epsilon_{ac} \end{aligned} \tag{6}$$

The key components of this equation are the interactions with coefficients γ_1 and γ_2. These

indicate how the elasticity of construction with respect to population differs by bedrock depth. In (6), the dependent variable can be measured in levels or as 1975-2015 growth.[12]

Table 1 presents the first stage coefficients on city mean bedrock depth interacted with ln 1975 city population. Panel A is for cities in all countries and Panel B is for cities in developing economies only. The first two columns show results for an indicator of whether any tall buildings were constructed by the indicated year. The third column shows the difference. The next two columns are analogous except ln total tall building height plus one in each year is the dependent variable. The final column shows results for the 1975-2015 change. Table A4 reports remaining first stage coefficients.

Table 1: First-Stage Estimates

	Tall Building Indicator			ln (Heights + 1)		
	1975	2015	Δ 1975-2015	1975	2015	Δ 1975-2015
	(1)	(2)	(3)	(4)	(5)	(6)
			Panel A: All Countries			
Bedrock Depth	0.0018***	0.0046***	0.0028***	0.0126***	0.0402***	0.0276***
× ln Pop 1975	[0.0005]	[0.0007]	[0.0007]	[0.0032]	[0.0062]	[0.0054]
(Bedrock Depth)^2	-0.0000***	-0.0000***	-0.0000**	-0.0002***	-0.0003***	-0.0002**
× ln Pop 1975	[0.0000]	[0.0000]	[0.0000]	[0.0000]	[0.0001]	[0.0001]
R-Squared	0.14	0.24	0.08	0.18	0.33	0.18
			Panel B: Developing Economies			
Bedrock Depth	0.0004	0.0036***	0.0032***	0.0030	0.0292***	0.0262***
× ln Pop 1975	[0.0005]	[0.0007]	[0.0007]	[0.0028]	[0.0060]	[0.0056]
(Bedrock Depth)^2	-0.0000	-0.0000***	-0.0000**	-0.0000*	-0.0002**	-0.0002**
× ln Pop 1975	[0.0000]	[0.0000]	[0.0000]	[0.0000]	[0.0001]	[0.0001]
R-squared	0.13	0.24	0.13	0.14	0.29	0.22

Notes: Each column is a separate regression of the indicated variable at top on the variables indicated on the left, a quadratic in mean city bedrock depth, log 1975 city population, and country fixed effects. Regressions in Panel A have 12,849 observations and those in Panel B have 11,257 observations. Remaining coefficients are reported in Table A4.

Evident in Table 1 is that coefficients on the interaction between mean bedrock depth and population (γ_1 and γ_2) grow in magnitude over time for both outcomes. Analogous results for 1990 and 2000 reveal that this growth is monotonic in year (not reported). Also of note is that γ_1 and γ_2 are estimated to be approximately 0 in 1975 in developing economies. These locations had very little height in 1975 regardless of bedrock conditions or population. Therefore, for developing country cities, to a first approximation one can view our analysis as using the 2015 level of tall building height as the key measure of the 1975-2015 change in heights.

Before discussing the main results, we consider the implications of these first stage results for identification of causal impacts of heights on urban structure. The main idea for identification is

[12]We also considered earthquake risk and exposure to Hong Kong as alternative sources of identifying variation in city heights. Both of these alternative potential instruments are also cost shifters. However, identification checks reveal them to provide less broad-based identifying variation than does bedrock depth, causing both of these alternatives to identify treatment effects that are more local. Estimates using these alternative instruments follow the same patterns as those presented in this section.

that bedrock depth is a supply factor that is uncorrelated with factors driving demand for height at the city level. However, in order to operationalize this idea, it turns out to be important to interact bedrock depth with a measure of static demand strength, for which we use ln 1975 city population. Bedrock depth by itself is not a strong enough source of identifying variation to generate first stage predictions of height or height growth that are sufficiently powered to be useful in determining causal effects of heights.

Given the need to use interactions as the source of identifying variation, the key identification assumption is more subtle than simply that bedrock is exogenous to city demand shocks. Instead, the identifying assumption is that historically larger cities on more favorable bedrock did not change in different ways from historically larger cities on less favorable bedrock relative to historically smaller cities on favorable relative to unfavorable bedrock. This double difference over time (making a triple difference) is the key argument needed for identification.

As such, any threats to identification would come from correlations between bedrock and latent city demand growth that was different for large and small cities. This would occur if bedrock depths more favorable for tall building construction also somehow allowed large cities to have greater post-1975 growth potential. Our empirical analysis in the following section examines the potential for such omitted variable bias to exist.

3 Empirical analysis

For 12,877 agglomerations a in 182 countries c, long difference regressions of the form in (7) make up the heart of our empirical analysis. Our primary dependent variables of interest y_{ac} are the 1975-2015 growth rates of population or built up area in agglomeration a of country c.[13] Controls for a quadratic in mean city bedrock depth, log 1975 city population, and country fixed effects are included.

$$y_{ac} = \beta \Delta \ln \left(Heights_{ac} + 1 \right) + \alpha_1 MBD_{ac} + \alpha_2 MBD_{ac}^2 + \alpha_3 \ln Pop_{ac75} + \kappa_c + \varepsilon_{ac} \tag{7}$$

We primarily examine IV versions of this estimation equation, in which log population in 1975 interacted with a quadratic in city mean bedrock depth enters as instruments for $\Delta \ln \left(Heights_{ac} + 1 \right)$.

As is formalized in the model in the following section, one can view (7) as capturing differences in the quantities of real estate demanded for cities with exogenously different amounts of heights. One central parameter that influences these responses is the elasticity of population with respect to urban utility (ζ). In a closed city, in which ζ is 0, the real estate supply shock from the lower cost of height manifests as lower floorspace rents and shorter commutes, a clear welfare gain for city residents that manifests as a much more compact city. Empirically, this scenario maps to a large negative built area elasticity and a zero population elasticity, both with respect to city heights. As ζ grows, in-migration responds more, thereby bidding up rents and lengthening

[13] An alternative option is to specify (7) as a regression of an outcome measured in 2015 on 2015 heights and indicated controls plus the dependent variable in 1975. Because the sum of heights in 1975 is near 0 in the vast majority of cities in our sample, this alternative specification yields very similar results.

commute times. The result is smaller welfare gains for city residents but more opportunity for outsiders to benefit from the city's improved infrastructure. Empirically, this means larger positive population responses and smaller magnitude negative built area responses.

The inclusion of the mean bedrock depth controls in (7) is not necessary for identification but does make identification stronger. Without these controls, we would be relying on their exclusion from the demand equation for heights for identification. While we think it reasonable that bedrock depth is not a demand factor, bedrock depth on its own does not provide much identifying variation in heights. Instead, we need to interact bedrock depth with a level demand factor, for which we use 1975 ln city population, in order to predict supply shocks to heights with sufficient power. For this reason, we leave in the bedrock depth controls in (7). However, excluding them does not affect any of our results.

We note that OLS estimates of β in (7) are muted relative to IV estimates at 0.05 for the population outcome and -0.09 for the built area outcome. As standard threats to identification would typically bias both OLS coefficients in the same direction, we conclude that these smaller magnitudes primarily reflect measurement error in heights. If demand factors were a central driver of city growth in heights, conditional on controls, the OLS population and built area elasticities would both be biased upwards. IV estimates that correct this endogeneity problem would thus be smaller (or more negative) than corresponding OLS estimates for both outcomes. Instead, measurement error, which seems sensible, would lead to attenuation bias. By only using buildings over 55 meters tall to measure heights, we do not measure all buildings that are relevant to real estate supply. There are many idiosyncracies in how much tall building occurs that disconnects it from fundamental supply and demand forces. On the taller side, this includes prestige skyscrapers that are not by themselves economically viable. On the shorter side, local zoning regulations may lead to considerable construction up to a cap that is high but below 55 meters in some cities. By isolating common supply factors for identification, we smooth out these idiosyncracies, thereby increasing the magnitudes of estimated coefficients.

3.1 Main IV Results

Table 2 presents our headline empirical results. Panel A shows results for all cities and Panel B shows results for cities in developing economies only. The first column shows that a 100 log point increase in heights leads to about a 12 percent increase in city population. This magnitude of height increase is the average for cities in the top tercile of 1975 population, while the average city had 1975-2015 height growth of 46 log points. The second column of Table 2 shows that a 100 log point increase in heights caused the built-up land area of a city to decline by about 17 percent. This is very similar to the 15 percent response for total city area. Putting the results in Columns 1 and 3 together, it is clear that exogenous height growth has substantially increased population density. When population density is explicitly put on the left hand side of the regression, the estimated heights coefficient is 0.27, matching the population coefficient in column 1 minus the area coefficient in column 3.

The final column of Table 2 shows results for the growth rate in lights at night 1990-2015, a

Table 2: Main IV Results

Period s-t:	Δ ln Pop 1975-2015	Δ ln Built Area 1975-2015	Δ ln Urban. Area 1975-2015	Δ ln Pop Dens. 1975-2015	Δ ln Lights 1990-2015
			Panel A: All Countries		
Δ ln(Heights+1)	0.12***	-0.17***	-0.15**	0.27***	0.15***
	[0.03]	[0.04]	[0.06]	[0.07]	[0.06]
			Panel B: Developing Economies		
Δ ln(Heights+1)	0.13***	-0.16***	-0.18**	0.31***	0.17***
	[0.03]	[0.04]	[0.08]	[0.08]	[0.06]

Notes: Each entry is from a separate regression of the indicated variable at top using the full sample in Panel A and cities in developing economies only in Panel B. Equation (7) shows the regression specification used. Δln(Heights+1) is instrumented with an interaction between bedrock depth and ln Pop 1975. See Table 1 for first stage results. The first stage F statistic is 28.42 for all regressions in Panel A and 22.84 for all regressions in Panel B. Table A5 reports coefficients on control variables for Panel A.

measure of total city economic growth due to heights. This is not significantly different from the population growth result in the first column. We note that lights per capita is also estimated to positively respond to heights, with an elasticity of 0.04 (or 0.06 for developing economies), but is not statistically significant (unreported).[14] Results for developing economies, representing 87% of the cities in our data, are very similar to those for the full sample.

These results are robust to a number of specification checks. One potential concern is that trends in the amenity value of cities, or other demand factors, may be differentially correlated with bedrock depth in large versus small cities. However, inclusion of additional controls for infrastructure and regional connectedness, including subways, roads, and measures of market access, do not affect results. Controls for location and topography (natural amenities) also do not affect results. Cities with shallow bedrock may find it more costly to expand their infrastructure. As such, another way we evaluate the potential importance of infrastructure is to verify that results hold excluding cities on bedrock up to 6 meters deep (the 25th percentile of the bedrock depth distribution) from the sample. Finally, using 100 meters rather than 55 meters as the height cutoff to define tall buildings also has no affect on results. Table A7 presents all of these results for the full sample and cities in developing economies only.[15]

As country fixed effects are included, variation across cities within countries with more variation in city size interacted with bedrock depth identifies IV coefficients of interest. In contrast, within-country variation in heights for all countries identifies corresponding OLS coefficients. While almost all countries have cities of many different populations represented, only larger countries tend to have much variation in bedrock depth. Indeed, Table A8 shows that the IV population elasticity estimates are almost identical for the 7,473 cities in countries

[14] Estimated population and built area elasticities are 0.11 and -0.24 respectively using 1990 as the base year. Those using 1975 levels rather than 1975-2015 changes are 0.09 and -0.11, respectively. (Table A6).

[15] We also verify that estimates are robust to controlling for distance to mines and/or oil and gas fields, or excluding cities within 50 km of either from the estimation sample. While access to natural resources may also influence construction costs, we undertake these checks with the idea that cities with natural resource oriented economies may have different trends in demand than other cities.

with the greatest variation in bedrock depth (Gini index above 0.75) and at least 6 cities; built area elasticities using this sample are a bit more muted at -0.13 rather than -0.17. OLS estimates of population elasticities draw closer to IV estimates in the high Gini index sub-sample relative to the full estimation sample, such that the two are no longer significantly different. This is evidence that our IV estimates reflect local average treatment effects within high bedrock variation countries and that there is relevant measurement error in heights. Estimated built area elasticities exhibit similar patterns but with larger remaining IV-OLS gaps in the high Gini index sub-sample.

Finally, we provide evidence that our estimated elasticities primarily capture migration of people from rural areas to cities rather than displacement between cities. Borusyak et al. (2022) demonstrates the econometric challenges associated with endogenous migration flows between regions in the empirical setting in which local outcomes are regressed on exogenous region-specific shocks for the universe of regions in a country. As our data does not include rural units, our analysis is not subject to these biases provided that city growth in response to exogenously assigned heights draw only from the rural hinterland rather than from other cities.

We carry out three types of exercises to evaluate the prevalence of displacement in our data. First, we explore robustness to different levels of regional and sub-national fixed effects. As migration occurs at higher rates more locally, we expect there to be greater displacement between cities for fixed effects covering smaller regions. If coefficient estimates do not grow with the use of more local fixed effects, that is evidence that our estimated elasticities reflect rural-urban migration. Second, we explore robustness to a sub-sample that only includes countries with urbanization rates below 20% in 1975, in which the vast majority of migrants to cities must have come from rural areas. Finally, in the spirit of the fix proposed in Borusyak et al. (2022), we control for the accessibility to heights in alternative cities that are likely to be viewed by migrants as substitutes.[16]

Table A9 shows the results of the first two exercises. IV estimates for population grow by at most 0.03 when including finer fixed effects and decline by 0.02-0.03 when using sub-region rather than country fixed effects. None of these differences are statistically different from our headline population elasticity estimate of 0.13 for developing economies. The final column of Table A9 shows results for the sample restricted to countries that were less than 20% urban in 1975. The population elasticity estimated for this sample remains stable at 0.13. Built area elasticities are somewhat more sensitive to the inclusion of various levels of fixed effects and sample. These estimates grow in magnitude to as much as -0.25 with alternative fixed effects. However, the estimated area elasticity shrinks to -0.08 for the sub-sample of rural countries, with a large standard error of 0.05. Once again, none of these estimates are statistically different from our primary built area elasticity estimate of -0.16 for developing economies.

For the third exercise, we calculate market potential (MP) terms that summarize accessibility of each city ac to other population centers and heights. We calculate the MP for heights for city

[16]Fully carrying out the proposed fix in Borusyak et al. (2022) requires observing migration flows in a base period; unfortunately, this is information we do not have for most countries in our data.

a in country c and year t as

$$MP^H_{act} = \sum_{a' \in C(a), \neq a} \frac{Heights_{a'ct} Pop_{a'c75}}{dis(a,a')^\alpha}. \tag{8}$$

That is, we sum heights times population in all other cities in the country of city a, discounting by the distance between city a and a' raised to the power α, which we vary between $\frac{1}{3}$ and 3. From these measures in 1975 and 2015, we build $\Delta \ln MP^H_{act}$ to include as a control variable in regressions.

As heights in other cities may be endogenous to trends in demand factors in city ac, we build an instrument for $\Delta \ln MP^H_{act}$ that follows the same logic as our instruments used in the main analysis. In particular, we build instruments by replacing $Heights_{a'c75}$ in (8) with $Pop_{a'c75} MBD_{a'c}$ or $Pop_{a'c75} MBD^2_{a'c}$. Then, analogous to our main estimation equation (7), we also control for three additional terms capturing the discounted sums of 1975 city populations and bedrock depths by replacing $Heights_{ac75}$ in (8) with Pop_{ac75}, MBD_{ac}, or MBD^2_{ac} and taking logs.

Table A10 shows the results with these market potential controls. The big message is that we find no evidence that displacement effects between cities in our sample are driving elasticity estimates. We show OLS results for $\alpha = 0.33, \alpha = 0.5$ and $\alpha = 1$, and IV results for $\alpha = 2$ and $\alpha = 3$. As bedrock depth tends to be highly spatially correlated, we need strong spatial decay in order for instruments to be able to separate out height growth in other cities from that in city ac. But whether instrumenting for $\Delta \ln MP^H$ or not, estimated population and built area elasticities remain very stable. We come to the same conclusion when only including the largest 5 cities in the country in MP terms or when controlling separately for height growth in each of these cities (unreported). The coefficient on the height market potential control is 0 or positive when instrumented, which may reflect a growth effect of improved access to markets. The lack of movement in our main elasticity estimates of interest indicates that MP terms are conditionally uncorrelated with our instruments for height growth in city ac.

3.2 Heterogeneity in Estimates

Table 3 shows heterogeneity of our main IV estimates by region of the world. The first column presents population and built area growth coefficients for all developing economy cities in Asia except the Middle East of 0.17 and -0.20, respectively. Remaining cities in the developing world generate similar estimates of 0.15 for population and -0.26 for built area, though these are slightly underpowered with a first stage F-statistic of 7.9. Because most of our data is for the developing world, and the population and land use pressures are greatest in these countries, we focus most of our policy analysis on this sample. No developing economy region other than Asia has enough observations to generate strong first stage identification.

The third column in Table 3 presents results for cities in developing economies that we infer to have relatively lax building restrictions. We defer the discussion of these results to Section 3.4 below.

Table 3: IV Results by World Region

	Developing Economies			Developed Economies		
	Asia x MENA	Others	Unconstrained	Total	USA+Can	Others
			Panel A: Δ ln Pop			
Δ ln(Heights+1)	0.17***	0.15**	0.22***	-0.02	0.30**	0.01
	[0.03]	[0.07]	[0.05]	[0.03]	[0.12]	[0.02]
			Panel B: Δ ln Built Area			
Δ ln(Heights+1)	-0.20***	-0.26***	-0.38***	-0.04	-0.67*	-0.04
	[0.04]	[0.09]	[0.09]	[0.03]	[0.35]	[0.03]
First Stage F	20.92	7.881	11.88	14.28	5.771	13.64
Observations	6,990	4,267	5,557	1,592	372	1,268

Notes: Each entry is from a separate IV regression using data from cities in world regions indicated in column headers over the indicated time period. "Asia x ME" refers to countries in Asia except the Middle East. "Unconstrained" refers to countries with no history of communism and with below median regulatory environments. Section 3.4 explains in more detail how this sample is selected.

Estimates in the right block of Table 3 are for cities in developed economies. These are subject to more complicated interpretation, as the majority of large cities in developed economies had significant heights in 1975. Moreover, these countries had largely completed their transitions from rural to urban by 1975. While we find no overall average impact of heights on city structure in developed economies for the 1975-2015 period, estimated coefficients are quite large in magnitude, though under-powered, for cities in the USA and Canada. This pattern fits with the idea that land use and building height restrictions are relatively lax in North America and severe in Europe, which contributes most of the observations to the other developed economies sample. However, we caution that the estimates for North America are more likely to in part reflect displacement between cities rather than rural-urban migration. Cities in Eastern Europe are a major driver of the 0 results for developed economies, which is consistent with their mostly centrally planned histories.

To further understand why estimates differ for developing and developed economies, we look back in time to the 1850-1975 period for cities in Europe and West Asia and 1920-1975 for cities in the US. These are periods of development that better match the sorts of changes experienced in developing economies during the 1975-2015 period, including structural change out of agriculture and rapid urbanization. Moreover, no tall buildings existed in Europe in 1850 and few existed in the USA in 1920. For Europe, we use data from Bairoch (1988), which has city populations until 1850. For the US, we use decennial census data. We start in 1920 in the USA, predating the roaring 20's construction boom, so that variation in initial city size is large enough to generate some first stage identifying power.

As we do not have city footprints in 1850 or 1920, we focus on estimating population elasticities. The associated regression specifications are the same as above except for the different base years. For these earlier periods, we estimate separate population elasticities for 1,095 cities in Europe and West Asia and 324 cities in the USA that are both 0.21 (SEs of 0.10

and 0.17, respectively). Both are a bit underpowered with first stage F-statistics of 5.4 and 4.1, respectively. However, they are robust to a number of specification checks and sample restrictions.[17] The big message is that the 0 estimate for developing economies only applies to the modern era; we find population elasticities that are in line with those for the developing world in the period of European and American development.

Next, we examine the distinction between impacts of commercial versus residential heights. While we can observe building use in the Emporis data, we do not have separate instruments for these two types of buildings. Instead, we make use of the fact that country-specific industrial structure and land use planning regimes influence the extent to which tall buildings host residential or commercial tenants. Service-oriented economies tend to have a higher share of tall buildings in commercial. Higher income economies with fewer restrictions on urban sprawl also tend to have a higher share commercial. For example, the US fits both criteria. In the developing world, Egypt and Pakistan also have about 50% of their tall buildings dedicated to commercial uses. In contrast, countries with land constraints and fewer office workers tend to have a higher share of tall buildings in residential use. Example countrie include Brazil, India, and South Korea. Because the residential share of tall buildings is in part driven by such country-specific factors (and we have country fixed effects), we can learn about impacts of the construction of residential versus commercial heights by restricting the sample to only include cities in countries with at least some baseline share of tall buildings in residential use. We do this recognizing that various sources of unobserved heterogeneity between countries are interacting with height growth to generate these effects.

Figure 6 shows estimates by country residential share of tall buildings. The top portion shows the positive estimated population height elasticities and the bottom portion shows the built area height elasticities. Red lines use subsets of cities in the developing world and blue lines use subsets of cities worldwide. Moving from left to right, the sample becomes more constrained to only include cities in countries with at least the residential share of tall buildings indicated on the horizontal axis.

The results in Figure 6 are striking. Cities in countries that built more residential heights accommodated more population and saved more land, especially in the developing world. Population elasticities rise from 0.13 to 0.21 when using close to the full developing world sample (countries with at least 50% of tall buildings residential) to just those countries with at least 90% residential. The residential impact is even greater for built area. Built area elasticities monotonically decline from -0.13 to -0.50, with more than half of this decline driven by the progressive exclusion of countries with 70-75% tall buildings in residential.

The broad implication of evidence in Figure 6 is that the type of tall buildings matters. As residential real estate is much more space intensive than offices per-capita, it is not surprising that residential buildings have bigger effects than commercial buildings. The model developed in the following section is parameterized to respect this observation.

[17] For the USA, we can get the first stage F up to 7.7 by excluding Las Vegas and controlling for 1920 city heights, with no effect on the elasticity estimate.

Figure 6: Effects of Heights by Country Tall Building Residential Share

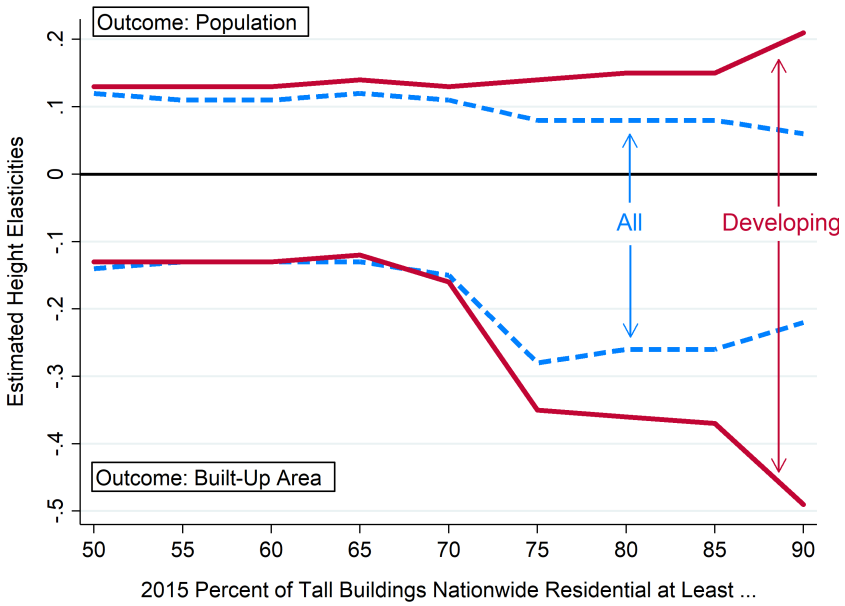

Notes: This figure shows four sets of estimated coefficients on the change in log heights in IV regressions of the form in (7). The top portion of the graph indicates coefficients for which the 1975-2015 change in log population is the outcome. The outcome in the bottom half of the graph is 1975-2015 change in log city built area. Moving from left to right, the sample becomes increasingly constrained to include only countries with at least the fraction of tall buildings nationwide in residential use indicated on the horizontal axis. Red lines are coefficients for cities in the developing world only. Blue lines include all cities with at least the indicated residential share.

3.3 Aggregate Impacts of Height

Here we provide an accounting of the extent to which post-1975 expansions in building heights have accommodated city population and land savings. With the rapid rate of urbanization occurring in many developing economies, cities are facing historic population pressures. Moreover, the land surrounding the largest cities in most countries is among the most productive land for (Henderson et al., 2018). How well has the tall building construction that has occurred since 1975 mitigated these pressures in aggregate?

To carry out these aggregation calculations, we refine our main height elasticity estimates in Tables 2 and 3 by focusing on heterogeneity by city population. For separate samples of Asian cities outside the Middle East and other cities in the developing world, we estimate instrumental variables locally weighted regressions (IV-LWR) by city population. This process is the same as standard IV estimation of (7), but with a separate coefficient on the change in heights estimated for each observation in the data set. These estimates are calculated using a separate weighted IV regression for each observation, with greater weights assigned to observations that are closer in 1975 city ln population. See Appendix I.2 for further details.

Figure 7 shows the results for city population growth as an outcome. Evident in this figure is the non-monotonicity in height effects by city population, with the largest causal effects of heights for the smallest and largest cities. For Asian cities, the population elasticity of height is about 0.3 for cities of 50,000 residents in 1975, falling to 0.11 at a population of 1 million and then rising to 0.16 for the very large cities (right axis). For other cities in the developing world,

estimates follow the same pattern and are slightly larger but are also less precisely estimated. We calculate analogous estimates for the built area outcome. For both regions, these hover around -0.20, do not vary much by 1975 city population, and are less precisely estimated than the population responses. First stage F-statistics (left axis) are shown in shaded pink and are strong for all city sizes in the Asian sample but only for small cities in other areas. Plots of estimated local height elasticities for the entire sample and all developing world cities are in Figures A7 and A8.

Figure 7: IV-Locally Weight Regression Population Estimates: Developing World

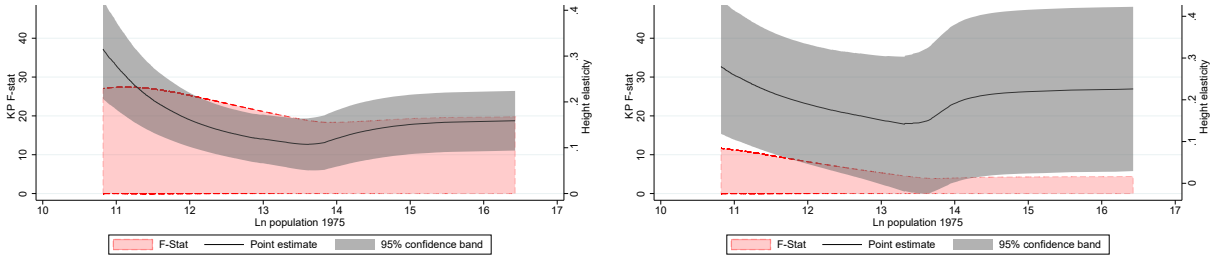

(a) Asian Cities

(b) Other developing cities

Notes: Figures show non-parametric estimates of height elasticities estimated with an LWR-IV approach. In each LWR, we estimate the height elasticity from a regression of the 1975-2015 long-difference in log city population against the long-difference in log building height using a second-order polynomial of bedrock depth interacted with initial 1975 log population as instrumental variables. Controls are a second-order polynomial of bedrock depth, initial log population, and country fixed effects. We use a Gaussian kernel with a locally varying bandwidth that is inversely related to the density of observations. Confidence bands are at the 95% level.

Armed with these estimated elasticities, we obtain the predicted city-specific absolute change in population and built area $\widehat{\Delta y_{ac}}$ caused by the actual change in height observed in the data, $\Delta H_{ac75-15}$. We begin with values of the outcome in the initial period y_{ac75} and apply estimated causal height elasticity parameters $\widehat{\beta^a}$ for city a. The following expression shows how we calculate the resulting city-specific change in the outcome predicted by our city-specific regression estimates and 1975-2015 growth in heights.

$$\widehat{\Delta y_{ac}} = y_{ac75} \times \left(\exp\left(\widehat{\beta^a} \times \Delta \ln \left(Heights_{ac} + 1 \right) \right) - 1 \right) \tag{9}$$

This procedure takes the observed height growth as exogenous. Therefore, it only allows us to calculate the 1975-2015 population growth or built area savings that occurred had all of the heights constructed during this time period been assigned in a way that is uncorrelated with covariates or the error term in (7). If that is not the case, this calculation likely somewhat overstates the growth in population and decline in built area that can be attributed to tall building construction.

Table 4 show the results of this exercise by six indicated 1975 city population categories, with cutoffs set on a logarithmic scale. First, note that in Asia there were only 108 cities in the top three size categories of cities over 1.2 million people, out of 7,464 cities total. However, these cities constructed 85% of the heights over the 1975-2015 period. Elsewhere in the developing

world, these top cities built two-thirds of the heights during this period. Indeed, city population is a good predictor for height growth.

Table 4: Aggregate Effects of 1975-2015 Tall Building Construction

City Pop. (2015)	Number of Cities	1975-2015 Δ Height (km)	Share of Height Δ	% of Pop Accomm	% of Area Saved	% Tree Cover	% Other Veg	Other Nonveg
Panel A: Asian Cities, except Middle East								
< 162,755	5837	73	0.03	1	1	8	73	19
to 442,413	1282	96	0.03	6	6	10	72	14
to 1,202,604	237	233	0.08	18	15	6	72	22
to 3,269,017	87	865	0.30	75	32	11	76	13
to 8,886,111	16	1,119	0.39	66	39	11	73	15
> 8,886,111	5	471	0.16	59	38	10	77	13
All	7,464	2,855	_	23	17	10	75	15
Panel B: Cities in Other Developing Regions								
< 162,755	3559	39	0.03	2	5	14	78	8
to 442,413	379	138	0.12	16	15	15	75	10
to 1,202,604	90	210	0.18	32	33	18	68	14
to 3,269,017	31	292	0.26	58	35	11	67	22
to 8,886,111	5	55	0.05	39	37	21	58	21
> 8,886,111	3	407	0.36	42	39	18	66	16
All	4,067	1,141	_	18	21	16	68	16

Notes: Estimates in each panel are based on separate sets of locally weighted regressions of Δ ln Pop or Δ ln built area on the change in log heights. Estimated elasticities for each city are applied to the 1975-2015 height growth in each city to determine the associated predicted city-specific population accommodated and built area saved.

Given that the largest cities built the lion's share of new tall buildings, it is natural that the main impacts are concentrated in these types of cities. In particular, for the smallest Asian cities, only 1 percent of 2015 population is accommodated in tall buildings constructed 1975-2015, saving 1 percent of the built area. These percent impacts increase monotonically to 75 percent and 32 percent, respectively, for cities between 1.2 and 3.3 million in 1975 population. These substantial effects mainly come from the fact that these cities built so many tall buildings during this time period, though treatment effects for the largest cities are also a bit greater. Above 1.2 million, the impacts flatten out some near these high levels, in which tall building construction accommodates about 70 percent of population and saves 35 percent of built area in Asian cities. Outside of Asia, the patterns of effects are similar though a bit muted, as the largest non-Asian developing country cities built fewer tall buildings than those in Asia.

One big message from Table 4 is that the technological changes that facilitated the construction of tall buildings has fundamentally altered the largest cities in the world. It has allowed them to accommodate a large fraction of their 2015 populations (over half in Asian cities in 2015) and allowed their built up footprints to be smaller by up to 39 percent.

The final three columns of Table 4 provide an accounting of the types of land saved through tall building construction. For each city with 1975-2015 height growth, we calculate the city's land savings. We then generate a buffer around the city boundary to match the area of land

saved and aggregate the various land uses. This exercise shows that about 10% of saved land around Asian cities is tree canopy and 75% is non-tree vegetation, with slightly larger shares around the larger cities. In other regions, even more tree canopy is saved at up to 20%, though less land of other types is saved. Both in Asia and elsewhere in the developing world, tall buildings have saved land that is at least 80% covered in some sort of vegetation.

While tall buildings has saved peripheral land around cities from urbanization, they have also caused urbanized regions to become less green. In particular, we show that the construction of tall buildings has crowded out agriculturally suitable land, tree canopy and cropland within 2015 urbanized regions. To quantify these responses, we run regressions similar to those in Table 2 but with changes in various measures of land as dependent variables. Table 5 presents these results. Panel A shows results for all cities and Panel B shows results only for cities in developing economies.

Table 5: Land-Use Changes Inside 2015 Urbanized Boundaries

Time Period	1975-2015	(2)-(4) 1982 - 2015			(5)-(7) 2000 - 2015		
Weight	Agric Suit	None			None		
Dep. Var.: Δ Log ... Area	Built	Urbanized	Tree Cover	Short Veg.	Short Veg.	Cropland	Urban Veg.
	(1)	(2)	(3)	(4)	(5)	(6)	(7)
			Panel A: All Economies				
Avg Frac of Area, Base Year	0.56	0.17	0.09	0.72	0.73	0.18	0.55
Coeff. on Δ ln Height	-0.16***	0.16***	-0.22**	-0.02**	-0.07***	-0.07*	-0.06***
	[0.04]	[0.03]	[0.03]	[0.01]	[0.03]	[0.04]	[0.01]
Impact on Frac of Total	-0.090	0.027	-0.019	-0.014	-0.051	-0.013	-0.033
			Panel B: Developing Economies				
Avg Frac of Area, Base Year	0.57	0.18	0.08	0.72	0.73	0.25	0.48
Coeff. on Δ ln Height	-0.14***	0.21***	-0.24***	-0.02**	-0.08***	-0.05	-0.07***
	[0.04]	[0.03]	[0.04]	[0.01]	[0.03]	[0.04]	[0.02]
Impact on Frac of Total	-0.080	0.038	-0.019	-0.014	-0.058	-0.013	-0.034

Notes: Each column in each panel is associated with a separate IV regression of the growth rate in land with the use indicated at top on the change in log heights using the same specification as in table 2. In the first column, the regression is weighted by agricultural suitability of the built area in the city. Entries in top rows indicate the aggregate share of year 2015 urban land in the indicated use in the respective base year. The bottom row indicates the fraction of aggregate urban land area gained of each type indicated in column headers based on initial aggregate shares calculated across all cities in our data worldwide and regression coefficients.

The first column of Table 5 presents results from the same regression as in Table 2 column 2, except that observations are weighted by the fraction of city land that is suitable for agriculture. This object has an average of 0.56 across cities in our sample. The estimated coefficient of -0.16 is almost identical to that in Table 2, indicating that there is not much selection of tall buildings into cities that are suitable or unsuitable for agriculture.

Results in the following column indicates that heights promoted infill urbanization. An approximate doubling of heights increased urbanization of 2015 urban land from a base of 17%

by 16% for all cities and 21% for developing country cities betweeen 1982 and 2015. As these base year percentages are calculated aggregating across all cities in our data, these estimates imply that 2.7% of 2015 urban land area overall and 3.8% in developing country cities was urbanized due to 1982-2015 height growth.

Results in the following two columns show that an approximate doubling of heights reduced tree cover by 22 percent and short vegetation by 2 percent within urbanized areas, using data from 1982 and 2015. When multiplied by the initial fractions of 2015 definition agglomerations that were covered by tree canopy or vegetation, we see that 1.9% of urbanized land in 2015 was converted from tree cover and 1.4% of the urbanized land in 2015 was converted from short vegetation given an approximate doubling of heights 1975-2015. These impacts are approximately the same in all cities and developing country cities only.

Column (5) shows analogous results for short vegetation over the 2000-2015 period. For this period, we observe the amount of short vegetation that is cropland and urban vegetation. The total impact of doubling heights on short vegetation is larger at 5.1% of 2015 area lost for all cities and 5.8% lost for cities in developing economies. Column (6) shows a small negative effect of heights on cropland within urbanized areas, which accounts for about one-quarter of the short vegetation lost because of tall building construction since 2000. As seen in Column (7), most of the rest is accounted for by urban vegetation, which includes yards and parks. While tall buildings save land from urban development, they also remove a significant amount of urban vegetation in already developed areas.

3.4 Model-Relevant Estimates

The main objective of our empirical work has been to recover averages of population and built area elasticities with respect to building heights across all cities in the world and for various sub-samples. It is these averages that are most relevant for developing a retrospective understanding of how tall buildings have influenced for the sizes and shapes of cities. However, these averages surely mask many dimensions of underlying heterogeneity, including height limits and land use regulation.

The model developed in the following section describes an environment in which only fundamental supply and demand forces determine a city's equilibrium heights, population and area. There is no role in the model for height restrictions or land use regulation. As such, credible model quantification requires elasticity estimates for a sub-sample of cities that are unregulated. Moreover, an empirically grounded city level measure of regulatory restrictiveness will be useful in determining how large the welfare gains from full deregulation could be.

To identify the countries with the least restrictive regulations, we begin with a city-level regression using data from 2010, 2015 and 2020 of heights on various city level demand and supply factors including city and country population, GDP, and geographical constraints (bedrock depth, altitude, ruggedness, etc.). Coefficients from this regression are reported in Barr and Jedwab (2023). Aggregating the data at the country level, we select the 42 developing economies with population-weighted mean residuals above 0 as the least regulated countries. We only

include countries in the developing world with no history of communism.[18]

As expected, the elasticity estimates for this sample, reported in the third column of Table 3, are larger than our broader average estimates reported in Table 2. In particular, for this relatively unconstrained sample, we find a population elasticity of 0.22 and an area elasticity of -0.38, both of which are statistically significant.

4 Theoretical Analysis

This section develops a theory that facilitates conceptual and quantitative analysis of the role of tall buildings in shaping urban economic development. This version of the standard urban monocentric city model follows in the tradition of Muth (1969), while incorporating and expanding on the real estate development technology in Section 2.4. This "representative city" model is intended to be flexible enough to capture the key forces that link tall building construction to urban growth and change that are common to cities of many different shapes, sizes, and stages of development. The model is stylized but can also be applied quite generally to cities in our data. In Section 4.2, we quantify the model. This includes matching observed population and area elasticities. In Section 4.3, we use the quantified model to conduct counterfactuals that allow us to calculate the welfare effects associated with the adoption of the tall-buildings technology and the consequences of relaxing the inferred height restrictions for all cities in our data.

4.1 Model Setup

We expand on the standard urban model with endogenous heights (Duranton and Puga, 2015; Ahlfeldt and Barr, 2022) by allowing workers to have the discrete choice of entering the city, following Ahlfeldt et al. (2022)'s approach to modelling labour market entry. Thus, we obtain an *imperfectly* open city which nests the conventional closed-city and open-city model versions of the monocentric model as special cases. The model generates a positive and finite height elasticity of population and a negative and finite height elasticity of area through a floor space supply channel, as is observed in the data. These responses strike a balance between the 0 population and large negative area elasticity in a closed-city model (Alonso, 1964) and the large population and small positive area response in an open-city model (Ahlfeldt and Barr, 2022). We walk through each component of the model below.

Environment: We consider a circular city of endogenous radius. The city is embedded in a country of $\bar{N}$ workers, which also has a rural hinterland. $\mathcal{L}(x) = 2\ell\pi x$ units of land are available for development at each distance x from an exogenously located historic city center,

[18]This selected set of low regulation countries includes Brazil, Kenya, Panama, the Philippines, and Thailand. If we also include developed economies, which would include Germany, Israel, Spain, South Korea, Taiwan and the US, we get larger elasticity estimates. However, we are concerned that these may reflect displacement between cities in addition to urban growth.

where $\ell = [0, 1]$ is the fraction of land that is developable. The area beyond the endogenous city margin at $x = x_1$ is the rural hinterland.

Workers: All workers are ex-ante identical and choose to live inside or outside the city. The utility of worker ν is described by:

$$U(\nu) = \max_{o}[U^o \exp(a^o(\nu))], \tag{10}$$

where $o \in \{inside, outside\}$ and $a^o(\nu)$ is an idiosyncratic taste shock for living in location o. Workers living in the agricultural hinterland receive an exogenous subsistence utility $U^{o=outside} = \widetilde{U}^{1/\zeta}$. All workers choosing to live in the city enjoy the same endogenous utility $U^{o=inside} = \bar{U}$. The idiosyncratic shocks $a^o(\nu)$ are drawn from the same Gumbel distribution with distribution function

$$G(a^o(\nu)) = \exp[-\exp(-\zeta a^o(\nu) - \Gamma)]. \tag{11}$$

$\zeta > 0$ is the taste dispersion parameter and Γ is the Euler-Mascheroni constant, included so that the Gumbel shocks are mean 0.

Utility maximization delivers the urban population N as share μ of the country population $\bar{N}$.[19]

$$N = \mu\overline{N} = \frac{\overline{U}^{\zeta}}{\overline{U}^{\zeta} + \widetilde{U}}\overline{N} \tag{12}$$

The resulting elasticity of urban population with respect to urban utility (the migration elasticity) is $\zeta(1 - \mu)$, with $1 - \mu$ reflecting the stock of available rural residents at risk of moving to the city.

City utility depends on a local amenity, tradeable goods consumption g, and residential floor space f^R. Workers choices of residential locations, on floors s in buildings located at CBD distance x, all must deliver the same utility level $U(x, s) = \bar{U}$ in equilibrium. Utility is Cobb-Douglas with a floor space expenditure share of $0 < (1 - \alpha^R) < 1$. The amenity value of each location $A^R(x, s)$ depends on horizontal (x) and vertical (s) locations. Put together, we have

$$U(x, s) = A^R(x, s)\Big(\frac{g}{\alpha^R}\Big)^{\alpha^R}\Big(\frac{f^R(x, s)}{1 - \alpha^R}\Big)^{1-\alpha^R}. \tag{13}$$

The amenity decays with CBD distance and rises with height, taking the following form:

$$A^R(x, s) = \bar{a}^R e^{-(\tau^R \max(0, x - \underline{x}^R))} s^{\tilde{\omega}^R}$$

$\tilde{\omega}^R > 0$ is the height elasticity of the residential amenity, capturing benefits such as better views or less exposure to noise and pollution. $\tau^R > 0$ determines the rate at which utility declines in distance from the edge of a central recreational district located at $x = \underline{x}^R$, with $\bar{a}^R$ the amenity

[19] See Ahlfeldt et al. (2022) for a formal derivation. This is almost isomorphic to using Frechet random utility draws with dispersion parameter ζ, with the advantage that this formulation justifies cases in which $0 < \zeta < 1$.

within this district. $\tau^R > 0$ generates the centripetal force of rising residential demand nearer to the city center.[20] Workers face the budget constraint

$$y = p^R(x,s) f^R(x,s) + g,$$

in which the endogenous wage y can be spent on housing, with endogenous unit price $p^R(x,s)$, and the tradeable good.

Utility maximization and imposing $U(x,s) = \bar{U}$ yields the residential bid rent for location (x,s) of

$$p^R(x,s) = A^R(x,s)^{\frac{1}{1-\alpha^R}} y^{\frac{1}{1-\alpha^R}} \bar{U}^{-\frac{1}{1-\alpha^R}}. \tag{14}$$

Averaging across all floors of a building of height $S^R(x)$ at any location, x delivers the horizontal residential bid rent

$$\bar{p}^R(x) = \frac{1}{1+\omega^R} \left[\frac{\bar{a}^R y}{\bar{U}} e^{-(\tau^R \max(0, x - \underline{x}^R))}\right]^{\frac{1}{1-\alpha^R}} S^R(x)^{\omega^R}, \tag{15}$$

where $\omega^R = \frac{\tilde{\omega}^R}{1-\alpha^R}$ is the height elasticity of residential rent. This follows the form asserted in Section 2.4.

Firms: Atomistic perfectly competitive firms produce the tradeable good using labor l and commercial floor space f^C with the Cobb-Douglas production function

$$g(x,s) = A^C(x,s) \left(\frac{l}{\alpha^C}\right)^{\alpha^C} \left(\frac{f^C(x,s)}{1-\alpha^C}\right)^{1-\alpha^C}. \tag{16}$$

Productivity at each location is shifted by

$$A^C(x,s) = \bar{a}^C N^\beta e^{-(\tau^C \times \max(0, x - \underline{x}^C))} s^{\tilde{\omega}^C}.$$

$\tilde{\omega}^C > 0$ is the height elasticity of productivity, that captures benefits such as signaling and workplace amenity effects (Liu et al., 2018). The agglomeration elasticity of productivity $\beta > 0$ describes how productivity increases in city employment N (Combes and Gobillon, 2015). $\tau^C > 0$ determines the rate at which productivity declines in distance from the edge of a central urban core at $\underline{x}^C$ and with the $\bar{a}^C$ exogenous productivity within this core. One way to rationalize this setting is to assume that all workers have to meet within this center to exchange knowledge.[21]

Profit maximization and imposing zero profits delivers the commercial bid rent

$$p^C(x,s) = A^C(x,s)^{\frac{1}{1-\alpha^C}} y^{\frac{\alpha^C}{\alpha^C - 1}}.$$

Averaging across all floors of a building with height $S^C(x)$ at each location x delivers the

[20] By imposing a constant amenity within the central district, we avoid the peaking of bid-rents and profit-maximizing heights at unrealistically high levels in the city center.

[21] By flattening productivity within the core, we avoid the peaking of bid-rents and profit-maximizing heights at unrealistically high levels.

horizontal commercial bid rent

$$\bar{p}^C(x) = \frac{1}{1+\omega^C}[\bar{a}^C N^\beta e^{-(\tau^C \times \max(0, x-\underline{x}^C))}]^{\frac{1}{1-\alpha^C}} y^{\frac{\alpha^C}{\alpha^C-1}} S^C(x)^{\omega^C}, \tag{17}$$

where $\omega^C = \frac{\tilde{\omega}^C}{1-\alpha^C}$ is the height elasticity of commercial rent. This form resembles (15).

Developers and Land Use: We extend the representative developer's problem laid out in Section 2.4 to index by type of use, commercial (C) or residential (R). Using (15) for residents and (17) for firms, the use-specific profit-maximizing building height matches (3), indexing all parameters by use. We require $\theta^U > \omega^U$ and $p^U(x) > c^U(1+\theta^U)$ for the solution to be well-behaved.

The developer may be subject to a height limit $\bar{S}^U$ imposed by the planning system. Conditional on building type U, the developer's resulting choice of height is thus

$$\tilde{S}^U(x) = \min(S^{*U}(x), \bar{S}^U). \tag{18}$$

Inserting into (2) and imposing zero profits, we obtain the use-specific bid rent for land[22]

$$r^U(x) = a^U(x)(\tilde{S}^U)^{1+\omega^U} - c^U(\tilde{S}^U)^{1+\theta^U}. \tag{19}$$

If planning restrictions do not bind, this function is declining in CBD distance x, reflecting greater willingness to pay for accessibility to the center.

At each location x, land is allocated to the use highest bid-rent use, given residential and commercial bid-rents in (19) and agricultural bid-rent r^A. Under the restriction that the commercial rent gradient is steeper than the residential rent gradient, which is consistent with plausible parameter values, there is a distance x_0 at which commercial and residential land rents equate ($r^C(x_0) = r^R(x_0)$). At shorter distances, commercial developers outbid residential developers when competing for land; thus this x_0 defines the boundary of the central business district (CBD).[23] Similarly, there is a distance x_1 where residential and agricultural land rents intersect ($r^R(x_1) = r^A$) and the city ends.

Spatial equilibrium. For given values of the city-wide endogenous objects $\{y, N, U\}$, all location-specific endogenous variables are uniquely determined. We obtain floor space rents from (17) and (15), heights via from (18), and use-specific land rents from (19). Land use then goes to the highest bidder, pinning down x_0 and x_1.

Real estate markets clear, implying that all floor space supplied at distance x, $\mathcal{L}(x)S^U(x)$,

[22] $a^C(x) = \frac{1}{1+\omega^C}[\bar{a}^C N^\beta e^{-(\tau^C \times \max(0, x-\underline{x}^C))}]^{\frac{1}{1-\alpha^C}} y^{\frac{\alpha^C}{\alpha^C-1}}$ and $a^R(x) = \frac{1}{1+\omega^R}[\frac{\bar{a}^R y}{U} e^{-(\tau^R \max(0, x-\underline{x}^R))}]^{\frac{1}{1-\alpha^R}}$.

[23] In our quantification, two parameter restrictions together ensure a commercial center surrounded by a residential area: The housing share in production is smaller than the housing share in consumption and $\tau^C > \tau^R$.

is input into either consumption or production:

$$\begin{aligned} F^C(x) &= \mathcal{L}(x)S^C(x), x \in [0, x_0] \\ F^R(x) &= \mathcal{L}(x)S^R(x), x \in (x_0, x_1), \end{aligned} \tag{20}$$

where $F^C(x)$ is the total input of floor space of all firms at x and $F^R(x) = \bar{f}^R(x)n(x)$ is total floor space consumption by all workers $n(x)$ at x. Using $F^C(x)$ from Eq. (20) and the marginal rate of substitution in Eq. (**??**), we obtain labor demand at each location:

$$L(x) = \frac{\alpha^C}{1-\alpha^C}\frac{\bar{p}^C(x)}{y^C}\mathcal{L}(x)S^C(x) \tag{21}$$

Using $F^R(x)$ from Eq. (20) in the Marshallian demand function, labor supply at any location is given by

$$n(x) = \frac{\mathcal{L}(x)S^R(x)}{y^R}\frac{\bar{p}^R(x)}{1-\alpha^R}. \tag{22}$$

General equilibrium: Aggregate labor market clearing means that

$$L = \int_0^{x_0} L(x)dx = \int_{x_0}^{x_1} n(x)dx = N. \tag{23}$$

Using Eq. (21) in Eq. (23) delivers

$$y = \frac{\alpha^C}{1-\alpha^C}\frac{\int_0^{x_1}\bar{p}^C(x)\mathcal{L}(x)S^C(x)dx}{N}. \tag{24}$$

We further assume housing market clearing so that

$$(1-\alpha^R)yN = \int_{x_0}^{x_1}\bar{p}^R(x)\mathcal{L}(x)S^R(x)dx. \tag{25}$$

Using Eq. (15), we can solve Eq. (25) for urban utility:

$$\bar{U} = \left[\frac{\frac{1}{1+\omega^R}y^{\frac{1}{1-\alpha^R}}\int_{x_0}^{x_1}\tilde{A}(x)^{\frac{1}{1-\alpha^R}}(S^R(x))^{(1+\omega^R)}\mathcal{L}(x)d(x)}{(1-\alpha^R)yN}\right]^{1-\alpha^R} \tag{26}$$

Eqs. (12), (24), and (26) constitute the exactly identified system of equations that solves for the general-equilibrium constants $\{y, U, N\}$.

Welfare: Given Gumbel-distributed preference shocks, expected utility across all workers living inside and outside the city can be expressed as follows:[24]

$$\mathcal{V} = \left(\widetilde{U} + \overline{U}^{\zeta}\right)^{\frac{1}{\zeta}} \tag{27}$$

[24]See Ahlfeldt et al. (2022) for a formal derivation.

Given our perfectly symmetric city, the aggregate land rent is defined by:

$$\mathcal{R} = \int_{x_1}^{x_0} r^R(x)\mathcal{L}(x)dx + \int_{x_0}^{0} r^C(x)\mathcal{L}(x)dx + \int_{x_1}^{\bar{x}} r^A\mathcal{L}(x)dx \tag{28}$$

Intuition: To give a sense of the key forces in the model, Figure 8 shows how key elasticities change with the migration elasticity ζ. Anticipating model quantification in the following subsection, this figure also provides intuition on how ζ is identified.

At the left of the graph is a closed city, in which ζ is 0. In this environment, reductions in the cost of height θ and associated new tall buildings does not draw in any population but makes the city more compact. The associated supply shock to city real estate lowers rents. The greater spatial concentration of production raises wages through an agglomeration force.

Moving to the right in Figure 8, it becomes easier for people to move into the city. This results in higher population, area, and rent elasticities. At $\zeta = 3$, the real estate supply shock effect of lowering the cost of height gets balanced by the general equilibrium migration response such that rents do not respond to heights. For greater values of ζ, where population elasticities are very large, rent elasticities are slightly positive.

Figure 8: Height elasticities in model by preference heterogeneity (ζ)

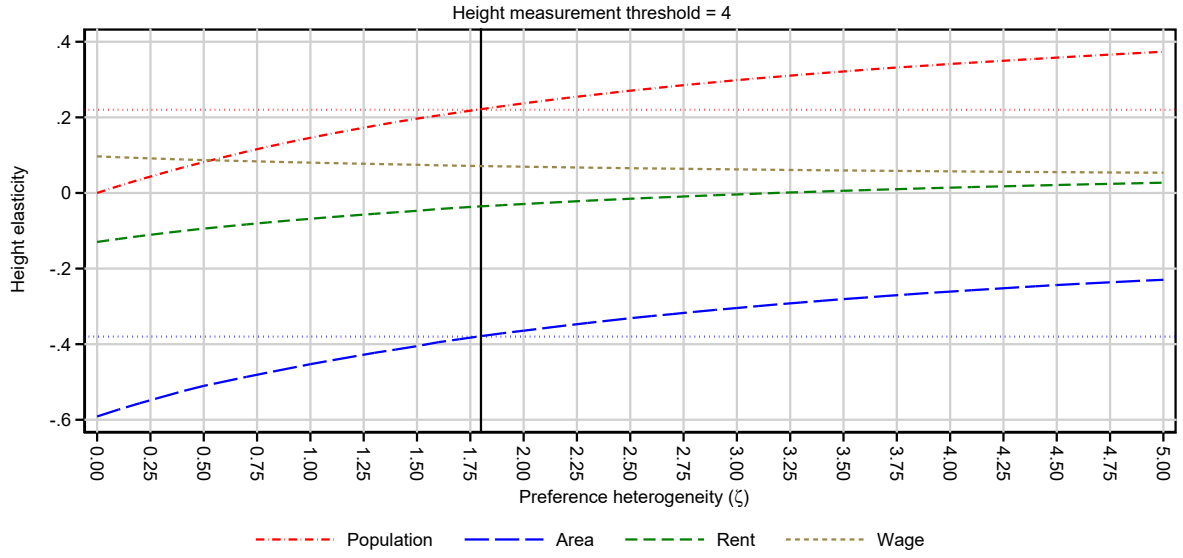

Note: Dotted horizontal lines are our estimates of the height elasticity of population and the height elasticity of area from cities that are unconstrained by height regulation (the empirical moments).

4.2 Quantification

We take parameters $\{\alpha^U, \beta, \omega^U, \theta^U, \tau^U, \underline{x}^U, \bar{a}^U, \tilde{c}^U, \bar{S}^U, r^a, \zeta, \ell, \tilde{U}\}$ and the endowments $\{\bar{N}, \bar{x}\}$ as given and treat $\{y, N, \bar{U}\}$ as city-wide endogenous objects for which we solve, along with the location-specific variables $\{L(x), n(x), \bar{p}^U(x), r^U(x), \tilde{S}^U(x)\}$ using a numerical procedure which we describe in Appendix section J.1. We summarize our choices in Table 6 and provide a brief rationale below. For details, we refer to Appendix Section J.2.

Our primary objective is to find a parametrization that rationalizes the height elasticities estimated in Section 3.4. We are not interested in matching the building height profile (or any other gradient) of a particular city. Instead, we generate a stylized city with a height profile that is consistent with the data when interpreted through the lens of the canonical urban land use model. To this end, we estimate the semi-elasticity of height with respect to distance from the city center from our data and exploit that there is a direct mapping from this reduced-form parameter to the structural amenity decay parameter (τ^U) within our model. Similarly, we let the data speak and set the share of built-up land ℓ to the observed mean ratio of built-up area over total land area. We set $\underline{x} = 1$, which results in an urban core with an area of slightly more than a square mile, a size that is anecdotally ascribed to the densest and most productive economic clusters, such as the City of London. We set $\bar{N} = 10\text{M}$ and $\bar{x} = 100\text{km}$, which generates a country population density of about 300 workers per km^2, about the value observed for the UK. The scale parameters $\{\bar{a}^U, \tilde{c}^U, r^a, \tilde{U}\}$ do not affect the height gradient, but they govern how attractive the city is relative to the rural hinterland and, hence, how many workers the city attracts. We generally invert $\tilde{c}^U$ for given values $\{\bar{a}^U, \tilde{c}^U, r^a\}$ to rationalize a given city population.

This leaves us with the preference heterogeneity parameter, ζ. For our purposes, it is a central parameter since it governs the migration response to any shock that affects the attractiveness of the city. The larger ζ, the more workers will move into the city in response to a positive shock to the supply of tall buildings. Since more workers use more floor space, the total land area will shrink less than the population density increases. If ζ was sufficiently large, the city could even expand vertically and horizontally. To identify ζ, we use a simulated method of moments (SMM) approach, treating the height elasticity of population and the height elasticity of area as moments that we match in model and data. Intuitively, we solve the model under varying values of θ^U for a given value of ζ, which delivers variation in population and area that mimics the bedrock-induced variation in the cost of height in our empirical analysis. In each run, we also compute a measure of tall building height. Log-linear regressions of model-generated population and area against model-generated heights produce our moments in the model.

One complication that arises in matching the moments is that our building heights data is bottom-coded at 55 m. We address this feature of our data by generating a height measure within the model that aggregates all heights above a height threshold $\mathcal{T}$. Since the truncated aggregate height measure is highly sensitive to the fuzziness of the height gradient, there is no one-to-one mapping from the threshold in the data (55 m) to $\mathcal{T}$. Therefore, we treat $\mathcal{T}$ as an additional parameter to be identified by our SMM approach. We find that under $\mathcal{T} = 4$ and $\zeta = 1.8$, we exactly match our moments. As long as $\mathcal{T} \geq 4$, we obtain a ζ value of slightly below two. The implied elasticity of labor supply to the city of about 1.5 is in line with reduced-form estimates in the literature (Beaudry et al., 2014). Our ability to comfortably reproduce the empirical moments within our model under a canonical parametrization adds to our confidence in the identification strategy proposed in Section 3.

Table 6: Baseline parameterization

	Parameter	Value	Further reading
$1-\alpha^C$	Share of floor space at inputs	0.15	Lucas and Rossi-Hansberg (2002)
$1-\alpha^R$	Share of floor space at consumption	0.33	Combes et al. (2019)
β	Agglomeration elasticity of production amenity	0.03	Combes and Gobillon (2015)
θ^C	Commercial height elasticity of construction cost	0.5	Ahlfeldt and McMillen (2018)
θ^R	Residential height elasticity of construction cost	0.55	Ahlfeldt and McMillen (2018)
ω^C	Commercial height elasticity of rent	0.03	Liu et al. (2018)
ω^R	Residential height elasticity of rent	0.07	Danton and Himbert (2018)
τ^C	Production amenity decay	0.03	Appendix Section J.2
τ^R	Residential amenity decay	0.03	Appendix Section J.2
ζ	Preference heterogeneity	1.8	Appendix Section J.2

Notes: Parameter values for $\{\alpha^U, \beta, \theta^U, \omega^U\}$ are borrowed from Ahlfeldt and Barr (2022) recommend these as suitable for stylized presentations and simple counterfactual analysis. The last column provides a references for the interested reader for further reading, but not necessarily the source of a point estimate. We set the scale parameters to $\bar{a}^C = \bar{a}^R = 2, \tilde{c}^C = \tilde{c}^R = 150, r^a = 50$, $\bar{N} = 10$M, $\bar{x} = 100$km and invert $\tilde{U}$ so that $\mu = 0.2$. There are no binding height limits in the baseline parametrization ($\bar{S}^C = \bar{S}^R = \infty$).

4.3 Counterfactuals

We are now ready to use the quantified model to explore the welfare effects of the tall-buildings technology as well as height limits that stand in the way of its adoption. To this end, we simulate the model with and without binding height constraints. In doing so, we account for variation in demand and supply conditions on the market of height which generate rich heterogeneity in the welfare effect.

4.3.1 Illustrative examples

We begin with some illustrative examples to develop the intuition for the mechanisms through which the welfare effect operates in the model. The starting point is the equilibrium derived under the baseline parameterization from Table 6 which we illustrate in the first row of Figure 9. Intuitively, the slopes of the use-specific floor-space bid-rent functions determine the slopes of the height gradients and the land bid-rent curves which, in turn, determine the land use pattern. Notice that the discontinuities in floor space rents and heights at the within-city land use boundary arise endogenously as a result of a net-cost of height $\theta^U - \omega^U$ that is smaller for commercial developments.

In the second row, we solve the model under the same parameterization, except that we increase the cost of height by 20% to emulate the effect of having less favorable bedrock. For the interested reader, we report changes in aggregate outcomes from the baseline to the counterfactual equilibrium in Table A12 in the Appendix. In keeping with intuition, building heights fall because—for given floor space rents—building tall is less profitable. In response, the city area expands by 17.8%. The relocation of firms and residents to more peripheral locations increases commuting costs by 2.9% and lowers productivity by about 0.9%. Due to the reduction in floor space supply, commercial rents increase by 11.2%. Although residents live farther from the center, residential rents increase by 1.2%. Lower productivity and higher commercial rents reduce labor demand, lowering the wage by 3.1%. Due to the lower wage, greater commuting

costs, and higher resident rents, indirect utility in the city, $\bar{U}$, net of any idiosyncratic component, falls by 6.6%. Since living in the city has become less attractive, the population falls by 8.9%. Expected utility across all workers inside and outside the city, $\mathcal{V}$, falls by 1.3%. Aggregate land values fall by 1%. There is redistribution from owners of land in the center, where the intensity of land use falls, to owners of rural land that is being converted into urban land as the city expands.

Figure 9: Urban spatial structure, cost of height, and regulation

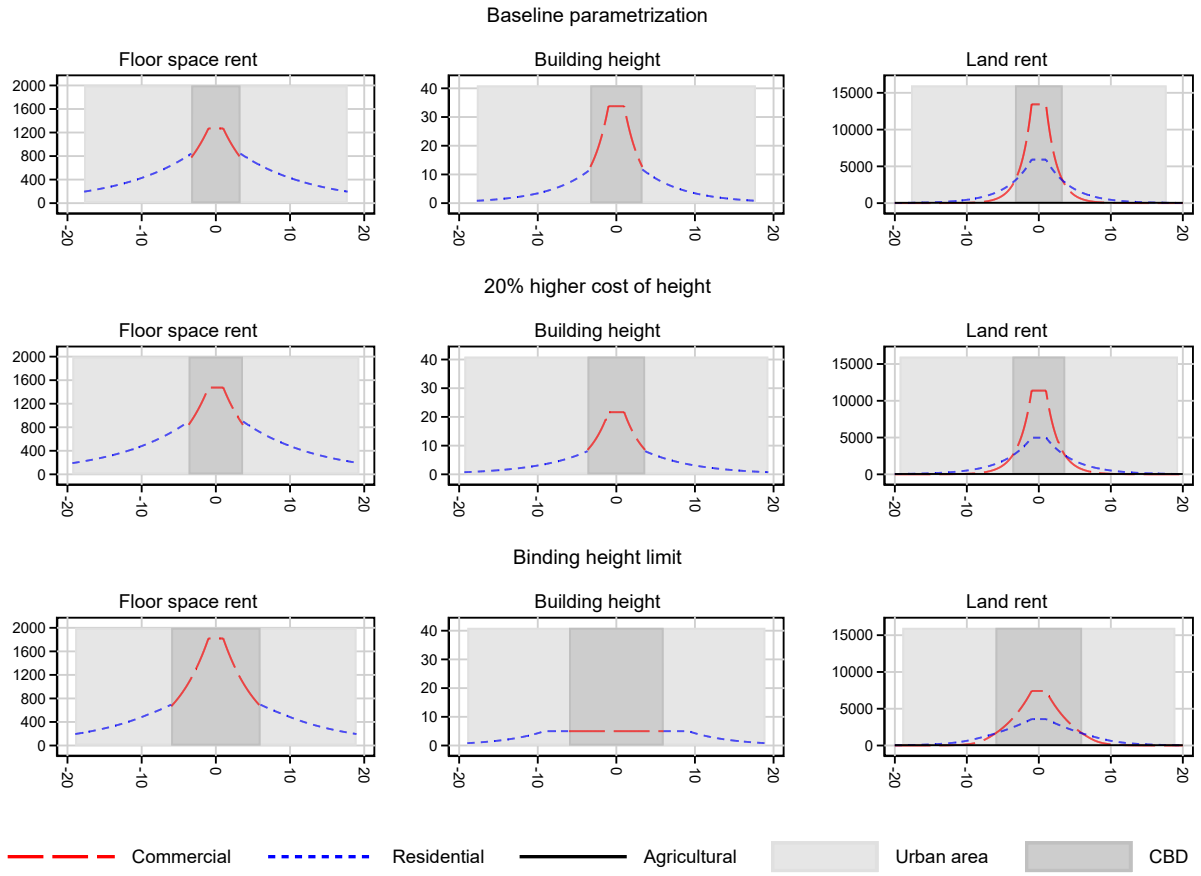

Note: Figure illustrates the solution to the model laid out in Section 4 under the parameter values from Table 6 (upper panels), a counterfactual where we increase the cost of height to $\theta^C = 0.6, \theta^R = 0.65$ (middle panels), and a counterfactual in which we introduce a height limit of $\bar{S}^C = \bar{S}^R = \mathcal{T} = 4$. See Table A12 in the Appendix for the impact of the greater cost of height and a binding height limit on aggregate outcomes.

In the third row, we set $\bar{S}^C = \bar{S}^R = \mathcal{T} = 4$, which results in an even flatter city than under the increased cost of height. Given that the CBD normally hosts the tallest buildings of the city, it is no surprise that the height cap results in a substantial horizontal expansion of the CBD. Although we have imposed a tighter constraint on vertical growth, the horizontal area of the city, at 14%, increases less than in the cost counterfactual. Because the vertical compression of the CBD is stronger than in the cost counterfactual, the horizontal expansion of the CBD is more pronounced. Therefore, the increase in commuting cost (8%) and the reduction in average productivity (8%) are also stronger. Wages also fall more (8%). The result is a reduction in housing demand that is so large that, despite the negative shock to residential floor space supply, residential rents fall substantially (14.8%). The increase in commuting costs and the lower wage,

however, dominate the effect of rents on indirect utility in the city, which decreases by 10.9%, leading to a fall in expected utility, $\mathcal{V}$ by 2.1%. Population falls by 15%, 50% more than in the cost counterfactual. Driven by the conversion of rural into residential and residential into commercial land use, aggregate land values increase increases by some notable 15%. Therefore, the height limit redistributes income from the mobile to the immobile factor. An important lesson from this counterfactual exercise that has been overlooked in the literature focusing on the residential sector (Brueckner and Sridhar, 2012) is that a major welfare cost of height limits arises from firms being pushed out of the locations where they are most productive.

4.3.2 Heterogeneity in welfare effects

Intuitively, the welfare effect of a height regulation must be related to its "bite". If we introduce the same height limit into a city with a lower cost of height, the effect should be larger since the regulation will have a greater bite. Indeed, it turns out that if we introduce the same height limit as in the third row of Figure 9 under a 20% greater cost of height, the impact on population and expected utility falls by about one third; the effect on area about halves (see Table A12 in the appendix). The standard approach in the literature to measuring the bite of height regulations is to compute the height gap (Jedwab et al, 2022, Barr and Jedwab, 2022). It represents the percentage fraction of the total height that would have been developed in the market equilibrium which has remained undeveloped due to height restrictions.

Empirically, the height gap can be established by comparing a city's total height to the total height of the tallest cities with similar characteristics, such as population, GDP per capita, or earthquake risk. In our model, the height gap is straightforward to compute by comparing solutions under binding and nonbinding height limits.[25]

We exploit this feature of the model to illustrate how the welfare effect associated with a height gap depends on population and cost of height. In doing so, we solve the model varying height cost (θ^U) and height limit ($\bar{S}^U$), and rural utility $\tilde{U}$ values. Concretely, we exploit that there is a unique mapping from urban and rural utility to population in Eq. (12) to find $\{\bar{S}^U, \tilde{U}\}$ values that rationalize any given combination of population and height gap using a procedure that we describe in Algorithm 4. We use this procedure to compute welfare effects for all combinations of height costs $\{0.2, 0.3, ..., 1\}$, height gaps $\{0\%, 10\%, ..., 100\%\}$, in each case for a small city of half a million and a large city of two million. It is worth recalling that for a given cost of height and a given height gap, the only reason why a city has a larger population is that it possesses greater demand for height.

Figure 10 confirms that losing height is more costly in terms of expected utility loss if the cost of height in a city is low, e.g. due to favorable bedrock. Lowering the cost of height from 0.6 to 0.3 about triples the relative utility loss at any given height gap in a city with a population of 2M. Demand conditions also matter. Holding the cost of height constant, we observe greater effects in cities that are larger. So, one important conclusion from Figure 10 is that height limits,

[25] Since we compute the height gap aggregating all heights exceeding $\mathcal{T} = 4$, the height gap can range between 0 and 100%.

even when expressed in terms of their relative effects on total height, tend to be more costly in cities with fundamentals that increase demand for and supply of height.

As already discussed in the context of Figure 9, vertical compression means horizontal expansion. This implies a significant increase in the value of land in more remote parts of the city and, in particular, land that is being converted from residential into commerical and rural into urban use. Figure 10 reveals that this uplift is generally large enough to more than compensate for the decline in land rent in the more constrained parts of the city. Again, the effect on aggregate land rent is much greater in cities with a lower cost of height where the loss of tall building height is particularly consequential. Holding the cost of height constant, there is little variation in population, which reveals that demand-side factors play a limited role.

Figure 10: Heterogeneity in welfare effects

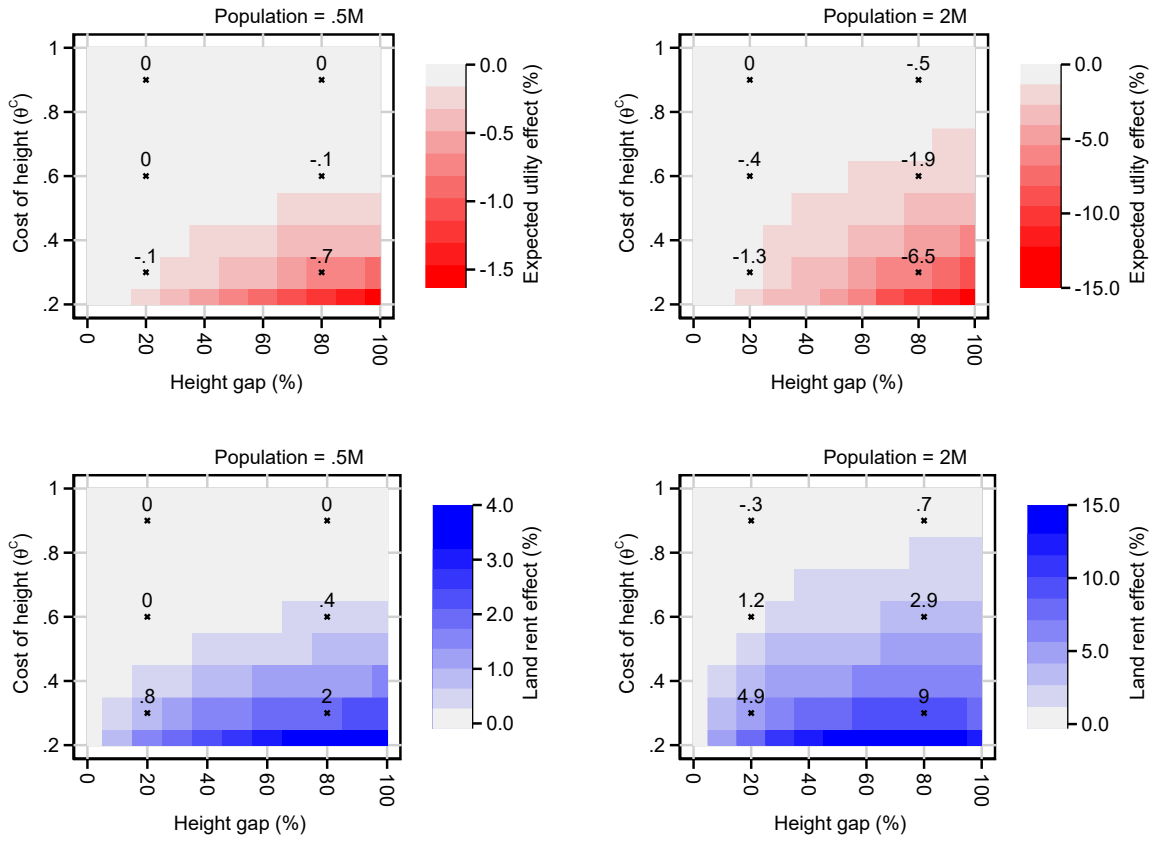

Note: To generate each panel, we solve the model under different values of $\{\theta^C\}$, setting $\theta^R = \theta^C + 0.05$. We find values of $\{\tilde{S}, \tilde{U}\}$ to rationalize a given combination of population and height gap, conditional on given θ^U values. We hold all other parameter values constant at the value described in Table 6. The height gap is the fraction of free-market total tall-building height that is not developed due to a height limit.

4.4 The Contribution of Tall Buildings to Welfare

We now return to our sample for 12,877 real-world cities with the aim of using the model to evaluate the welfare effects of tall buildings. To this end, we use the same procedure as in Figure 10 to invert the model and rationalize observed values of population and height gap conditional on the observed cost of height for each city in our data (see Algorithm 4 in the appendix for

details). As is discussed in Section 3, population is covered in the GHS-UCDB data introduced in Section 3. We obtain city-specific estimates of the cost of height using bedrock depths reported by Shangguan et al. (2017) and our non-parametric estimate of the relationship between bedrock depth and the cost of height illustrated in Figure A4.

To obtain a measure of the height gap for each city, we build on the analysis in Barr and Jedwab (2023). Using the same underlying regression model that was used to identify low regulation countries, as discussed in Section 3.4, they build predicted (log) heights for each city in the sample. After partitioning the sample into 1,000 bins of about 13 cities each using these predicted heights, we obtain the 90th percentile value in actual (log) heights in each bin. This is assumed to be the unconstrained amount of heights built given fundamental supply conditions conditional on city observables about demand and supply that generate the binned prediction. We construct our height gap measure for city i in bin b as:

$$Gap_{ib} = \max\left([1 - \frac{\ln Heights_{ib}}{\ln Heights_{b}^{90}}], 0\right) \tag{29}$$

By construction, Gap_{ib} goes from 0% to 100%. We emphasize that while this gap measure is likely to be correct on average conditional on observables, it is less likely to be accurate for specific cities.[26]

In Table 7, we tabulate the city-populated-weighted mean welfare effect by world region. We report the incidence on the mobile (labour) and immobile (land) factors for two scenarios. First, we calculate the welfare consequences of going from no height restrictions ($\bar{S}^U = \infty$) to a complete ban on tall buildings ($\bar{S}^U = \mathcal{T}$). The result is the welfare cost associated with banning all equilibrium tall buildings in the model. Second, we calculate the welfare consequences of going from no height restrictions ($\bar{S}^U = \infty$) to the actual height gaps (Gap_{ib}), which delivers the welfare cost associated with current height regulations.

Table 7 presents the welfare results. They indicate that on a global scale tall buildings have the potential to increase worker welfare by 3.2%, relative to having no tall buildings (bottom row). About two-thirds of the height potential has been realized under current regulations; worker welfare could increase by 1.0% if current height constraints were relaxed. However, there is significant heterogeneity across world regions. Since a relatively large fraction of the US urban population lives in large cities, and bedrock conditions are generally favorable, the welfare potential for North America is more than twice as large as the global average, though most of it has been realized. The region with the most to gain is South Asia, where only about half of the potential 4.1% has been realized. East Asia and Europe/Central Asia have realized over three-quarters of their small welfare potentials of less than 3%.

On the flip side, land owners stand to lose from deregulating heights. Of the 3.15% increase in land value associated with going from unregulated heights to no heights, about 60% (1.85 percentage points) has been realized due to height restrictions. Magnitudes of counterfactual

[26] Gaps are about 0% for Chicago, Seoul, Sao Paulo and Manila, 3% for NYC and Shanghai, 9% for Bangkok, 10% for Paris and Mexico City, 13% for London and Los Angeles, 17% for Ho Chi Minh City, and 23% for Dhaka and Karachi.

Table 7: Wefare effects of tall buildings by world regions

World region	City characteristics				Expected utility ($\mathcal{V}$)		Agg. land rent ($\mathcal{R}$)	
	Urban pop. (BN)	Share large cities	Cost of height θ	Est. height gap	No tall building	Actual height limit	No tall building	Actual height limit
East Asia & Pacific	1.03	55.76%	1.01	43.36%	-2.37%	-0.30%	2.25%	0.57%
Europe & Central Asia	0.36	41.06%	0.76	37.79%	-2.58%	-0.43%	2.54%	1.24%
Latin America & Caribbean	0.35	52.79%	0.73	40.50%	-2.99%	-0.68%	3.10%	1.58%
Middle East & North Africa	0.25	48.82%	0.81	66.46%	-3.48%	-1.45%	3.35%	2.79%
North America	0.17	67.35%	0.65	26.97%	-6.59%	-1.06%	6.00%	3.29%
South Asia	0.90	37.17%	0.66	44.37%	-4.10%	-1.88%	4.06%	2.99%
Sub-Saharan Africa	0.43	33.69%	0.68	51.40%	-2.75%	-1.33%	2.70%	2.11%
Mean	3.49	46.49%	0.79	44.57%	-3.23%	-1.00%	3.15%	1.85%

Notes: Model-based estimates are matched to real-world cities based on population, cost of height and height gap, an empirical estimate of how much of the potential height has not been realized taken from Barr & Jedwab, 2023. Welfare estimates are population-weighted averages by region. Height ban means no tall building exceeding four floors. Large city population share is the share of urban population in cities with a population of at least 1M.

changes in real estate values exhibit a similar pattern across world regions as worker welfare, though with the opposite sign.

Finally, it is important to realize that—while already large—the welfare effect of height limits is likely to grow over time. The history of tall buildings is one of technological innovations that have lowered the cost of height. The exact rate is difficult to estimate, but extant estimates suggest that the cost-of-height parameter, θ, has declined by 2% per year in the long run (see Ahlfeldt and Barr (2022) and Appendix Section H.5). Even if this rate halves, the cost of height will fall by 20% within a generation. Our simulations suggest that even if cities adjust to keep the relative bite of height regulation constant, the welfare cost will increase significantly, especially in regions, such as East Asia and the Pacific, where the cost of height is currently particularly large.

5 Conclusion

We demonstrate that tall buildings make cities more productive, compact, and affordable. As the cost of building tall structures decreases with further technological progress, this potential will only increase into the future. Hence, the potential cost of height restrictions are large.

While this study emphasizes the benefits of allowing cities to build tall, there may also be amenity and productivity costs from the associated congestion that we have not considered. A priority for future research should be to measure such costs.

References

Ahlfeldt, Gabriel M. and Daniel P. McMillen, "Tall buildings and land values: Height and construction cost elasticities in Chicago, 1870-2010," *Review of Economics and Statistics*, 2018, *100* (5), 861–875.

_ **and Elisabetta Pietrostefani**, "The economic effects of density: A synthesis," *Journal of Urban Economics*, 2019, *111* (February), 93–107.

_ **and Jason Barr**, "Viewing urban spatial history from tall buildings," *Regional Science and Urban Economics*, 11 2020, p. 103618.

_ **and** _ , "The economics of skyscrapers: A synthesis," *Journal of Urban Economics*, 5 2022, *129*, 103419.

_ **, Duncan Roth, and Tobias Seidel**, "Optimal minimum wages," *CEPR Discussion Paper 17026*, 2022.

Alonso, William, *Location and Land Use*, Cambridge, MA: Harvard Univ. Press, 1964.

Bairoch, Paul, *Cities and economic development: from the dawn of history to the present*, University of Chicago Press, 1988.

Barr, Jason, "Skyscrapers and the Skyline: Manhattan, 1895–2004," *Real Estate Economics*, 2010, *38* (3), 567–597.

_ , "Skyscraper Height," *Journal of Real Estate Finance and Economics*, 2012, *45* (3).

_ , *Building the Skyline: The Birth and Growth of Manhattan's Skyscrapers*, Oxford University Press, 2016.

_ **and Remi Jedwab**, "Exciting, boring, and nonexistent skylines: Vertical building gaps in global perspective," *Real Estate Economics*, 2023.

_ **, Troy Tassier, and Rossen Trendafilov**, "Depth to Bedrock and the Formation of the Manhattan Skyline, 1890–1915," *The Journal of Economic History*, 2011, *71* (4), 1060–1077.

Baum-Snow, Nathaniel, "Did Highways Cause Suburbanization?," *Quarterly Journal of Economics*, 2007, *122* (2), 775–805.

_ , "Urban transport expansions and changes in the spatial structure of us cities: Implications for productivity and welfare," *Review of Economics and Statistics*, 2020, *102* (5), 929–945.

_ **and Lu Han**, "The Microgeography of Housing Supply," *Working paper*, 2019.

_ **, J Vernon Henderson, Matthew A Turner, Qinghua Zhang, and Loren Brandt**, "Does investment in national highways help or hurt hinterland city growth?," *Journal of Urban Economics*, 2020, *115*, 103124.

_ **, Loren Brandt, J Vernon Henderson, Matthew A Turner, and Qinghua Zhang**, "Roads, Railroads, and Decentralization of Chinese Cities," *The Review of Economics and Statistics*, 1 2017, *99* (3), 435–448.

Beaudry, Paul, David A. Green, and Benjamin M. Sand, "Spatial equilibrium with unemployment and wage bargaining: Theory and estimation," *Journal of Urban Economics*, 2014, *79*, 2–19. Spatial Dimensions of Labor Markets.

Bertaud, Alain and Jan Brueckner, "Analyzing building-height restrictions: predicted impacts and welfare costs," *Regional Science and Urban Economics*, 2005, *35* (2), 109–125.

Borusyak, Kirill, Rafael Dix-Carneiro, and Brian Kovak, "Understanding migration responses to local shocks," *Available at SSRN 4086847*, 2022.

Brueckner, Jan and Kala Seetharam Sridhar, "Measuring welfare gains from relaxation of land-use restrictions: The case of India's building-height limits," *Regional Science and Urban Economics*, 2012, *42* (6), 1061–1067.

_ **and Ruchi Singh**, "Stringency of land-use regulation: Building heights in US cities," *Journal of Urban Economics*, 2020, *116*.

Brueckner, Jan K., "The structure of urban equilibria: A unified treatment of the muth-mills model," *Handbook of Regional and Urban Economics*, 1987, *2*, 821–845.

Brueckner, Jan, Shihe Fu, Yizhen Gu, and Junfu Zhang, "Measuring the stringency of land use regulation: The case of China's building height limits," *Review of Economics and Statistics*, 2017, *99* (4), 663–677.

Bryan, Gharad and Melanie Morten, "The Aggregate Productivity Effects of Internal Migration: Evidence from Indonesia," *Journal of Political Economy*, 12 2018.

Burchfield, Marcy, Henry G Overman, Diego Puga, and Matthew A Turner, "Causes of sprawl: A portrait from space," *The Quarterly Journal of Economics*, 2006, *121* (2), 587–633.

Caliendo, Lorenzo, Maximiliano Dvorkin, and Fernando Parro, "Trade and Labor Market Dynamics: General Equilibrium Analysis of the China Trade Shock," *Econometrica*, 5 2019, *87* (3), 741–835.

Combes, Pierre-Philippe and Laurent Gobillon, "The Empirics of Agglomeration Economies," in Gilles Duranton, J Vernon Henderson, William C B T Handbook of Regional Strange, and Urban Economics, eds., *Handbook of Regional and Urban Economics*, Vol. 5, Elsevier, 2015, pp. 247–348.

_ , Gilles Duranton, and Laurent Gobillon, "The identification of agglomeration economies," *Journal of Economic Geography*, 2011, *11* (2), 253–266.

_ , _ , and _ , "The Costs of Agglomeration: House and Land Prices in French Cities," *The Review of Economic Studies*, 10 2019, *86* (4), 1556–1589.

Curci, Federico, "Vertical and horizontal cities: in which direction should cities grow?," *Working paper*, 2017.

_ , "The taller the better? Agglomeration determinants and urban structure," *Working paper*, 2020.

Danny, Deng Yongheng E. Solganik Tsur Somerville Ben-Shahar and Z. Hongjia, "The Value of Vertical Status: Evidence from the Real Estate Market," 2022.

Danton, Jayson and Alexander Himbert, "Residential vertical rent curves," *Journal of Urban Economics*, 2018, *107*, 89–100.

Desmet, Klaus, DÃ¡vid KrisztiÃ¡n Nagy, and Esteban Rossi-Hansberg, "The Geography of Development," *Journal of Political Economy*, 1 2018, *126* (3), 903–983.

Duranton, Gilles and Diego Puga, "Urban Land Use," in Gilles Duranton, J. Vernon Henderson, and William C. Strange, eds., *Handbook of Regional and Urban Economics*, Vol. 5, Elsevier, 2015, chapter 8, pp. 467–560.

_ and _ , "The Economics of Urban Density," *Journal of Economic Perspectives*, 2020, *34* (3), 3–26.

_ and Matthew A. Turner, "Urban Growth and Transportation," *The Review of Economic Studies*, 2012, *79* (4), 1407–1440.

Emporis, *Emporis* 2022.

Faber, Benjamin, "Trade Integration, Market Size, and Industrialization: Evidence from China's National Trunk Highway System," *The Review of Economic Studies*, 7 2014, *81* (3), 1046–1070.

Florczyk, A., M. Melchiorri, C. Corban, M. Schiavina, L. Maffenini, M. Pesaresi, P. Politis, F. Sabo, S. Carneiro Freire, D. Ehrlich, T. Kemper, P. Tommasi, D. Airaghi, and L. Zanchetta, "Description of the GHS Urban Centre Database 2015," *Publications Office of the European Union*, 2019.

Gibbons, Stephen, Teemu Lyytikäinen, Henry G Overman, and Rosa Sanchis-Guarner, "New road infrastructure: the effects on firms," *Journal of Urban Economics*, 2019, *110*, 35–50.

Glaeser, Edward, *Triumph of the City: How Our Greatest Invention Makes Us Richer, Smarter, Greener, Healthier, and Happier* 2012.

Gollin, Douglas, Casper Worm Hansen, and Asger Mose Wingender, "Two Blades of Grass: The Impact of the Green Revolution," *Journal of Political Economy*, 2021, *129* (8), 2344–2384.

Gonzalez-Navarro, Marco and Matthew A Turner, "Subways and urban growth: Evidence from earth," *Journal of Urban Economics*, 2018, *108*, 85–106.

Gyourko, Joseph and Raven Molloy, "Regulation and housing supply," in "Handbook of regional and urban economics," Vol. 5, Elsevier, 2015, pp. 1289–1337.

Harari, Mariaflavia, "Cities in bad shape: Urban geometry in India," *American Economic Review*, 2020, *110* (8), 2377–2421.

Harris, John R and Michael P Todaro, "Migration, Unemployment and Development: A Two-Sector Analysis," *The American Economic Review*, 2 1970, *60* (1), 126–142.

Heblich, Stephan, Stephen J Redding, and Daniel M Sturm, "The Making of the Modern Metropolis: Evidence from London," *The Quarterly Journal of Economics*, 11 2020, *135* (4), 2059–2133.

Henderson, J Vernon, Tanner Regan, and Anthony Venables, "Building the city: from slums to a modern metropolis," *The Review of Economic Studies*, 2021, *88* (3), 1157–1192.

_ , Tim Squires, Adam Storeygard, and David Weil, "The global distribution of economic activity: nature, history, and the role of trade," *The Quarterly Journal of Economics*, 2018, *133* (1), 357–406.

Hilber, Christian AL and Wouter Vermeulen, "The impact of supply constraints on house prices in England," *The Economic Journal*, 2016, *126* (591), 358–405.

Hsieh, Chang-Tai and Enrico Moretti, "Housing Constraints and Spatial Misallocation," *American Economic Journal: Macroeconomics*, 2019, *11* (2), 1–39.

Jedwab, Remi and Adam Storeygard, "The Average and Heterogeneous Effects of Transportation Investments: Evidence from Sub-Saharan Africa 1960â2010," *Journal of the European Economic Association*, 06 2021, *20* (1), 1–38.

_ , Jason Barr, and Jan Brueckner, "Cities without Skylines: Worldwide Building-height Gaps and their Implications," 2020.

Koster, Hans R A, Jos van Ommeren, and Piet Rietveld, "Is the sky the limit? High-rise buildings and office rents," *Journal of Economic Geography*, 5 2013, *14* (1), 125–153.

Liu, Crocker, Stuart S Rosenthal, and William C Strange, "The Vertical City: Rent Gradients and Spatial Structure," *Journal of Urban Economics*, 2018, *106*, 101–122.

_ , _ , and _ , "Employment Density and Agglomeration Economies in Tall Buildings," *Regional Science and Urban Economics*, 2020, *84*.

Lucas, Robert E Jr. and Esteban Rossi-Hansberg, "On the Internal Structure of Cities Author," *Econometrica*, 2002, *70* (4), 1445–1476.

McFadden, Daniel, "The measurement of urban travel demand," *Journal of Public Economics*, 1974, *3* (4), 303–328.

Mills, Edwin S, "An Aggregative Model of Resource Allocation in a Metropolitan Area," *The American Economic Review*, 1967, *57* (2), 197–210.

Muth, R, *Cities and Housing*, Chicago: Chicago University Press, 1969.

Nase, Ilir and Jason Barr, "Game of Floors: The Determinants of Residential Height Premiums," 2023.

NGDC, *Global Radiance Calibrated Nighttime Lights* 2015.

Redding, Stephen J. and Esteban Rossi-Hansberg, "Quantitative Spatial Economics," *Annual Review of Economics*, 2017, *9* (1), 21–58.

_ and Matthew A. Turner, "Transportation Costs and the Spatial Organization of Economic Activity," in "Handbook of Regional and Urban Economics," Vol. 5 2015.

Rosenthal, Stuart S and William C Strange, "The attenuation of human capital spillovers," *Journal of Urban Economics*, 2008, *64* (2), 373–389.

Schleier, Merill, *The Skyscraper in American Art, 1890â1931* 1986.

Shangguan, Wei, Tomislav Hengl, Jorge Mendes de Jesus, Hua Yuan, and Yongjiu Dai, "Mapping the global depth to bedrock for land surface modeling," *Journal of Advances in Modeling Earth Systems*, 2017, *9* (1), 65–88.

Song, Xiao-Peng, Matthew C Hansen, Stephen V Stehman, Peter V Potapov, Alexandra Tyukavina, Eric F Vermote, and John R Townshend, "Global land change from 1982 to 2016," *Nature*, 2018, *560* (7720), 639–643.

Storeygard, Adam, "Farther on down the Road: Transport Costs, Trade and Urban Growth in Sub-Saharan Africa," *The Review of Economic Studies*, 04 2016, *83* (3), 1263–1295.

Tan, Ya, Zhi Wang, and Qinghua Zhang, "Land-use regulation and the intensive margin of housing supply," *Journal of Urban Economics*, 2020, *115*, 103199.

United Nations, *World Urbanization Prospects: The 2018 Revision* 2018.

World Bank, *World Development Indicators* 2022.

ONLINE APPENDIX NOT FOR PUBLICATION

H Data and stylized facts

H.1 Value of tall buildings

We observe the volume of buildings indexed by i in city m, V_{im}. The height of a building is S_{im}. A simple way of measuring the value of building i, v_{im} is:

$$v_{im} = \frac{\bar{p}_{im}}{\delta_m} V_{im}$$

where $\bar{p}_{im}$ is the average rent per square meter and δ_m is a city-specific discount rate used to compute the present value of a perpetual stream of revenues. Since the monocentric standard urban model has received great support in data (see Liotta et al., 2022, for evidence from a global sample of cities), it is reasonable to express rent as

$$\bar{p}_{im} = \bar{p}_m^0 \times \exp\left(-\tau_m DCBD_{im}\right) + \varepsilon_{im},$$

where r_m^* is the rent at the central business district (CBD) of city m, $DCBD_{im}$ is the distance from the CBD in km, and $\tau_m > 0$ is a decay parameter that governs how quickly rents decay in distance from the CBD.

Ahlfeldt and Barr (2022a) show that under canonical assumptions, this decay parameter is a linear transformation of the semi-elasticity of height with respect to distance from the CBD. We estimate this this semi-elasticity by city and then use the result from Ahlfeldt and Barr (2022a) to compute city-specific rent gradients as $\tau_m = -\frac{\partial \ln S_{im}}{\partial DCBD_{im}} \times 0.2$. We can further use equilibrium condition for profit-maximizing building height derived in (Ahlfeldt and Barr, 2022a) to express the rent at the CBD as:

$$\bar{P}_m^0 = \tilde{c}\left(S_m^0\right)^{0.5},$$

Where S_m^0 is the height at the CBD.

Our object of interest is the share of the value of buildings exceeding 55 meters at total stock:

$$TBS = \frac{\sum_m \sum_i v_{im} \times \mathbb{1}(S_{im} > 55)}{\sum_i v_{im}}$$

Assuming $\mathbb{E}(\varepsilon_{im}|m) = 0$, we can combine all ingredients to compute our object of interest as

$$TBS = \frac{\sum_m \sum_i (S_m^0)^{0.5} \exp\left(-\tau_m DCBD_{im}\right) V_{im} \times \mathbb{1}(S_{im} > 55)}{\sum_m \sum_i (S_m^0)^{0.5} \exp\left(-\tau_m DCBD_{im}\right) V_{im}}.$$

Ahlfeldt and Barr (2022b) show that tall building represent a source of "big data" from which one can infer the spatial distribution of economic activity. Thus, we use our data set of tall buildings to identify the city centre as the median coordinate. Having recovered city center it is then straightforward to estimate to estimate the city specific height gradient $\frac{\partial \ln S_{im}}{\partial DCBD_{im}}$.

H.2 Summary Statistics

Table A1: Summary Statistics

		City Population in 1975			
		< 100k	100k-500k	> 500k	
		(1)	(2)	(3)	(3) - (2)
Avg Sum of Heights >55 m in 1975		3	36	1,441	1,404
Frac of Cities with Tall Bldgs in 1975		0.01	0.09	0.41	0.32
MBD	Mean 1975-2015 Δ ...				
<10m	ln Pop	0.55	0.45	0.55	0.10
	ln Built Area	0.46	0.76	0.75	-0.01
	ln (Heights + 1)	0.05	0.37	2.05	1.68
	Heights (m)	9	72	5,206	5,134
	Any Tall Bldgs	0.01	0.06	0.21	0.15
	Observations	3,876	788	113	
10m - 30m	ln Pop	0.46	0.29	0.42	0.13
	ln Built Area	0.50	0.60	0.55	-0.05
	ln (Heights + 1)	0.21	1.20	3.40	2.20
	Heights (m)	63	694	26,540	25,846
	Any Tall Bldgs	0.03	0.18	0.32	0.14
	Observations	4,561	1,547	313	
> 30m	ln Pop	0.47	0.27	0.44	0.17
	ln Built Area	0.73	0.94	0.78	-0.16
	ln (Heights + 1)	0.10	0.69	4.09	3.40
	Heights (m)	26	220	11,780	11,560
	Any Tall Bldgs	0.02	0.11	0.46	0.35
	Observations	1,151	436	89	

Note: Each city in the main estimation sample is one observation. Entries in columns (1), (2) and (3) are conditional means as a function of 1975 city population and city mean bedrock depth (MBD). All differences in the final column are statistically significant at the 5 percent level except growth in population for cities with bedrock depths between 0 and 10 meters and built area for cities with bedrock depths between 0 and 10 or 10 and 30 meters.

The final column in Table A1 explicitly shows that height growth was greater in cities of over 500 thousand residents in 1975 than in those cities with between 100 and 500 thousand residents at all three indicated bedrock depths. Differencing relative height growth between intermediate and shallow bedrock depths, we see that larger cities on intermediate depth bedrock experienced more rapid 1975-2015 height growth than did those cities on shallow bedrock. We note that secondary Chinese cities are heavily over-represented in the deep bedrock category for large cities at the bottom of Column (3). In many of these locations, the post-1990 construction boom did not respond to standard market forces.

H.3 Data on Tall Buildings

The full Emporis data set includes 693,855 buildings worldwide. These include buildings of various types, heights and sizes. While Emporis attempted to collect extensive information about the world's buildings, it could not do so comprehensively. As a result, we are concerned about the selection of buildings recorded in the data set. Our empirical strategy requires measuring the universe of buildings above some height cutoff. To determine this height cutoff, we inspect the following nonparameteric density of building heights in the full Emporis data set.

Figure A1: Distribution of Building Heights (m) in Emporis circa 2022

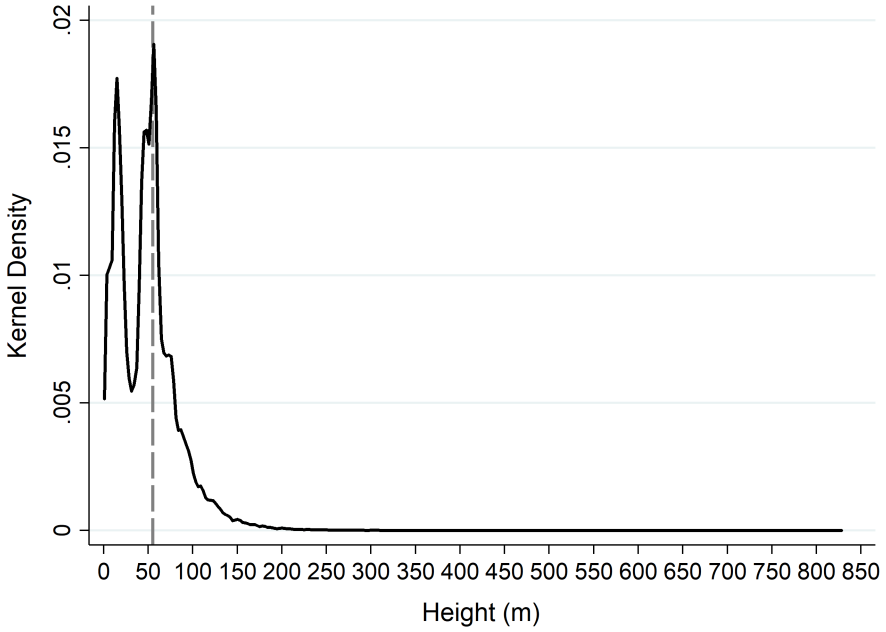

Notes: This figure shows the kernel density of heights (meters) for all 693,855 "existing [completed]" buildings in Emporis (accessed 02-07-2022). We only include "building with towers", "high-rise building", "low-rise building", "multi-story building", and "skyscraper" property types.

Evident in Figure A1 is a spike in the distribution of building heights at just above 55 meters. It is for this reason that we use the 55 meter height threshold above which to measure the sum of heights for each city.

For a subset of our tall buildings data set, we observe not only the height of a tall building, but also the cost of construction (excluding cost of land acquisition) and the floor area. In this section, we describe how we process the data to generate the heat maps in Figure 3 and 4 and provide complementary LWR estimates using bivariate kernels that provide non-parametric point estimates of the cost-bedrock relationship by height groups aongside confidence bands.

H.3.1 Descriptive statistics

In Table A2, we provide summary statistics of the Emporis data used in this section. Panel A summarizes sample that we restrict to US cities to ensure that variation in the cost of height over a long time is identified within one country that roughly follows a common trend. We use

this sample in Figures 3, A2, and A5 and Table A3. Panel B summarizes the multinational sample that we use in Figures 4, A4, and A3 for cross-sectional analyses.

Table A2: Summary statistics of Emporis data

	Mean	SD	Min	Max
Panel A: 591 observations in 93 US cities				
Construction year	1988.23	23.95	1902.00	2021.00
Height (m)	102.15	55.72	55.03	541.33
Bedrock depth (m)	19.66	14.72	2.50	113.01
Ln construction cost	7.05	1.20	3.18	10.98
Ln cost (residulized)	-0.00	0.53	-1.61	2.65
Panel B: 1,033 observations in 206 cities in 55 countries				
Construction year	1994.98	21.00	1902.00	2021.00
Height (m)	113.42	71.52	55.00	828.00
Bedrock depth (m)	20.08	13.05	0.00	117.53
Gross floor area (m^2)	53972.87	61268.07	934.00	9.8e+05
Ln construction cost	7.12	1.58	-5.25	10.98
Ln cost (residulized)	-0.00	0.85	-7.60	5.14

Notes: Unit of observation is buildings in Emporis data.

H.3.2 Residualized log unit cost

The cost of constructing a tall building depends on a range of factors that are unrelated to the height of the building and the depth of bedrock such as the price of labour or construction materials. Therefore, we residualize observed construction cost $C_{i,m(i),c(i),t}$ per unit of floor area $F_{i,m(i),c(i),t}$ of a building i, constructed in city m in country c during decade t using the following regression:

$$\ln C_{i,m(i),c(i),t} - \ln F_{i,m(i),c(i),t} = \mu_{m(i)} + \eta_{c(i),t} + \varepsilon^{C}_{i,m(i),c(i),t},$$

where $\mu_{m(i)}$ is a time-invariant fixed effect controlling for arbitrary demand and supply shifters at the city level and $\eta_{c(i),t}$ is a country by decade effect that controls for time-varying effects such as increasing demand due to economic growth or varying costs of construction materials. From this regression, we recover the residual, $\varepsilon^{C}_{i,m(i),c(i),t}$, as a relative cost measure that describes log deviations from country-trend-adjusted city averages.

H.3.3 LWR using a bivariate kernel

As discussed in Section 2, innovations in construction technology may have affected the construction cost for buildings of different height differently. Intuitively, improvements in mainframe computing and software that allow for refined structural engineering to withstand collateral wind loads should have had a greater impact on the cost of building very tall buildings. Likewise, the engineering literature suggests that in determining construction cost, building height and bedrock depth interact in a complex fashion. For tall buildings, there is generally

a cost-minimizing bedrock depth, but this depth is likely to vary by height—taller buildings require deeper foundations—and so does the importance of bedrock—bedrock is generally more important to anchor taller buildings. To evaluate such complex relationship non-parametrically, we employ a locally weighted regressions approach (Cleveland and Devlin, 1988; McMillen, 1996) using a bivariate kernel.

Let's assume we have a set of variables $s \in \{s^1, s^2\}$ that determine construction cost. For each combination of grid values along those dimensions $\tilde{s}^1 \in \tilde{S}^1, \tilde{s}^2 \in \tilde{S}^2$ we run the locally weighted regression

$$\varepsilon_i^C = \bar{\varepsilon}^{\tilde{s}^1,\tilde{s}^2} + \tilde{\varepsilon}_i^{\tilde{s}^1,\tilde{s}^2}$$

using the Gaussian kernel weight

$$\begin{aligned} W_i^{\tilde{s}^1,\tilde{s}^2} &= \frac{w_i^{\tilde{s}^1,\tilde{s}^2}}{\sum_{j=i}^{J} w_j^{\tilde{s}^1,\tilde{s}^2}}, \text{where} \\ w_i^{\tilde{s}^1,\tilde{s}^2} &= \prod_{s=\in\{s^1,s2\}} \frac{1}{\kappa^s\sqrt{\pi}} \exp\left[-\frac{1}{2}\left(\frac{s_i - \tilde{s}}{\kappa^s}\right)^2\right]. \end{aligned} \tag{30}$$

where κ^s are bandwidth parameters.

Hence, we run $\tilde{S}^1 \times \tilde{S}^2$ locally weighted regressions to recover $\tilde{S}^1 \times \tilde{S}^2$ parameters $\bar{\varepsilon}^{\tilde{s}^1,\tilde{s}^2}$ which are local means that we plot on the height-bedrock plane in Figures 3 and 4. This amounts to 112 (years) $\times$ 195 (height values) = 21,840 regressions in 3 and 35 (bedrock depth values) $\times$ 195 (height values) = 6,825 regressions in Figure 4.

H.3.4 LWR using a univariate kernel

The strength of the heatmaps in Figure 3 and 4 is to provide an accessible presentation of a non-parametric function in two dimensions. In doing so, we focus on point estimates and abstract from confidence bands. For an illustration of the latter, subdivide the data set in groups defined by building height and estimate the the relationships between cost and either the year of construction or bedrock height groups using LWR and univariate kernels that are otherwise identicaal to Eq. (30). Since we include only one dimension in our kernel, we use smaller bandwidth parameters. The blue and the red lines for 100-150 m and 150-250 m in Figures A3 and A2 roughly correspond to the blue and red lines in Figures 4 and 3.

The results presented in A2 confirm that the construction cost of very tall buildings exceeding 150 m in the US have fallen significantly more that in other height categories. In particular, costs in this category have fallen throughout the study period on which we focus in the main stages of the analysis.

The results presented in Figure A3 confirm that the cost-minimizing bedrock depth for buildings of about 125 m is about 18 m, whereas it is 25 m for buildings of about 200 m. The additional insight from the confidence bands is that we can reject that the cost is the same at lower or greater depths. Another relevant finding from Figure A3 is that the point estate of cost for short buildings and deep bedrocks are associated with a large standard error.

Figure A2: Construction cost as function of height and construction year

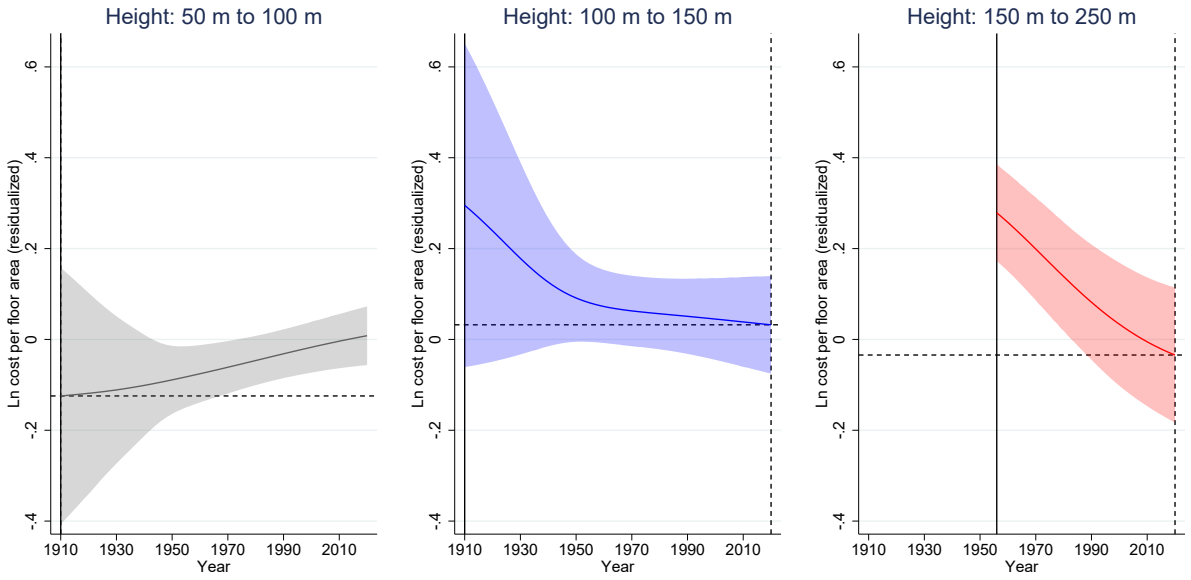

Notea: The sample consists of 591 constructions in US cities (see Panel A in Table A2). Ln cost per floor area is residualized to control for city fixed effects and country-by-decade of construction effects. We use locally weighted regressions with a univariate Gaussian kernel and a bandwidth of $\kappa = 25$ to estimate local means of the cost measure for varying bedrock depths. Confidence bands are at the 95% level.

Figure A3: Construction cost as function of height and bedrock depths

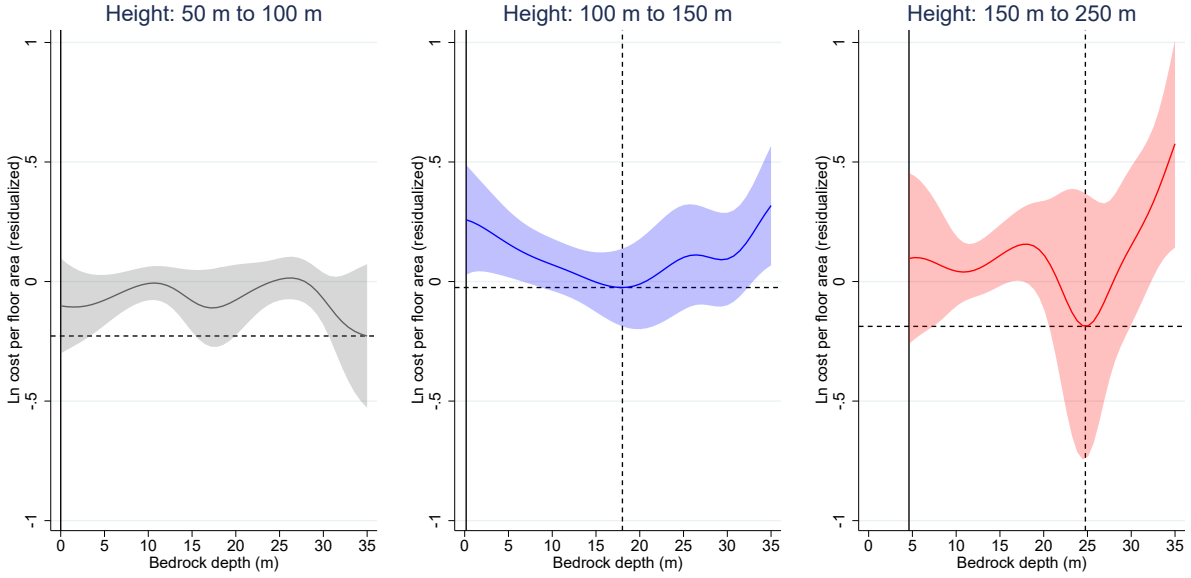

Note: The sample consists of 1,033 constructions in 206 cities in 55 countries (see Panel A in Table A2). Ln cost per floor area is residualized to control for city fixed effects and country-by-decade of construction effects. We use locally weighted regressions with a univariate Gaussian kernel and a bandwidth of $\kappa = 4$ to estimate local means of the cost measure for varying bedrock depths. Confidence bands are at the 95% level.

H.4 Cost of height and bedrock depth

A convenient way of summarizing the cost of height is the elasticity of per-unit construction cost with respect to height (Ahlfeldt and McMillen, 2018; Ahlfeldt and Barr, 2022a). The

engineering literature and stylized evidence discussed in Section 2 suggests that this elasticity should non-linearly depend on bedrock depth. Intuitively, bedrock very close to the surface makes the construction of taller buildings relatively more expensive since these require deeper foundations and removing bedrock is costly. Similarly, very deep bedrock makes the construction of taller buildings relatively more expensive since bedrock is more important as an anchor for the foundations of taller buildings.

To empirically substantiate this notion, we use a LWR-IV approach to causally estimate how unit costs change in height depending on bedrock depth. We require a demand-side instrumental variable to remove the effect of supply-side factors such as ruggedness that could be correlated with sub-soil geology. We use distance from the CBD as and instrumental variable since it affects building heights via the demand side (Brueckner, 1987; Ahlfeldt and Barr, 2022a) and has empirically been shown to be a strong predictor of height (Ahlfeldt and McMillen, 2018; Ahlfeldt and Barr, 2022a). The city center is defined as the median coordinate of buildings exceeding 100 m height and or the tallest building where building exceeds 100 m. Concretely, we estimate a first stage

$$\ln h_{i.m(i),c(i),t} = \alpha^{\tilde{b}} \ln DCBD_{i,m(i)} + \tilde{\mu}^{\tilde{b}}_{m(i)} + \tilde{\eta}^{\tilde{b}}_{c(i),t} + \tilde{\varepsilon}^{\tilde{b}}_{i,m(i),c(i),t} \tag{31}$$

and a second stage:

$$\ln C_{i,m(i),c(i),t} - \ln F_{i,m(i),c(i),t} = \theta^{\tilde{b}} \widehat{\ln h}_{i.m(i),c(i),t} + \mu^{\tilde{b}}_{m(i)} + \eta^{\tilde{b}}_{c(i),t} + \varepsilon^{\tilde{b}}_{i,m(i),c(i),t} \tag{32}$$

for each LWR $\tilde{b} \in \tilde{B}$ using a weighted 2SLS estimator. $h_{i,m(i),c(i),t}$ is the height of building i, constructed in city m in country c during decade t, $DCBD_{i,m(i)}$ is distance from the city center defined as the median coordinate of buildings with $h_i \geq 100$ m (or the tallest building if it is smaller), $\ln C_{i,m(i),c(i),t} - \ln F_{i,m(i),c(i),t}$ is the log of the cost per unit of floor area, $\{\mu^{\tilde{b}}_{m(i)}, \mu^{b}_{m(i)}\}$ are city fixed effects, $\{\eta^{\tilde{b}}_{c(i),t}, \eta^{b}_{c(i),t}\}$ are country by decade fixed effects, and $\{\tilde{\varepsilon}^{\tilde{b}}_{i,m(i),c(i),t}, \varepsilon^{\tilde{b}}_{i,m(i),c(i),t}\}$ are error terms.

In each LWR $\tilde{b} \in \tilde{B}$ we weigh observations by the Gaussian kernel weight

$$\begin{aligned} W^{\tilde{b}}_i &= \frac{w^{\tilde{b}}_i}{\sum_{j=i}^{J} w^{\tilde{b}}_j}, \text{where} \\ w^{\tilde{b}}_i &= \frac{1}{\kappa^{\tilde{b}}\sqrt{\pi}} \exp\left[-\frac{1}{2}\left(\frac{b_i - \tilde{b}}{\kappa^{\tilde{b}}}\right)^2\right]. \end{aligned} \tag{33}$$

Notice that Eq. (33) uses a univariate version of the same kernel as in Eq. (30), except that we employ a LWR-specific bandwidth. This is because we wish to allow for a more flexible fit via a smaller bandwidth in the in the more populated part of the bedrock distribution where we also expect more variation in θ, whereas we wish to reduce standard errors in the right tail of the bedrock distribution that is more sparsely populated and where we expect less variation in θ.

To this end, we use a variant of Scott's rule of thumb for bandwidth selection and define

$$\kappa^{\tilde{b}} = \mathcal{M} \frac{3.49 \hat{\sigma}^{\tilde{b}}}{\left(N^{\tilde{b}}\right)^{\frac{1}{3}}},$$

where the standard deviation $\hat{\sigma}^{\tilde{b}}$ and the number of observations $N^{\tilde{b}}$ are computed for rolling subsamples that satisfy $|b_i - \tilde{b}| \leq \mathcal{B} = 10$. We scale the rule-of-thumb bandwidth by a factor of $\mathcal{M} = 2$ since the non-parametric estimation of derivatives generally requires larger bandwidths than the estimation of levels (Henderson and Parmeter, 2015, Section 5.9).

Figure A4: Cost of height as function of bedrock depths

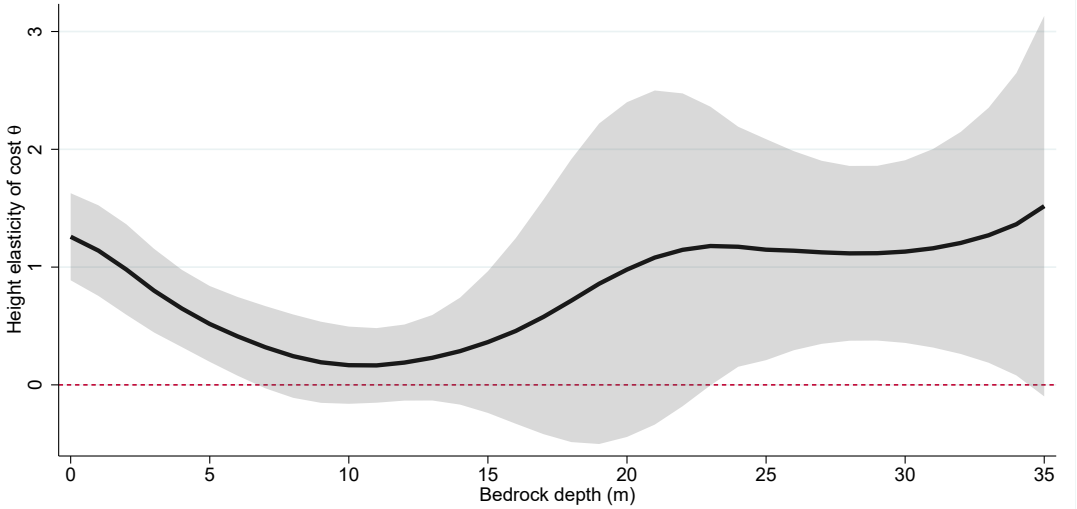

Notes: We show non-parametric estimates of the cost of height from an LWR-IV approach. In each LWR, we estimate the height elasticity from a regression of the log of construction cost per floor area against building height, controlling for city fixed effects and country by decade of construction effects. The sample consits of 1,033 constructions in 206 cities in 55 countries (see Panel A in Table A2). We use distance from the city center as an instrumental variable for height to remove the effects of unobserved factors that affect construction cost (such as ruggedness) that could be correlated with bedrock. The city center is defined as the median coordinate of buildings exceeding 100 m height and or the tallest building where building exceeds 100 m. The median first-stage F-statistic is 10.4. We use a Gaussian kernel with a locally varying bandwidth that is inversely related to the density of observations. Confidence bands are at the 95% level.

The results in Figure A4 support the engineering-based hypothesis that bedrock at intermediate intermediate depths reduces the construction cost of tall buildings. Within the sample of buildings for which we observe height, construction cost, and floor area, the marginal cost of increasing height is minimized at a bedrock depth of about 10 to 15 m. At depths below about 5 m or greater than 23 m, the cost of height is significantly larger. This range is roughly consistent with the descriptive evidence from Figures 4 and A3, given an average building height of 109 m in our sample. Yet, it appears that the causal estimation approach yields somewhat lower optimal bedrock depths, perhaps because deeper bedrock is correlated with other geological factors that add to construction cost. More importantly, the results from Figure A4 support the idea that as demand for height increases over time, cities with bedrock within an intermediate range will have a greater ease of accommodating that demand, resulting in lower barriers to growth.

H.5 Cost of height over time

As discussed in more detail by Ahlfeldt and Barr (2022a), several technological innovations have contributed to the emergence of tall buildings as an increasingly widespread urban phenomenon. Around the turn from the 19$^{\text{th}}$ to the 20$^{\text{th}}$ century, the elevator and and the steel frame made tall commercial and residential structures economically viable. From the 1960$^{\text{th}}$, mainframe allowed for more sophisticated structural engineering that allowed for lighter and taller buildings that could withstand large collateral wind loads. Improvements in software and hardware have ever since allowed to design tall buildings more efficiently. In the near future, the magnetic elevator is expected to remove yet another barrier to vertical growth.

It is, therefore, reasonable to expect a secular downward trend in the cost of height. Indeed, indirect evidence from correlations of land prices and building heights substantiates this hypothesis (Ahlfeldt and McMillen, 2018; Ahlfeldt and Barr, 2022a). We use our construction cost data set to directly test the hypothesis that the height elasticity of construction cost has decreased over time. Since different parts of the world have adopted the skyscraper technology at different points in time, we focus on the US—the only country where we can estimate the cost of height throughout the 20$^{\text{th}}$ century—to avoid changes in our estimates of the cost of height over time being driven by the international composition of the sample. In Table A3, we report the results from instrumental variable regressions of a log cost measure against the log of height and an interaction with a yearly time trend. We normalize this trend to have a value of zero in 1975, the beginning of our observation period in the main stages of our analyses. Hence, the coefficient on the non-interacted log height variable gives the height elasticity of cost in 1975 while the coefficient on the interaction reveals how this elasticity changes over time. All estimates control for city fixed effects, decade fixed effects and a yearly time trend. Columns (1) presents OLS estimates. Column (2) presents 2SLS estimates where the log distance from the city center (the median coordinate of bildings exceeding 100 m or the tallest building if shorter) and its interaction with a time trend serve as instrumental variables. Both models confirm the hypothesis that the cost of height has decreased over time. The OLS estimates point to a reduction in the height elasticity of costs by slightly less than one percentage point per year. The 2SLS estimates are significantly larger, pointing to a reduction of 2.2 percentage points per year.

To allow for greater flexibility in the time trend, we use LWR-IV specification similar to the one described by Eqs (31), (32) and, (33). The only difference is that we use the year instead of bedrock as a covariate in the univariate kernel and employ a constant bandwidth of $\kappa = 30$ since we have no priors regarding when we should expect greater changes in the cost of height. Figure A5 confirms that the height elasticity of cost has declined since the beginning of the 20$^{\text{th}}$ century. Hence, the evidence supports the notion of a secular downward trend in the cost of height that should act as supply-side driver of vertical growth.

Table A3: Cost of height over time

	(1) Ln cost per space		(2) Ln cost per space	
Ln height	0.255***	(0.08)	0.578**	(0.26)
Year - 1975	0.086***	(0.01)	0.146***	(0.04)
Ln height × Year - 1975	-0.008***	(0.00)	-0.022**	(0.01)
KPF	-		3.13	
City FE	Yes		Yes	
Decade FE	Yes		Yes	
IV	-		Yes	
Observations	554		554	
R^2	.819		-	

Notes: Unit of observation is building. All buildings with height $\leq$ 55 m excluded. The sample considts of 591 constructions in US cities (see Panel A in Table A2). Robust standard errors in parentheses are clustered on cities. In (1), instrumental variables are log distance from center and the interaction a yearly time trend. The city center is defined as the median coordinate of buildings exceeding 100 m height and or the tallest building where building exceeds 100 m.The sample used is the one summarized in Panel A of Table A2 (US cities). * $p < 0.1$, ** $p < 0.05$, *** $p < 0.01$.

Figure A5: Construction cost as function of height and bedrock depths

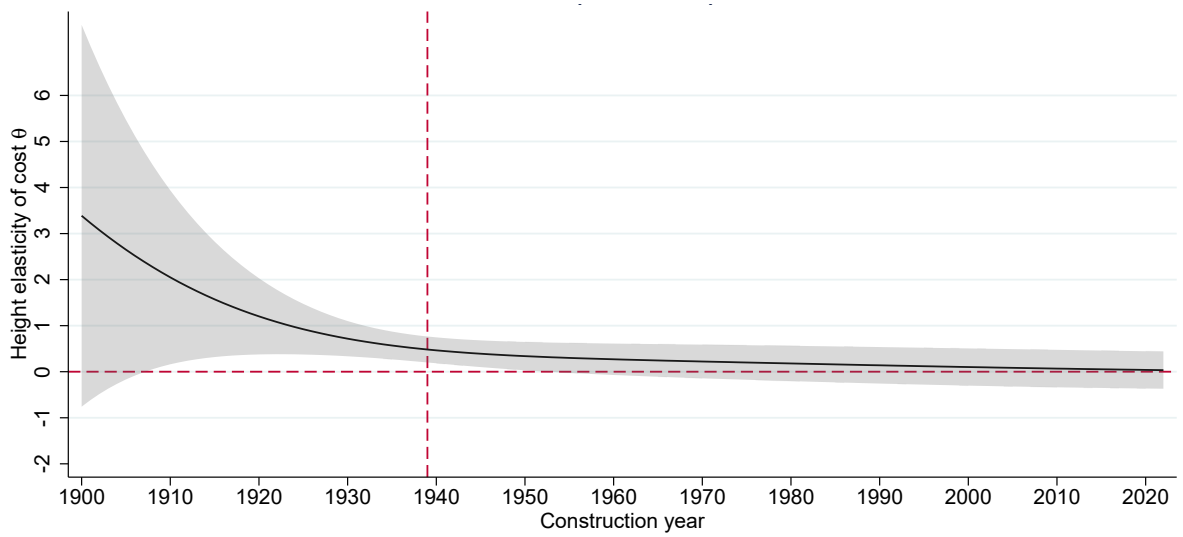

Notes: We show non-parametric estimates of the cost of height from an LWR-IV approach. In each LWR, we estimate the height elasticity from a regression of the log of construction cost per floor area against building height, controlling for city fixed effects and decade of construction effects. We use distance from the city center as an instrumental variable for height. The city center is defined as the median coordinate of buildings exceeding 100 m height and or the tallest building where building exceeds 100 m. We use locally weighted regressions with a univariate Gaussian kernel and a bandwidth of four to estimate local means of the cost measure for varying bedrock depths. Confidence bands are at the 95% level. The sample consists of 591 constructions in US cities (see Panel A in Table A2).

H.6 Further First Stage Evidence

Figure 5 shows that between 1975 and 2015 larger cities on more favorable bedrock experienced more rapid height growth. The following figure demonstrates that, as predicted, this comes from there being a more muted relationship in 1975 than in 2015, but both with the same shape.

Table 1 presents the main first stage coefficients. Remaining coefficients are shown in the following table.

Figure A6: Relationships Between Tall Buildings and ln 1975 Population by Bedrock Depth in 1975 and 2015

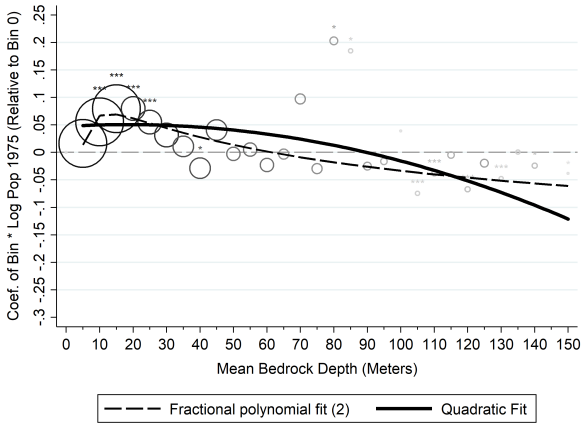

(a) Tall Building Indicator, 1975

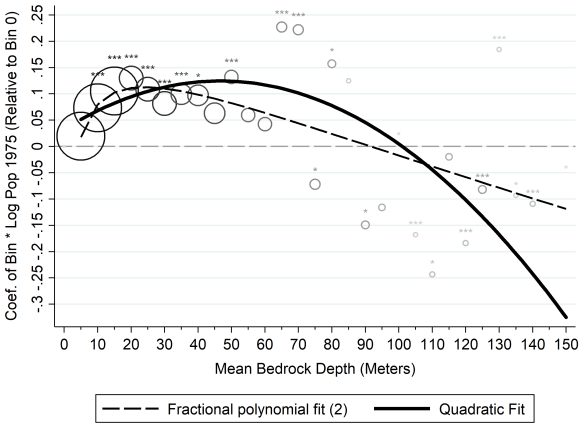

(b) Tall Building Indicator, 2015

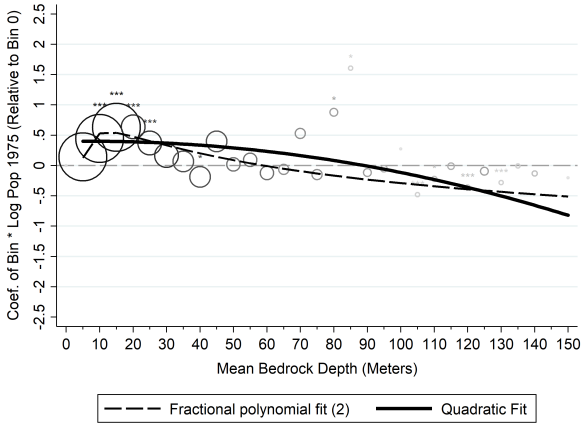

(c) ln Sum of Heights, 1975

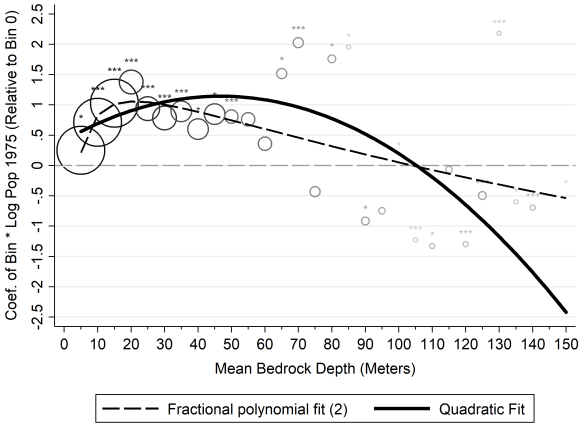

(d) ln Sum of Heights, 2015

Notes: The top panels graph coefficients on ln 1975 city population for each 5 meter bin of bedrock depth in which the dependent variable is an indicator for whether the city had any height growth. The bottom panels graph analogous coefficients in which the dependent variable is the ln sum of heights constructed. 1975 is on the left and 2015 is on the right.

I Empirical analysis

This section complements Section 3 in the main paper.

I.1 Robustness of Main IV estimates

Table A5 shows coefficients on control variables in Panel A of Table 2.

Table A6 shows robustness of our baseline results to various specification checks.

Table A7 shows that our baseline results are robust to controlling within (subways) and between (highways) city accessibility and various geographic feature that could be correlated with bedrock. Table A9 shows robustness with respect to various spatial fixed effects. Table A8 shows our IV estimates are not driven by a small number of countries with great variation in

Table A4: First-Stage Estimates: Remaining Coefficients

	Tall Building Indicator			ln (Heights + 1)		
	1975	2015	Δ 1975-2015	1975	2015	Δ 1975-2015
			Panel A: All Countries			
ln Pop 1975	0.0773***	0.1286***	0.0512***	0.5272***	1.0025***	0.4753***
	[0.0076]	[0.0093]	[0.0093]	[0.0498]	[0.0769]	[0.0653]
Bedrock Depth	-0.0208***	-0.0538***	-0.0330***	-0.1473***	-0.4721***	-0.3248***
	[0.0054]	[0.0079]	[0.0079]	[0.0362]	[0.0698]	[0.0612]
(Bedrock Depth)^2	0.0002***	0.0005***	0.0002**	0.0018***	0.0039***	0.0021**
	[0.0001]	[0.0001]	[0.0001]	[0.0004]	[0.0011]	[0.0009]
			Panel B: Developing Economies			
ln Pop 1975	0.0517***	0.1140***	0.0623***	0.2998***	0.8206***	0.5208***
	[0.0079]	[0.0098]	[0.0098]	[0.0477]	[0.0804]	[0.0674]
Bedrock Depth	-0.0048	-0.0420***	-0.0372***	-0.0353	-0.3417***	-0.3064***
	[0.0055]	[0.0078]	[0.0084]	[0.0323]	[0.0687]	[0.0638]
(Bedrock Depth)^2	0.0001	0.0003***	0.0003**	0.0005*	0.0025**	0.0020**
	[0.0000]	[0.0001]	[0.0001]	[0.0003]	[0.0010]	[0.0009]

Notes: This table reports additional coefficient estimates from regressions in Table 1. Regressions in Panel A have 12,849 observations and those in Panel B have 11,257 observations.

Table A5: Main IV Results: Remaining Coefficients

Period s-t:	Δ ln Pop 1975-2015	Δ ln Built Area 1975-2015	Δ ln Urban. Area 1975-2015	Δ ln Pop Dens. 1975-2015	Δ ln Lights 1990-2015
ln Initial Pop s	-0.12***	0.24***	-0.68***	-0.37***	-0.15***
	[0.03]	[0.03]	[0.06]	[0.04]	[0.04]
Bedrock Depth	0.00***	0.00***	0.02***	-0.00*	0.00**
	[0.00]	[0.00]	[0.00]	[0.00]	[0.00]
(Bedrock Depth)^2	-0.00	-0.00**	-0.00***	0.00	-0.00
	[0.00]	[0.00]	[0.00]	[0.00]	[0.00]

Notes: This table shows coefficients on control variables for our main IV regressions in Table 2 Panel A.

Table A6: Checks on the Main IV Specification

	1975-2015				1990-2015			
Outcome	ln Pop	ln BltAr	ln BltAr	Δ ln BltAr	Δ ln Pop	Δ ln BltAr	Δ ln Pop	Δ ln BltAr
2015 ln Heights	0.09***	-0.11***						
	[0.02]	[0.02]						
Δ ln Heights			-0.12***	-0.12***	0.11***	-0.24***	0.09***	-0.23***
			[0.03]	[0.03]	[0.03]	[0.05]	[0.03]	[0.05]
First Stage F	41.97	35.5	23.92	23.92	16.83	16.83	15.14	15.14
1975 ln Pop	Yes	Yes	Yes	Yes	No	No	Yes	Yes
1990 ln Pop	No	No	No	No	Yes	Yes	No	No
1975 ln Built Area	No	Yes	Yes	Yes	No	No	No	No

Notes: Results are analogous to those in Table 2. The first 2 columns show results of regressions of 2015 levels on 2015 log heights, controlling for 1975 levels. The following 2 columns are also for the 1975-2015 period. Remaining columns are for the 1990-2015 period.

bedrock depth.

Table A7: Robustness of Results in Table 2 with Various Controls

	(1)	(2)	(3)	(4)	(5)	(6)	(7)
Panel A:	Dependent Variable = Δ ln Population; All Countries						
Δ ln Height	0.12***	0.12***	0.09***	0.13***	0.13***	0.12***	0.13***
	[0.03]	[0.03]	[0.03]	[0.04]	[0.03]	[0.03]	[0.03]
Panel B:	Dependent Variable = Δ ln Built Area; All Countries						
Δ ln Height	-0.17***	-0.18***	-0.19***	-0.08**	-0.18***	-0.18***	-0.18***
	[0.04]	[0.03]	[0.04]	[0.04]	[0.03]	[0.03]	[0.04]
Observations	12,849	12,849	12,647	9,698	12,807	12,807	12,849
F-statistic	28.42	32.22	25.08	15.25	29.69	32.52	23.66
Panel C:	Dependent Variable = Δ ln Population; Developing Countries						
Δ ln Height	0.13***	0.14***	0.10***	0.17***	0.13***	0.13***	0.13***
	[0.03]	[0.03]	[0.04]	[0.06]	[0.03]	[0.03]	[0.03]
Panel D:	Dependent Variable = Δ ln Built Area; Developing Countries						
Δ ln Height	-0.16***	-0.19***	-0.18***	-0.10*	-0.18***	-0.19***	-0.16***
	[0.04]	[0.04]	[0.05]	[0.05]	[0.04]	[0.04]	[0.04]
Observations	11,257	11,257	11,169	8,141	11,234	11,234	11,257
F-statistic	22.84	24.04	16.22	9.167	24.15	24.34	20.76
Country FE	Yes	Yes	Yes	Yes	Yes	Yes	Yes
Infrastructure Controls	No	Yes	No	No	No	Yes	No
Drop Subway Cities	No	No	Yes	No	No	No	No
Drop Bedrock < 6 meters	No	No	No	Yes	No	No	No
Geographic Controls	No	No	No	No	Yes	Yes	No
Δ ln 100m+ Height	No	No	No	No	No	No	Yes

Notes: Each column presents separate estimates from a variation of the baseline model in Table 2 for the full sample of cities (panels A-B) and the sample of developing country cities (panels C-D). Infrastructure controls are second-order polynomials of log number of subway stations in 1975 and log market access in 1975. Market access for city i is the total sum of the 1975 population of other cities j in the same country weighted by the inverse of Euclidean distance between cities i and j. Geographic controls are second-order polynomials of log Euclidean distance from the coast, log Euclidean distance from a major lake, log mean altitude, the log of the standard deviation in altitude, log agricultural suitability, and log mean annual temperature (1961-1990).

I.2 Construction of Locally-weighted regression estimates

In Section 3, we present height elasticity estimates for various outcomes for groups of cities such as in developed or developing countries. To obtain city-specific estimates of a height elasticity, β^a, we estimate a locally weighted regressions (LWR) variant of our baseline instrumental variable strategy. Concretely, we estimate, for each city $\tilde{a} \in N$, the following second-stage specification:

$$\Delta \ln Y_{ac75-15} = \beta^{\tilde{a}} \Delta \ln H_{ac75-15} + \sum_{n=1}^{2} \alpha_n^{\tilde{a}} (B_{ac})^n + \alpha_3^{\tilde{a}} \ln P_{ac75} + \kappa_c^{\tilde{a}} + \mu_{ac}^{\tilde{a}}$$

In each LWR-IV regression indexed by $\tilde{a} \in N$, a second-order polynomial of city-level mean bedrock depth interacted with 1975 log city population serve as instrumental variables for $\Delta \ln H_{ac75-15}$. Notice that expect for the subscript $\tilde{a}$ that denote city-specific estimates, all variables are defined as in Section 3 in the main paper. In each LWR $\tilde{a} \in J$ we weigh observations by the Gaussian kernel weight

$$W_a^{\tilde{a}} = \frac{w_a^{\tilde{a}}}{\sum_{j=a}^{N} w_a^{\tilde{a}}}, \text{where}$$
$$w_a^{\tilde{a}} = \frac{1}{\kappa^{\tilde{a}}\sqrt{\pi}} \exp\left[-\frac{1}{2}\left(\frac{\ln P_a - \ln P^{\tilde{a}}}{\kappa^{\tilde{a}}}\right)^2\right],$$

Where $\kappa^{\tilde{a}}$ governs the bandwidth and $\ln P_a - \ln P^{\tilde{a}}$ gives the log difference between the population of any city a and the target city $\tilde{a}$ for which a local value of β is being estimated. Intuitively, a city a will receive a higher weight in a LWR $\tilde{a} \in J$, the more similar its population is to that of city $\tilde{a}$.

We employ a LWR-specific bandwidth because we wish to allow for a more flexible fit via a smaller bandwidth in the more populated part of the population distribution, whereas we wish to reduce standard errors in the right tail of the population distribution that is more sparsely populated. To this end, we use a variant of Scott's rule of thumb for bandwidth selection and define

$$\kappa^{\tilde{a}} = \mathcal{M}\frac{3.49\hat{\sigma}^{\tilde{a}}_{\ln P}}{(N^{\tilde{a}})^{\frac{1}{3}}},$$

where the standard deviation $\hat{\sigma}^{\tilde{a}}_{\ln P}$ and the number of observations $N^{\tilde{b}}$ are computed for rolling subsamples that satisfy $|\ln P_a - \ln P^{\tilde{a}}| \leq \mathcal{B} = 5$. We scale the rule-of-thumb bandwidth by a factor of $\mathcal{M} = 20$ since the non-parametric estimation of derivatives generally requires larger bandwidths than the estimation of levels (Henderson and Parmeter, 2015, Section 5.9). Importantly, these choices ensure that we can distinguish our point estimates from zero with nearly 95% confidence throughout the population distribution.

We present our LWR estimates of the height elasticity for the outcomes population, built-up area, and urban area in Figures A7, A8, and A9. We observe that the height elasticity of population is u-shaped with respect to initial city size. This pattern is suggestive of a sizable extensive-margin effect (introducing tall buildings) coupled with an intensive-margin effect (vertical growth conditional on having tall buildings) that increases in city size. It is noteworthy that the turning point is reached at a population of about $\exp(13.8) = 1M$, which has been found to about the threshold when cities typically adopt the skyscraper (buildings taller than 150 m) technology (Ahlfeldt and Barr, 2022a).

The convex intensive-margin effect is plausible as a vertical expansion is likely to have a greater impact on a city's capacity to accommodate residential and commercial uses when a city has exhausted its potential for horizontal expansion. Consistent with this hypothesis, we find that a large city's area (built-up and urban area) is relatively insensitive to a technology-induced increase in height (due to favorable bedrock). The implication is that less vertical growth

cannot easily be compensated by greater horizontal growth. In contrast, the land area is much more responsive to technology-induced vertical growth in small cities. This is intuitive since small cities can more easily grow horizontally if the cannot grow vertically (due to unfavorable bedrock conditions).

Figure A7: LWR estimates of height elasticity of population

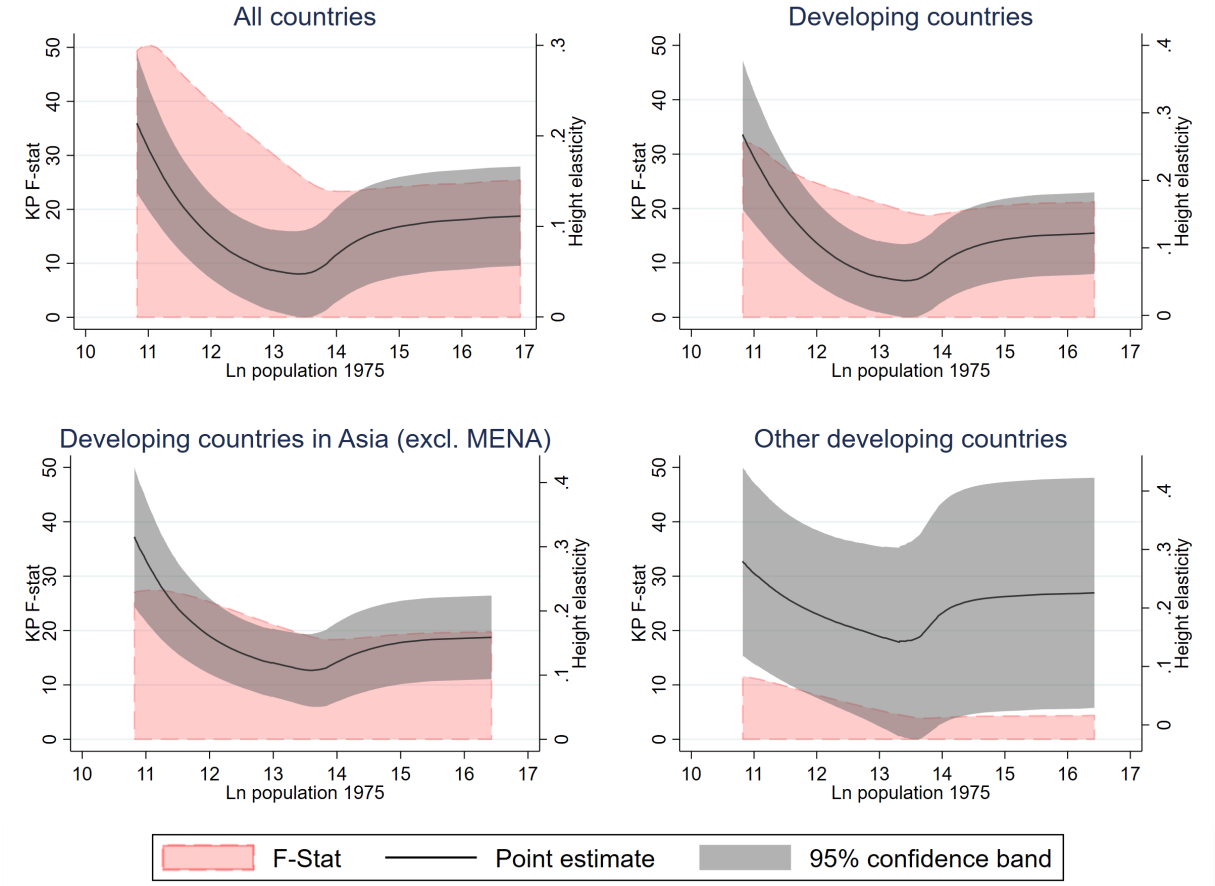

Note: We show non-parametric estimates of the height elasticity from an LWR-IV approach. In each LWR, we estimate the height elasticity from a regression of the 1975-2015 long-difference in the log outcome against the long-difference in log building height using a second-order polynomial of bedrock depth interacted with initial 1975 log population as instrumental variables. Controls are a second-order polynomial of bedrock depth, initial log population, and country fixed effects. We use a Gaussian kernel with a locally varying bandwidth that is inversely related to the density of observations. Confidence bands are at the 95% level.

I.3 Aggregated effects by category

It is straightforward to obtain the absolute change in an outcome ΔY_{a75-15} caused by change in height ΔH_{a75-15} based on the value of the outcome in the initial period Y_{a75} and a causally estimated value (capturing the supply-side channel, exclusively) of a height elasticity β^a for city a:

$$\Delta Y_{a75-15} = Y_{a75} \times (\exp(\beta^a \times \Delta H_{a75-15}) - 1) \tag{34}$$

This city specific-effect effects can then be aggregated to arbitrary groups. We present results for groups of developing-country cities in Table A11. For comparison, we also present results

Figure A8: LWR estimates of height elasticity of built-up area

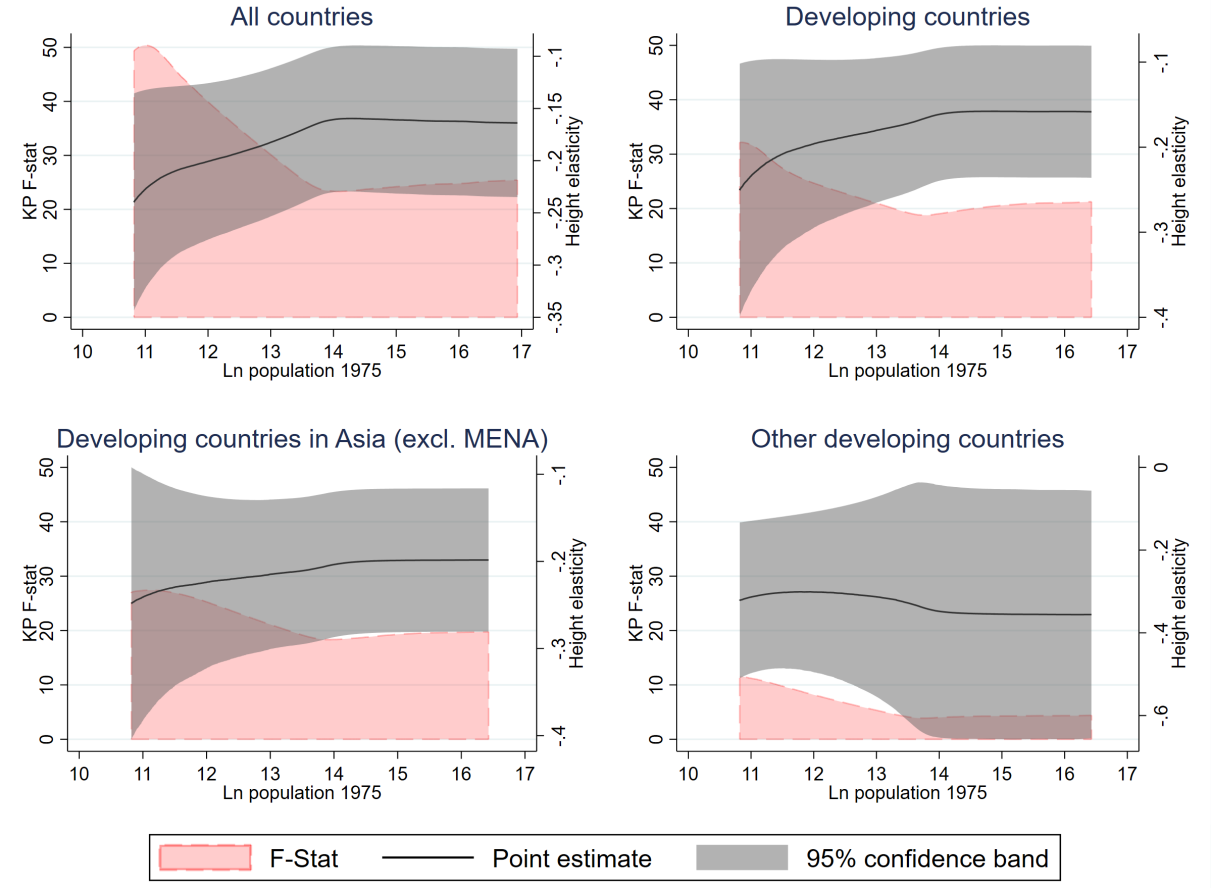

Note: We show non-parametric estimates of the height elasticity from an LWR-IV approach. In each LWR, we estimate the height elasticity from a regression of the 1975-2015 long-difference in the log outcome against the long-difference in log building height using a second-order polynomial of bedrock depth interacted with initial 1975 log population as instrumental variables. Controls are a second-order polynomial of bedrock depth, initial log population, and country fixed effects. We use a Gaussian kernel with a locally varying bandwidth that is inversely related to the density of observations. Confidence bands are at the 95% level.

for cities in the USA and Canada. Many other developed countries, in particular in Europe, impose strong height constraints. This implies that height and location of tall buildings are determined by planners instead of profit-maximizing developers, rendering the economic reasoning underlying our first-stage regressions inapplicable.

J Model

J.1 Equilibrium solver

For given values of $\{y, \bar{U}\}$, parameters $\{\alpha^U, \beta, \omega^U, \theta^U, \tau^U, \underline{x}^U, \bar{a}^U, \tilde{c}^U, \bar{S}^U, r^a, \zeta, \ell, \tilde{U}\}$, and the endowment $\bar{N}$ there is a unique mapping to all other endogenous object. Hence, the equilibrium can be references by $\{y, \bar{U}\}$. To solve for these equilibrium values, we implement an algorithmic procedure that we describe in pseudo-code in Algorithm 1.

Figure A9: LWR estimates of height elasticity of urban area

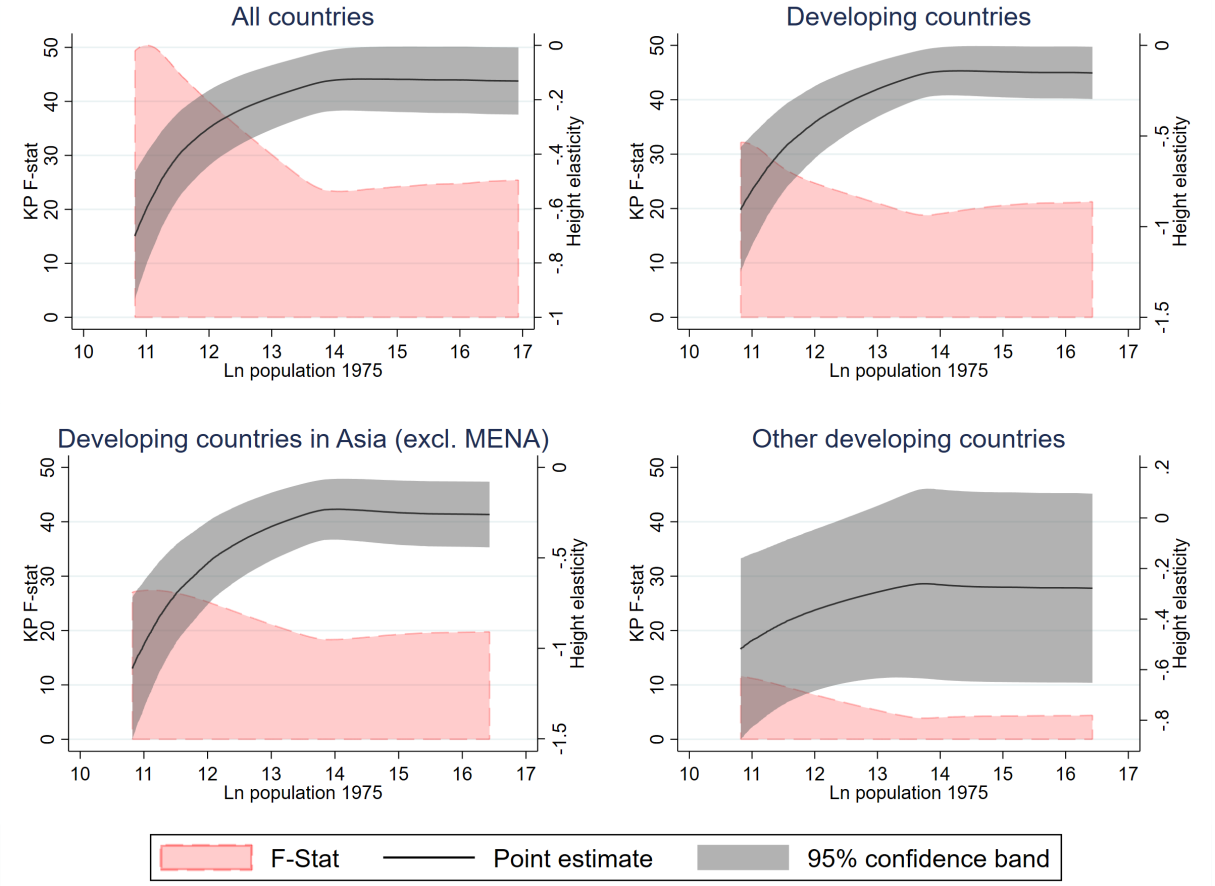

Note: We show non-parametric estimates of the height elasticity from an LWR-IV approach. In each LWR, we estimate the height elasticity from a regression of the 1975-2015 long-difference in the log outcome against the long-difference in log building height using a second-order polynomial of bedrock depth interacted with initial 1975 log population as instrumental variables. Controls are a second-order polynomial of bedrock depth, initial log population, and country fixed effects. We use a Gaussian kernel with a locally varying bandwidth that is inversely related to the density of observations. Confidence bands are at the 95% level.

Algorithm 1: Equilibrium solver

Data: Given values for primitives $\{\alpha^U, \beta, \omega^U, \theta^U, \tau^U, \underline{x}^U, \bar{a}^U, \tilde{c}^U, \bar{S}^U, r^a, \zeta, \ell, \bar{N}, \tilde{U}\}$
Guesses of equilibrium values of $\{\bar{U}, y\}$

while $\bar{U} \neq \widehat{\bar{U}}$ *or* $y \neq \hat{y}$ **do**
- Compute N using Eq. (12)
- Compute $\bar{p}^U(x)$ using Eqs. (15) & (17) Compute $\tilde{S}^U(x)$ using Eq. (18)
- Compute $r^U(x)$ using Eq. (19)
- Allocate land use using Eq. (**??**)
- Compute market-clearing wage $\hat{y}$ using Eqs. (21) and (23)
- Compute endogenous city-utility $\widehat{\bar{U}}$ using Eq. (26)
- Update guesses to weighted combination of old guesses and $\{U, \hat{y}\}$

Result: Equilibrium values of $\{\bar{U}, y\}$

J.2 Quantification

This section adds to Section 4.2 in the main paper.

J.2.1 Amenity decay (τ^U)

In the absence of binding height limits, we can use Eq. (18) to obtain:

$$\ln S^U(x_1) = \ln S^U(\underline{x}) - \frac{\tau^U}{(1-\alpha^U)(\theta^U-\omega^U)} x_1.$$

Since the land area of a city is $\mathcal{L} = \ell\pi(x_1)^2$, we can solve for the amenity decay parameter:

$$\tau^U = (1-\alpha^U)(\theta^U-\omega^U)\frac{\ln S^U(x_1) - \ln S^U(\underline{x})}{\sqrt{\frac{\mathcal{L}}{\ell\pi}}}$$

We assume that the average height of a residential building at the city margin, $\ln S^R(x_1)$, is about 1.5 floors (5 m). As a measure of residential height within the city core, $\ln S^R(\underline{x})$, we use the average height of the five tallest residential buildings in the city. Using the measure of city area, $\mathcal{L}$, observed in our data and the set values of parameters $\{\alpha^R, \theta^R, \omega^R, \ell\}$, we obtain a distribution of city-specific decay parameters summarized in Figure A10. We find that the decay parameter tends to be smaller in larger cities, maybe because these tend to be better connected by high-speed transport infrastructure such as highways and subways. Since, in our baseline parametrization, we target a city with a population with 2M, we set the decay parameter to 0.03 for both uses. Both rates of decay reflect the cost of moving workers in space (not goods), so it is reasonable to assume that they are comparable.

Figure A10: Amenity decay τ^R

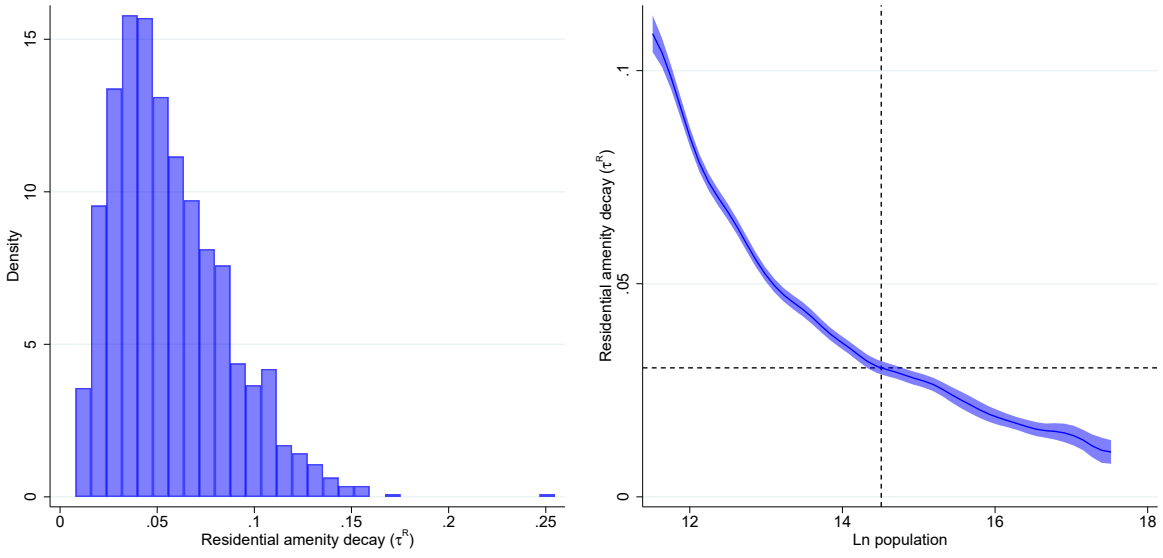

Note: The right panel reports estimates of conditional means obtained from locally weighted polynomial regressions.

J.2.2 Scale parameters $(\ell, a^U, c^U, r^a, \tilde{U})$

The scale parameters $\ell, a^U, c^U, r^a, \bar{N}, \tilde{U}$ do not affect the steepness of the height gradient, but they govern the attractiveness of the city relative to the rural hinterland and, hence, total population, area, and height.

The mean area in 2015 in our data is 22 km^2 (s.d. 114). The built-up area is 51 km^2 (s.d. 190). Since, on average, the total area is about twice the built-up area, we set $\ell = 0.5$. We set $a^C = a^R = 2, c^C = c^R = 150, r^a = 50, \bar{N} = 10\text{M}$ and use Eq. (12) to invert the rural utility

$$\tilde{U} = \frac{1-\mu}{\mu}\bar{U}^{\zeta} \tag{35}$$

for a chosen urbanization rate using a numerical procedure described in Algorithm 2.

Under these values we obtain a height of about 35 floors within the urban core in the baseline with $\mu = 0.2$, which is close to the mean height of the five tallest buildings in a city with a 2M population in our data.

Algorithm 2: $\tilde{U}$ inverter

Data: Given values of primitives $\{\alpha^U, \beta, \omega^U, \theta^U, \tau^U, \underline{x}^U, \bar{a}^U, \tilde{c}^U, \bar{S}^U, r^a, \zeta, \ell, \bar{N}\}$
Guess of $\tilde{U}$
User-chosen μ

while $\tilde{U} \neq \widehat{\tilde{U}}$ **do**
  Compute $\bar{U}$ using Algorithm 1
  Compute rural utility, $\widehat{\tilde{U}}$, using Eq. (35)
  Update guess of $\tilde{U}$ to weighted combination of old guess and $\widehat{\tilde{U}}$

Result: $\tilde{U}$ that rationalizes given μ

J.2.3 Preference heterogeneity

We seek to find the value of ζ under which the model generates our key moments in the data: Our estimates of the height elasticity of population, $\hat{\beta}^N$, and the height elasticity of area, $\hat{\beta}^{\mathcal{L}}$. In our empirical identification strategy, we exploit subsoil geography to ensure that we identify these parameters from variation in the cost of height, holding housing demand factors constant. Since we have full control over the data-generating process, it is straightforward to mimic this source of variation in the model.

To this end, we solve the model multiple times for values of $\theta \in \Theta$, where $\theta^C = \theta$ and $\theta^R = \theta + 0.05$ to maintain the same difference between the commercial and residential height elasticity as in the baseline specification in Table 6. Holding all other parameters constant, we obtain differences in equilibrium outcomes that are solely driven by variations in the cost of height. To operationalize our SMM approach, we nest this loop over $\theta \in \Theta$ within a search over a parameter space defined by $\zeta \in \mathcal{Z}$ and $\mathcal{T} \in \mathcal{R}$. Notice that we invert $\tilde{U}$ using Eq. (35) each time we adjust ζ, setting $\mu = \bar{\mu}$ and all parameters to the values in Table 6 to keep the city

population constant. For each combination of $\{\theta, \zeta, \mathcal{T}\}$, we solve the model and compute the endogenous outcomes city area

$$\mathcal{L}_\theta^{\zeta,\mathcal{T}} = \int_0^{(x_1)^{\theta,\zeta,\mathcal{T}}} \mathcal{L}(x)dx,$$

city population

$$N_\theta^{\zeta,\mathcal{T}} = \int_{(x_0)^{\theta,\zeta,\mathcal{T}}}^{(x_1)^{\theta,\zeta,\mathcal{T}}} (n(x))^{\theta,\zeta}dx,$$

and city tall building height

$$H_\theta^{\zeta,\mathcal{T}} = \int_0^{(x_1)^{\theta,\zeta,\mathcal{T}}} \mathcal{L}(x)\left((S^C(x))^{\theta,\zeta} - \mathcal{T}\right)dx + \int_{(x_0)^{\theta,\zeta,\mathcal{T}}}^{(x_1)^{\theta,\zeta,\mathcal{T}}} \mathcal{L}(x)\left((S^R(x))^{\theta,\zeta} - \mathcal{T}\right)dx. \tag{36}$$

For each combination of $\{\zeta, \mathcal{T}\}$, we run the following regressions on the model-based outcomes to recover our moments in the model $\{\tilde{\beta}^N, \tilde{\beta}^{\mathcal{L}}\}$:

$$\ln \mathcal{L}_\theta^{\zeta,\mathcal{T}} = c^{\mathcal{L},\zeta,\mathcal{T}} + \tilde{\beta}_{\zeta,\mathcal{T}}^{\mathcal{L}} \ln H_\theta^{\zeta,\mathcal{T}} + \tilde{\epsilon}_\theta^{\mathcal{L},\zeta,\mathcal{T}}$$
$$\ln N_\theta^{\zeta,\mathcal{T}} = c^{N,\zeta,\mathcal{T}} + \tilde{\beta}_{\zeta,\mathcal{T}}^{N} \ln H_\theta^{\zeta,\mathcal{T}} + \tilde{\epsilon}_\theta^{N,\zeta,\mathcal{T}}$$

We find our preferred combination of $\{\zeta, \mathcal{T}\}$ by minimizing the value of the residual sum of squares of the moments in model and data:

$$\zeta, \mathcal{T} = \arg \min_{\zeta \in \mathcal{Z}, \mathcal{T} \in \mathcal{R}} \sum_{o \in N, \mathcal{L}} \left(\hat{\beta}^o - \tilde{\beta}^o\right)^2 \tag{37}$$

We provide a compact summary of the procedure using pseudo code Algorithm 3.

Algorithm 3: Calibrating $\{\zeta, \mathcal{T}\}$

Data: Given values of primitives $\{\alpha^U, \beta, \omega^U, \theta^U, \tau^U, \underline{x}^U, \bar{a}^U, \tilde{c}^U, \bar{S}^U, r^a, \zeta, \ell, \bar{N}\}$
Moments in data $\{\widehat{\beta}^N, \widehat{\beta}^{\mathcal{L}}\}$
User-chosen μ

foreach $\zeta \in \mathcal{Z}$ **do**
  Use Algorithm 2 to invert $\tilde{U}$ so to match $\mu = 0.2(\Rightarrow)N = \mu\bar{N} = 2M)$ under baseline values of $\{\theta^C = 0.5, \theta^R = 0.55\}$
  foreach $\mathcal{T} \in \mathcal{R}$ **do**
    foreach $\theta \in \Theta$ **do**
      Use Algorithm 1 to solve for equilibrium outcomes of $\{\mathcal{L}_\theta^{\zeta,\mathcal{T}}, N_\theta^{\zeta,\mathcal{T}}, H_\theta^{\zeta,\mathcal{T}}\}$
    foreach $o \in N, \mathcal{L}$ **do**
      Regress $\ln o_\theta^{\zeta,\mathcal{T}}$ against $\ln H_\theta^{\zeta,\mathcal{T}}$ to obtain model moment $\tilde{\beta}^o$

Use moments in data $\{\widehat{\beta}^N, \widehat{\beta}^{\mathcal{L}}\}$ and model $\{\tilde{\beta}^N, \tilde{\beta}^{\mathcal{T}}\}$ in Eq. 37 to find $\{\zeta, \mathcal{T}\}$

Result: $\{\zeta, \mathcal{L}\}$ values that match moments in model and data

Guided by Figure A4, we define a grid of height costs $\Theta = \{0.2, 0.3, ..., 1\}$. Further, we set $\bar{mu} = 0.2$. We search over $\mathcal{Z} = \{0, 0, 1, ..., 5\}$ and $\mathcal{R} = \{0, 1, ..., 20\}$. For the moments in the data, we use $\hat{\beta}^N = 0.22$ and $\hat{\beta}^{\mathcal{L}} = -0.38$ from Table XXX estimated from a subset of cities that are relatively unconstrained by height regulation. Under $\zeta = 1.8$ and $\mathcal{T} = 4$, we almost exactly match the moments. Figure A11 plots the value of the objective function against the two dimensions of the parameter space. There is a clearly defined minimum in the objective function at our identified value of ζ. In contrast, the choice of $\mathcal{T}$ is less consequential. As long as $\mathcal{T} \geq 3$, the model generates height elasticities that are close to those estimated from data. It is plausible that we obtain the best fit under a value of $\mathcal{T} = 4$ (corresponds to about 15 m) that is smaller than the bottom-coding in the data (55 m). To see this, consider that the model generates an average height of 14 floors, which corresponds to 55 m. Setting $\mathcal{T} = 15$, we would generate a tall building height measure in the model of $H = 0$. In reality, we would most likely observe a positive value for H because the mean height of 55 m would be generated by a mix of taller and shorter buildings.

Figure A11: Value of objective function by $\zeta, \mathcal{T}$

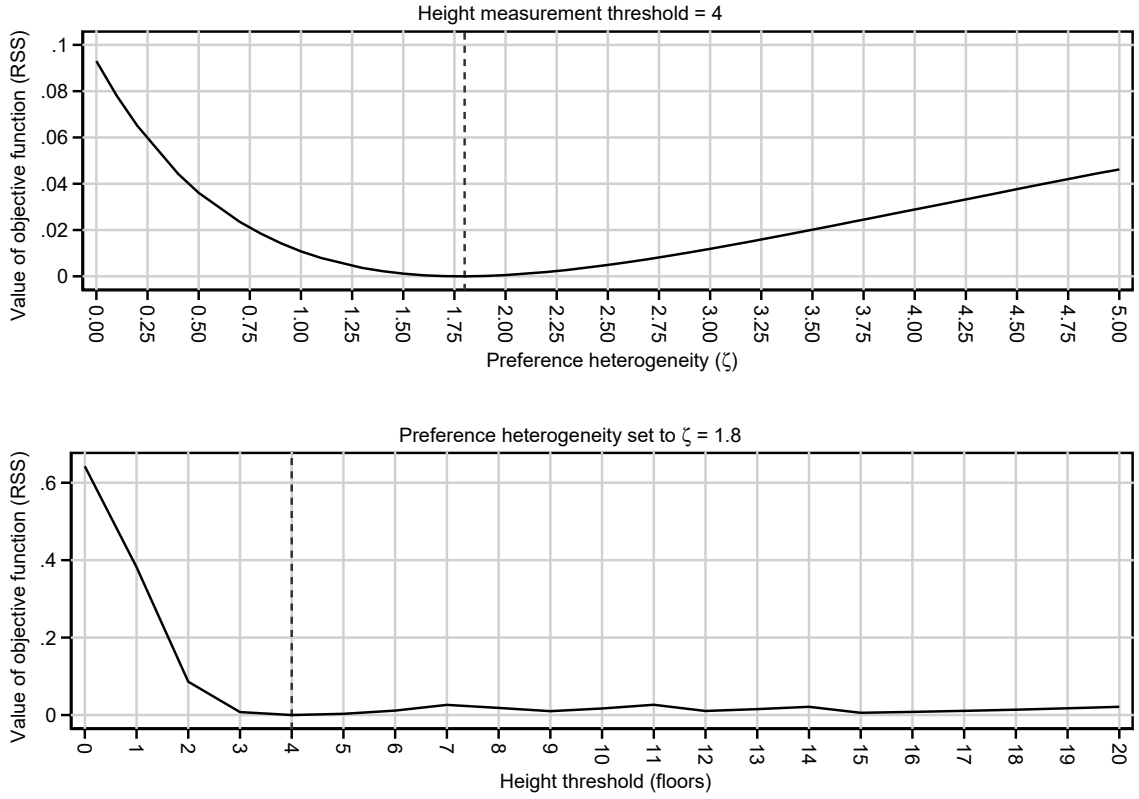

Note: Value of objective function is the residual sum of squares of moments in model and data (height elasticity of are and height elasticity of population).

Figure 8 provides some intuition into how matching moments in model and data pins down ζ. At $\zeta = 0$, workers are immobile. Therefore, the population does not respond to supply-induced changes in supply. Consequently, a vertical expansion leads to a relatively large contraction of the city area. Given a fixed population, the added supply of floor space results in lower rents. This implies lower costs to firms, leading to an expansion of floor space input, production, labor

demand, and, eventually, higher wages. At higher values of ζ, we observe a larger population response to the supply-driven reduction in rent. The larger the population response, the smaller the response in the other outcomes. Since the relationships between height elasticities and ζ are monotonic, we obtain the well-behaved objective functions displayed in Figure A11.

J.3 Counterfactuals

This section compliments Section 4.3 in the main paper.

J.3.1 Illustrative examples

Figure 9 in the main paper illustrates gradients in selected model outcomes under the baseline parameterization (first row) and two counterfactuals in which we increase the cost of height by 20% (second row) and add a binding height limit (third row). The first two columns in Table A12 report relative changes in various model outcomes from the baseline parameterization to these counterfactuals.

In keeping with intuition, both counterfactuals, which correspond to negative floor space supply shocks, deliver a lower urban indirect utiltiy, and consequentially, a lower urban population and expected utility, overall. As the city contracts vertically, it expands horizontally, resulting in a larger total urban area. As visible in Figure 9, the CBD expands horizontally, pushing the residential zone outwards. As a result, commuting costs, $\exp(\tau^R \times x)$, increase. This is one of the main mechanisms through which the height constraints will affect residents indirectly, even if a height limit primarily affects commercial developments. The other channel is the wage. For one thing, limits to vertical development displace firms to less productive locations. For another, the cost of commercial floor space increases. Both act as negative shocks to labor demand, lowering the equilibrium wage. Since greater commuting costs and lower wages imply lower housing demand, residential rents do not necessarily increase by much, even if residential floor space supply falls. Indeed, residential rents even decrease by about 15% in the counterfactual where we impose a height ban. Given the expenditure share on housing of one-third, the ceteris paribus effect on indirect utility amounts to about 5%. This effect compensates for commuting cost and wage effects, each of which amounts to about 8%, resulting in a negative net effect on indirect urban utility ($\bar{U}$) of about 11%. Since, in this example, we have an urban population share, μ, of slightly below one-fifth, the negative effect on expected utility in the total population is to about 2%.

J.3.2 Heterogeneity in welfare effects

Algorithm 4 uses pseudo code to describe the numerical procedure we use to compute welfare effects for cities of a given cost of height, population, and height gap, which we use in Sections 4.3.2 and 4.4.

Algorithm 4: Welfare effects

Data: Given values of primitives $\{\alpha^U, \beta, \omega^U, \tau^U, \underline{x}^U, \bar{a}^U, \tilde{c}^U, \bar{S}^U, r^a, \zeta, \ell, \bar{N}, \mathcal{T}\}$
City population, Pop_a, observed in data
Height gap, HG_a, observed in data
Bedrock depth, MBD_a, observed in data

Use MBA_a and non-linear mapping in Figure A4 to obtain cost of height, θ_a^C
Set $\theta_A^R = \theta_a^C + 0.05$
Set height limit in model to $\bar{S}^U = \mathcal{T}$
while *Height gap in model,* $\tilde{HG} < HG_a$ **do**
    Use Algorithm 2 to invert rural utility, $\tilde{U}$, that satisfies $\mu\bar{N} = Pop_a$
    Use Eq. (36) to compute constrained tall building height H
    Use Algorithm 1 to solve for counterfactual under no height limit, $\bar{S} = \infty$
    Use Eq. (36) to compute unconstrained tall building height H^*
    Compute $\tilde{HG} = \frac{H}{H^*} - 1$
    Marginally increase height limit in model, $\bar{S}$
Use Algorithm 1 to solve for $\mathcal{W}^{actual}$, where $\mathcal{W} \in \{\mathcal{V}, \mathcal{R}\}$, under calibrated height limit $\bar{S}$
Use Algorithm 1 to solve for welfare $\mathcal{W}^{ban}$ under counterfactual height limit $\bar{S} = \mathcal{T}$
Use Algorithm 1 to solve for welfare $\mathcal{W}^{market}$ under counterfactual height limit $\bar{S} = \infty$
Compute welfare effect of existing tall buildings $\hat{\mathcal{W}}^{actual} = \frac{\mathcal{W}^{actual}}{\mathcal{W}^{ban}} - 1$
Compute welfare potential of tall buildings $\hat{\mathcal{W}}^{potential} = \frac{\mathcal{V}^{market}}{\mathcal{W}^{ban}} - 1$
Compute welfare effect of existing height regulation $\hat{\mathcal{W}}^{regulation} = \frac{\mathcal{V}^{actual}}{\mathcal{W}^{market}} - 1$

Result: Effects of existing tall buildings, all potential tall buildings, and height limits on expected utility $\{\hat{\mathcal{V}}_a^{actual}, \hat{\mathcal{V}}_a^{potential}, \hat{\mathcal{V}}_a^{regulation}\}$ and land rent $\{\hat{\mathcal{R}}_a^{actual}, \hat{\mathcal{R}}_a^{potential}, \hat{\mathcal{R}}_a^{regulation}\}$ for city a

J.3.3 The contribution of tall buildings to welfare

Table A13 replicates Table 7 with the only difference being that we lower the cost of height, θ, by 20%. As a result, all welfare effects by about 50%.

Table A8: Estimates as a Function of Within Country Inequality in Bedrock

	All Countries					Developing Economies				
					Panel A: Δ ln Pop					
Δ ln Height	0.06***	0.06***	0.12***	0.09***	0.13***	0.08***	0.08***	0.13***	0.09***	0.12***
	[0.00]	[0.00]	[0.03]	[0.01]	[0.02]	[0.00]	[0.00]	[0.03]	[0.01]	[0.02]
					Panel B: Δ ln Built Area					
Δ ln Height	-0.01***	-0.01***	-0.17***	-0.03***	-0.13***	-0.02***	-0.02***	-0.16***	-0.03***	-0.12***
	[0.00]	[0.00]	[0.04]	[0.01]	[0.04]	[0.01]	[0.01]	[0.04]	[0.01]	[0.04]
Observations	12,849	12,781	12,781	7,473	7,473	11,257	11,223	11,223	7,402	7,402
Estimator	OLS	OLS	IV	OLS	IV	OLS	OLS	IV	OLS	IV
F-statistic			27.95		23.54			22.74		22.38
Countries in Sample	All	> 5 Cities	> 5 Cities	> 5 Cities	> 5 Cities	All	> 5 Cities	> 5 Cities	> 5 Cities	> 5 Cities
Gini Above 0.75 Only	No	No	No	Yes	Yes	No	No	No	Yes	Yes

Notes: IV regressions use the same specification as those in Table 2. OLS regressions simply do not instrument for change in heights. Differences across columns are in the indicated sample restrictions and estimator used. Gini Above 0.75 indicates that the Gini coefficient of the distribution of bedrock depth across cities within a country exceeds 0.75.

Table A9: Evidence of Displacement Effects: Robustness to Different Fixed Effects and Samples

	(1)-(4) All Economies				(5)-(9) Developing Economies				
					Panel A: Δ ln Pop				
Δ ln Height	0.12***	0.10***	0.15***	0.14***	0.13***	0.10***	0.16***	0.14***	0.13***
	[0.03]	[0.03]	[0.02]	[0.02]	[0.03]	[0.03]	[0.03]	[0.02]	[0.04]
					Panel B: Δ ln Built Area				
Δ ln Height	-0.17***	-0.22***	-0.23***	-0.21***	-0.16***	-0.21***	-0.25***	-0.22***	-0.08
	[0.04]	[0.04]	[0.04]	[0.03]	[0.04]	[0.05]	[0.04]	[0.03]	[0.05]
Level of FE	Baseline	Subregion	Admin 1	Admin 2	Baseline	Subregion	Admin 1	Admin 2	Baseline
Sample	Full	Full	Full	Full	Full	Full	Full	Full	<20% Urb
Observations	12,849	12,873	11,967	7,848	11,257	11,269	10,606	7,439	4,594
IV F-stat	28.42	26.74	35.51	35.52	22.84	20.02	28.96	35.23	9.77

Notes: Columns (1)-(8) present variants of the baseline empirical specification in 2 with the following alternative fixed effects. Subregion: 2018 United Nations Geoscheme, grouping countries into 20 world regions (e.g., South America, Central America, and North America); Admin 1: First-level administrative divisions that subdivide countries into large sub-national units (e.g., provinces for China); Admin 2: Second-level administrative divisions that subdivide countries into smaller sub-national units (e.g., prefectures for China). The final column (9) only uses cities in the sample of developing economies that were less than 20% urbanized in 1975.

Table A10: Including Controls for Market Potential

	Δ ln Pop					Δ ln Built Area				
					Panel A: Full Sample					
Δ ln(Hgt+1)	0.13***	0.13***	0.13***	0.13***	0.13***	-0.19***	-0.19***	-0.18***	-0.20***	-0.18***
	[0.03]	[0.03]	[0.03]	[0.03]	[0.03]	[0.03]	[0.03]	[0.03]	[0.04]	[0.04]
$\Delta \ln MP^H$	0.01**	0.01*	0.01	0.00	0.04*	-0.04***	-0.04***	-0.04***	0.19***	0.09***
	[0.01]	[0.01]	[0.01]	[0.02]	[0.02]	[0.01]	[0.01]	[0.01]	[0.04]	[0.03]
First Stage F	31.66	31.73	31.47	20.60	38.37	31.66	31.73	31.47	20.60	38.37
					Panel B: Developing Economies					
Δ ln(Hgt+1)				0.15***	0.14***				-0.20***	-0.17***
				[0.03]	[0.03]				[0.05]	[0.04]
$\Delta \ln MP^H$				-0.02	0.02				0.18***	0.10***
				[0.02]	[0.02]				[0.04]	[0.03]
First Stage F				22.73	35.38				22.73	35.38
Decay Param	0.33	0.5	1	2	3	0.33	0.5	1	2	3
IV $\Delta \ln MP^H$	No	No	No	Yes	Yes	No	No	No	Yes	Yes

Notes: The sample size is 12,849 Panel A and 11,257 in Panel B. Regressions have the same specification as in Table 2 with the addition of the indicated market potential term and unreported controls for spatially discounted population, mean bedrock depth and mean bedrock depth squared, as is explained in the text. Additional inclusion of individual controls for 1975 population and heights growth in the largest cities in the country or the closest cities in space yield population and built area elasticities that are within 0.01 of those reported in this table.

Table A11: Aggregate effects by country groups

	Pop (mill)	% of 2015	Area (sq km)	% of 2015
All countries	435	12%	-449	–15%
Developing countries	370	13%	-236	–15%
Developing Asia excl. MENA	200	20%	-119	–21%
Other developing countries	484	26%	-161	–17%

Notes: For developing countries, we aggregate city-specific height effects computed according to equation (34) using city-specific height elasticity estimates from Figures A7 and A8.

Table A12: Counterfactuals: Illustrative example

	20% higher cost of height	Binding height limit	Binding height limit under 20% higher cost of height
Total population	–8.91%	–15.06%	–10.07%
Total area	16.75%	13.97%	6.35%
Average commuting cost	2.92%	7.97%	4.83%
Average residential rent	1.23%	–14.86%	–10.59%
Average commercial rent	11.23%	6.33%	0.09%
Average productivity	–0.90%	–5.39%	–4.23%
Wage	–3.08%	–7.63%	–5.17%
Total land value	–1.02%	14.65%	9.85%
Urban utility ($\bar{U}$)	–6.61%	–10.90%	–6.86%
Expected utility ($\mathcal{V}$)	–1.29%	–2.09%	–1.21%

Notes: The first two scenarios directly correspond to the counterfactuals in the second and third rows of Figure 9. Averages are weighted by number of workers.

Table A13: Wefare effects of tall buildings by world regions: 20% lower cost of height

		City characteristics			Expected utility ($\mathcal{V}$)		Agg. land rent ($\mathcal{R}$)	
World region	Urban pop. (BN)	Share large cities	Cost of height θ	Est. height gap	No tall building	Actual height limit	No tall building	Actual height limit
East Asia & Pacific	1.03	55.76%	0.81	43.36%	-3.76%	-0.57%	3.69%	1.31%
Europe & Central Asia	0.36	41.06%	0.61	37.79%	-3.54%	-0.62%	3.61%	1.99%
Latin America & Caribbean	0.35	52.79%	0.58	40.50%	-4.35%	-0.98%	4.50%	2.52%
Middle East & North Africa	0.25	48.82%	0.65	66.46%	-5.57%	-2.48%	5.46%	5.21%
North America	0.17	67.35%	0.52	26.97%	-8.68%	-1.43%	8.26%	4.97%
South Asia	0.90	37.17%	0.53	44.37%	-5.75%	-2.82%	5.96%	4.73%
Sub-Saharan Africa	0.43	33.69%	0.54	51.40%	-3.93%	-2.00%	3.89%	3.29%
Mean	3.49	46.49%	0.63	44.57%	-4.72%	-1.57%	4.74%	3.12%

Notes: Model-based estimates are matched to real-world cities based on population, cost of height and height gap, an empirical estimate of how much of the potential height has not been realized taken from Barr & Jedwab, 2023. Compared to the actual cost of height used in Table 7, we have reduced the cost of height, θ, by 20%. Welfare estimates are population-weighted averages by region. Height ban means no tall building exceeding four floors. Large city population share is the share of urban population in cities with a population of at least 1M.

References

Ahlfeldt, Gabriel M. and Daniel P. McMillen, "Tall buildings and land values: Height and construction cost elasticities in Chicago, 1870-2010," *Review of Economics and Statistics*, 2018, *100* (5), 861–875.

_ **and Jason Barr**, "The economics of skyscrapers: A synthesis," *Journal of Urban Economics*, 5 2022, *129*, 103419.

_ **and** _ , "Viewing urban spatial history from tall buildings," *Regional Science and Urban Economics*, 11 2022, (94), 103618.

Brueckner, Jan K., "The structure of urban equilibria: A unified treatment of the muth-mills model," *Handbook of Regional and Urban Economics*, 1987, *2*, 821–845.

Cleveland, William S and Susan J Devlin, "Locally Weighted Regression: An Approach to Regression Analysis by Local Fitting," *Journal of the American Statistical Association*, 1988, *83* (403), 596–610.

Henderson, Daniel J. and Christopher F. Parmeter, *Applied Nonparametric Re- gression* 2015.

Liotta, Charlotte, Vincent Viguie, and Quentin Lepetit, "Testing the monocentric standard urban model in a global sample of cities,," *Regional Science and Urban Economics*, 2022, (97).

McMillen, Daniel P., "One Hundred Fifty Years of Land Values in Chicago: A Nonparametric Approach," *Journal of Urban Economics*, 7 1996, *40* (1), 100–124.